



Ecosystem service, biodiversity and socio-economic models for each case study

Deliverable D3.3

31st May 2022

Anna Cord¹, Stephanie Roilo¹, Michael Beckmann², Anne Paulus², Katharina Schneider², Predrag Lugonja³, Tijana Nikolic³, Fanny Langerwisch⁴, Marek Bednář⁴, Tomáš Václavík⁴, Paul Evans⁵, Arjan Gosal⁶, Rosemary Wool⁶, George Breckenridge⁶, Guy Ziv⁶, Jodi Gunning⁶

¹ *Technische Universität Dresden*

² *Helmholtz Centre for Environmental Research - UFZ*

³ *BioSense Institute*

⁴ *Palacký University Olomouc*

⁵ *UK Centre for Ecology and Hydrology*

⁶ *University of Leeds*

BESTMAP

**Behavioural, Ecological and Socio-economic Tools for Modelling
Agricultural Policy**



This project receives funding from the European Union's Horizon 2020 research and innovation programme under grant agreement No 817501.

Prepared under contract from the European Commission

Grant agreement No. 817501

EU Horizon 2020 Research and Innovation action

Project acronym: **BESTMAP**
 Project full title: **Behavioural, Ecological and Socio-economic Tools for Modelling Agricultural Policy**
 Start of the project: September 2019
 Duration: 48 months
 Project coordinator: Prof. Guy Ziv
 School of Geography,
 University of Leeds, UK
<http://bestmap.eu/>

Deliverable title: ESS, biodiversity and socio-economic models for each case study
 Deliverable n°: D3.3
 Nature of the deliverable: Other
 Dissemination level: Public

WP responsible: WP3
 Lead beneficiary: Technische Universität Dresden

Citation: Cord, A., Roilo, S., Beckmann, M., Paulus, A., Schneider, K., Lugonja, P., Nikolic, T., Langerwisch, F., Bednář, M., Václavík, T., Evans, P., Gosal, A., Wool, R., Breckenridge, G., Gunning, J. & Ziv, G. (2022). ESS, biodiversity and socio-economic models for each case study. Deliverable D3.3 EU Horizon 2020 BESTMAP Project, Grant agreement No. 817501.

Due date of deliverable: Month n°33
 Actual submission date: Month n°33

Deliverable status:

Version	Status	Date	Author(s)
1.0	Final	31 May 2022	Anna Cord ¹ , Stephanie Roilo ¹ , Michael Beckmann ² , Anne Paulus ² , Katharina Schneider ² , Predrag Lugonja ³ , Tijana Nikolic ³ , Fanny Langerwisch ⁴ , Marek Bednář ⁴ , Tomáš Václavík ⁴ , Paul Evans ⁵ , Arjan Gosal ⁶ , Rosemary Wool ⁶ , George Breckenridge ⁶ , Jodi Gunning ⁶ , Guy Ziv ⁶

¹*Technische Universität Dresden,*

²*Helmholtz Centre for Environmental
Research - UFZ,* ³*BioSense Institute,*

⁴*Palacký University Olomouc,* ⁵*UK
Centre for Ecology and Hydrology,*

⁶*University of Leeds*

The content of this deliverable does not necessarily reflect the official opinions of the European Commission or other institutions of the European Union.

Table of contents

Preface	5
Summary	5
Research goals	6
FAIR guiding principles	6
Models	6
Biodiversity	7
Model description	7
Case study examples	10
Food and fodder	14
Model description	14
Case study example	17
Carbon sequestration	18
Model description	18
Case study example	23
Water quality	25
Model description	25
Case study example	28
Socio-economic effects	33
Model description	33
Case study example	38
Obstacles and challenges	41
Outlook	41
Acknowledgements	43
References	43
Appendix	47
Biodiversity model factsheet	47
Food and fodder model factsheet	80
Carbon sequestration model factsheet	96
Water quality factsheet	111
Socio-economic effects model factsheet	126

Preface

This deliverable provides a report on the biodiversity and ecosystem services (ESS) models as well as the socio-economic statistical model, generated in the Work Package 3 (WP3) - Farming System Archetypes of BESTMAP. A general overview of the research goals and guiding principles under which the models were developed is given, followed by a detailed description of the four biophysical models (biodiversity, food and fodder, carbon sequestration and water quality) and of the socio-economic model, each with case study (CS) examples. This document is accompanied by model factsheets (see Appendix) which loosely follow the structure of the ODMAP (Overview, Data, Model, Assessment and Prediction) protocol developed by Zurell et al. (2020). The deliverable also discusses the obstacles and challenges encountered during the model adaptation and implementation in the different CS, and how the model outputs will be used in various other tasks within the project.

Summary

This deliverable presents the biodiversity, ESS and socio-economic models developed and adapted for each case study (CS) in BESTMAP. Understanding the environmental effects of currently subsidised measures like agri-environmental schemes (AES), ecological focus areas (EFA) and organic farming in the different project's CS is a first important step in assessing the effectiveness of such measures for environmental and biodiversity protection. It also contributes to the impact assessment of the current Common Agricultural Policy (CAP) and helps guide decisions for future CAP directions. This deliverable builds on the ideas and guidelines presented in the "MS4 - Directives for Modelling Approach in Case Studies", and directly employs the geospatial dataset collected and harmonised in "D3.1 - Case Study Base Layer dataset for each of the case studies". We here present four models on biodiversity and ESS, which estimate the impact of selected agri-environmental measures (AEM, used here as an umbrella term for agri-environment schemes, ecological focus areas and organic farming) on biodiversity, food and fodder, carbon sequestration and water quality. Additionally, a socio-economic model based on data from the Farm Accountancy Data Network (FADN) is described. All models are generated or adapted using open-source software, and the model scripts are made freely available and reusable. Moreover, the models are validated and uncertainty in the model results is assessed for all models and CS, thereby ensuring the reliability and correct interpretation of the model outputs. The core part of this deliverable is built from a general overview of each model's workflow, followed by examples of the model outputs from the different CS. Model factsheets with a detailed description of the input data, statistical approach, and outputs of each model, are attached to this deliverable and ensure transparency and reproducibility of all analyses (see Appendix). Modelling AEM effects across different countries, each with diverse agricultural policies, environmental conditions and data availability, is a challenging task; this deliverable also discusses problems and setbacks encountered during this process and how they were overcome. Lastly, we describe how the model outputs link to other ongoing and future activities within the project, and how they will be made available to the wider public, including local stakeholders, in the interactive BESTMAP dashboard.

1. Research goals

Biophysical and socio-economic modelling is one of the core tasks in the WP3 - Farming System Archetypes of BESTMAP, and is closely linked to activities in WP4 and WP5. The goal of this task is to estimate and map, in a spatially explicit way, the effects of selected agri-environmental measures (AEM) on biodiversity, ESS and socio-economic outputs for each of the five CS of the project. We here refer to AEM as an umbrella term for agri-environmental schemes, ecological focus areas and organic farming, as these practices are often similar in management and environmental objectives. Based on the results of the deliverable, other tasks within BESTMAP will implement the following: the model results will be used to identify trade-offs and synergies between biodiversity, ESS and socio-economic indicators in and across the five CS. Differences in the provision and flows of ESS and biodiversity between the different Farming System Archetypes (FSAs) will be assessed using the biophysical models' outputs. Useful policy indicators at the CS level will be developed from the biophysical models' results, and will later be upscaled to the European level. The indicators will be visualised either via the interactive dashboard, in which different policy scenarios and their effects will be explored, or in other ways (depending on the feedback from the CS co-design sessions). The biophysical models will also be applied to different AEM scenarios resulting from the agent-based modelling task, so that the environmental impacts of farmers' decisions can be directly estimated.

2. FAIR guiding principles

BESTMAP is committed to following the FAIR (Findability, Accessibility, Interoperability, and Reusability) guiding principles for scientific data - and model - management (Wilkinson et al., 2016), and strives to make all its outputs open access and reusable. BESTMAP's ESS and biodiversity models were selected from a comprehensive list of pre-existing open-source, spatially-explicit, calibrated and validated models (for further details on model selection, see MS4), which have been adapted for their application at the CS level and for the specific goal of detecting AEM effects on ESS and biodiversity. The model factsheets that accompany this deliverable describe in detail the input data, workflow (including calibration and validation), and output products for each of the models in each CS, to ensure the full reproducibility of the analyses and their results. The input data for the models were compiled and harmonised across CS in the Case Study Base Layer, a geospatial dataset described in the "D3.1 - Case Study Base Layer dataset for each of the case studies" stored in the UFZ GeoNetwork (<https://geonetwork.ufz.de>). The software (e.g. R <https://www.r-project.org/>, InVEST <https://naturalcapitalproject.stanford.edu/software/invest>, Python <https://www.python.org/>, QGIS <https://qgis.org/en/site/>) used for data preparation and modelling are all freely available, and the codes developed by the modellers for the adaptation and application of the models at CS level are stored in the UFZ GitLab page (<https://git.ufz.de/>), which hosts model-specific repositories. Finally, the outputs of the models will be made publically available via the UFZ GeoNetwork (<https://geonetwork.ufz.de>) at the end of the project. This ensures long-time data availability beyond the running time of the project.

3. Models

The BESTMAP modelling team held a virtual workshop in April 2020 to discuss and delineate the goals and directives for the biophysical and socio-economic models to be developed and adapted at the CS level ("MS4 - Directives for Modelling Approach in Case Studies"). As the primary goal of the biophysical modelling task was to investigate AEM effects on different ESS and biodiversity, the selection of both AEM and ESS to be modelled was tailored to this purpose. Multiple spatially-explicit open-source modelling suites and techniques for different ESS and biodiversity were reviewed, requirements regarding input data and parametrization collated and approaches for model validation selected. Models

were selected also on the basis of their ability to detect the environmental and socio-economic impacts of the implementation of different AEM at the field, farm and landscape level. The final list of selected and implemented models includes three ESS models (food and fodder, carbon sequestration and water quality), one biodiversity model and one socio-economic statistical model.

We originally selected a set of AES that occurred in all or most of the CS, and that were widely adopted. We later included ecological focus areas (EFA) to the AES groupings, as some of these are very similar in management to the AES and hence lead to similar environmental effects. Organic farming was also selected as one of BESTMAP's focal management practices, due to its growing popularity and widespread uptake across all CS. To ensure consistency and comparability of the AEM groupings across CS, we outlined definitions for each measures' group (see D2.5). The final list of modelled AEM are: buffer areas/strips, cover crops, land-use conversion to permanent grassland, land-use conversion to forest, maintaining permanent grassland, organic farming and fallow land. The frequency and spatial coverage of these seven AEM groups vary across CS, as does their relevance/impact for different ESS and biodiversity models, so not all AEM are considered in all models and CS.

To best visualise the contribution of the modelled AEM on ESS and biodiversity, we adopted a two-scenario approach: one land-use scenario reflects the current land-use management conditions for the year 2019, i.e. the most recent year for which land management data from the Integrated Administration and Control System and Land Parcel Identification System (IACS/LPIS) were available in the CS; in a second scenario, we removed all AEM from the landscape. ESS and biodiversity were modelled in both scenarios, and the difference between the two output maps allows us to clearly visualise the positive or negative effects of AEM on the selected ESS and biodiversity. All models were validated following established methods, as described in the next chapter for each model. Uncertainty in the model outputs can derive from incomplete or biased input data, model limitations as well as lack of knowledge and/or incorporation of associated or underlying processes. Uncertainty assessment is thus a fundamental factor for the correct interpretation of model outputs (Bryant et al., 2018); we performed uncertainty analyses for each model and CS.

3.1. Biodiversity

3.1.1. Model description

Authorship

Contact: Stephanie Roilo (stephanie.roilo@tu-dresden.de) for the models in DE, CZ, ES and UK; Tijana Nikolic (tijana.nikolic@biosense.rs) for the models in RS; Tomas Vaclavik (tomas.vaclavik@upol.cz) for the models in CZ.

Model name

Species distribution model (SDM; Figure 1) for selected farmland bird species.

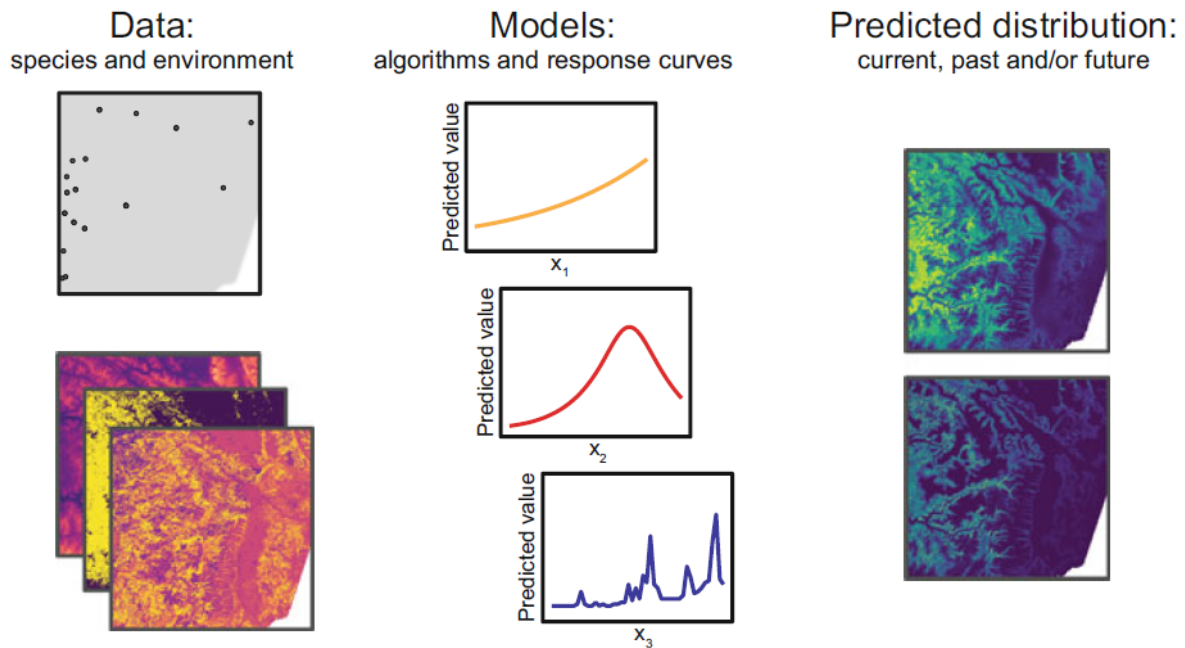


Figure 1: A general framework of species distribution models. Data on species location are linked to spatial data on the environment with quantitative models. Different model algorithms can vary considerably in the way they relate species responses to environmental gradients. With estimated response curves, species distributions are mapped in space and/or time. Ensemble models combine several model algorithms to deliver more robust forecasts (source: Fletcher & Fortin 2018).

Model objective

Main objective of the model is to estimate how the adoption of Agri-Environmental Measures (AEM) affects habitat suitability for a selected set of farmland bird species.

Model output

The model output consists of habitat suitability maps for the selected bird species.

Data specifications

Response data type: presence-only, georeferenced point occurrences of several farmland bird species.

Predictor types: geospatial (e.g. raster and shapefile data) information on climate, topography, anthropogenic disturbance, land cover and land-use, including land-use management information like AEM adoption extracted from the Integrated Administration and Control System (IACS) and Land Parcel Identification System (LPIS).

Assumptions

Model assumptions: 1. Species-environment equilibrium, 2. All relevant ecological drivers of farmland bird distributions are included in the models, 3. Bird dataset adequately covers fields with and without agri-environment measures.

Algorithms and workflow

Modelling techniques: We used ensemble SDMs to minimise the uncertainties arising from single algorithm models. The ensemble models were based on five modelling algorithms, namely generalised linear models and generalised additive models (GLM and GAM,

regression-based methods), random forest, generalised boosting models, and maximum entropy (RF, GBM, and MAXENT; machine-learning methods) as implemented in the biomod2 package version 3.4.6 (Thuiller et al. 2019).

Model workflow: We fitted 10 repetitions for each model by randomly subdividing the dataset into 70% training data and 30% testing data. Each model run was evaluated via cross-validation. We used the Area Under the Receiver Operating Characteristics Curve (AUC), the True Skills Statistics (TSS), specificity and sensitivity as evaluation metrics (Fletcher & Fortin 2018). To obtain a relevant combination of several unbiased (i.e., with fair accuracy) models, only models with an AUC value ≥ 0.7 were retained, and the ensemble model was constructed for each species by computing the weighted average of all remaining models. The weights were based on the AUC scores of each model, so that better performing models had a higher influence in the final ensemble. The models were then projected onto the current (as of 2019) environmental and agricultural conditions to obtain habitat suitability maps for each bird species.

Model validation

Each model run was evaluated via cross-validation, and the average across the 10 runs was computed to assess the performance of the final model. We used AUC, TSS, specificity and sensitivity as evaluation metrics.

Uncertainty estimation

Ensemble SDMs were developed with the specific goal of minimising the uncertainty in estimating species distribution deriving from single algorithm models (Araújo & New 2007, Wüest et al. 2020). Indeed, among the many potential sources of uncertainty in SDMs, such as algorithms, environmental datasets, species presences, variable collinearity, etc., the choice of modelling algorithm is thought to be the greatest source of uncertainty in SDM performance and prediction maps (Watling et al. 2015, Wüest et al. 2020). We therefore produced uncertainty maps calculated as the standard deviation of the prediction maps deriving from the model algorithms included in the ensemble model (Buisson et al. 2010; Senai & Worner 2019). Such maps highlight the areas of highest disagreement across single algorithm predictions.

Software

Software: We used the biomod2 package version 3.4.6 (Thuiller et al. 2019) in R version 4.0.2 (R Core Team 2020).

Code availability: the R code used for the preparation of the environmental variables at multiple spatial scales (approach adopted in DE, CZ and RS), fitting the models and producing the uncertainty maps, together with a README file, is available here: <https://git.ufz.de/bestmap/bestmap-biodiversity>

Linking the model outputs to indicators

The model results can be linked to the following policy indicators:

[C.35/I.18 Farmland Bird Index](#) (FBI) (European Commission 2021).

While the European Farmland Bird Index represents temporal trends of population sizes based on annual national bird surveys, we here aimed at developing an indicator that could detect the effects of AEM in a spatially-explicit way, and that could be compared across CS. We hence normalised all individual species' SDMs and we computed the average habitat suitability score across all modelled bird species. The output is an index of farmland birds'

habitat suitability, with high (positive) values indicating highly suitable habitat, and low (negative) values indicating unsuitable habitat.

Model specifications for each case study are available in the model factsheet in the appendix.

3.1.2. Case study examples

Mulde, DE

Figure 2 shows the modelled habitat suitability maps, under the two scenarios, for one example species: the red-backed shrike (*Lanius collurio*). Model performance was very good (Area Under the Receiver Operating Characteristics Curve = 0.91, sensitivity = 0.86, specificity = 0.83). For this species, the application of AEM, especially extensive grassland management, fallow land and organic farming, led to an increase in habitat suitability, as is evident by comparing the two maps (Figure 3). The uncertainty map for the current scenario highlights some areas of higher disagreement in the single algorithm predictions; these are areas with large proportions of fallow land and organic farming, for which the estimated species-environment relationships diverged across different algorithms.

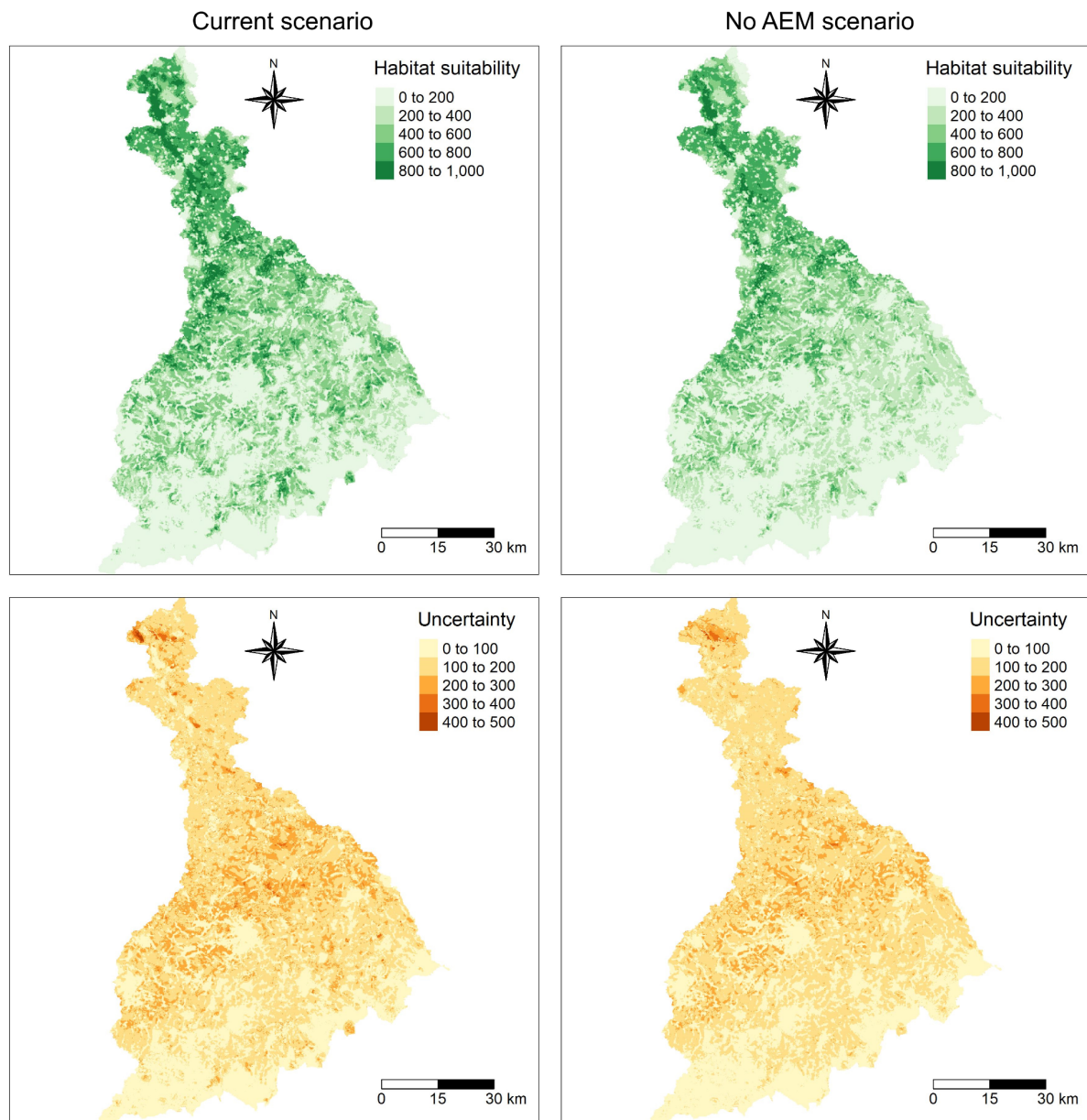


Figure 2: Modelled habitat suitability, ranging from 0 to 1000 as a measure of habitat quality, and the related uncertainty maps, calculated as standard deviation across the single model algorithms' predictions, for the red-backed shrike (*Lanius collurio*) in the Mulde river basin. The maps on the left refer to the current scenario, i.e. the land-use conditions as of 2019; the maps on the right refer to the "no AEM scenario", in which all modelled AEM groups are removed from the landscape.

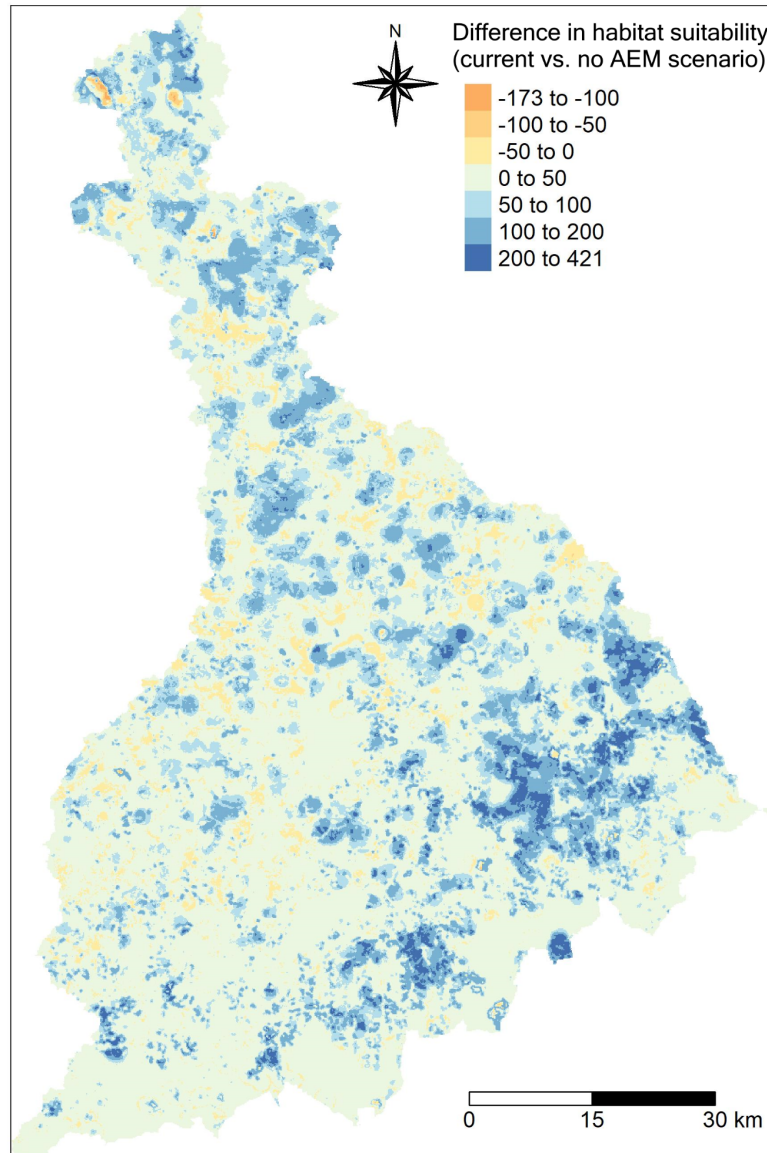


Figure 3: Difference in habitat suitability between the current and the no AEM scenario, for the red-backed shrike (*Lanius collurio*) in the Mulde river basin. Positive values (in blue) mark areas in which habitat suitability is higher when AEM are implemented, that is under current land-use conditions as of 2019. The opposite is true for areas with a negative change (in red).

Catalonia, ES

In Catalonia, bird occurrence data was only available in gridded format at 1km resolution. The model outputs are thus also at a coarser spatial resolution than in DE, CZ and RS, where georeferenced occurrence points of bird observations were available (see Appendix, biodiversity model factsheet). Figure 4 shows the modelled habitat suitability maps, under the two scenarios, for the skylark (*Alauda arvensis*) in Catalonia. Model performance was very good (Area Under the Receiver Operating Characteristics Curve = 0.82, sensitivity = 0.75, specificity = 0.77). For this species, the considered AEM, especially extensive grassland management and fallow land, were positively related to habitat suitability (Figure 5). In both scenarios, the uncertainty is highest in the southern tip of the CS.

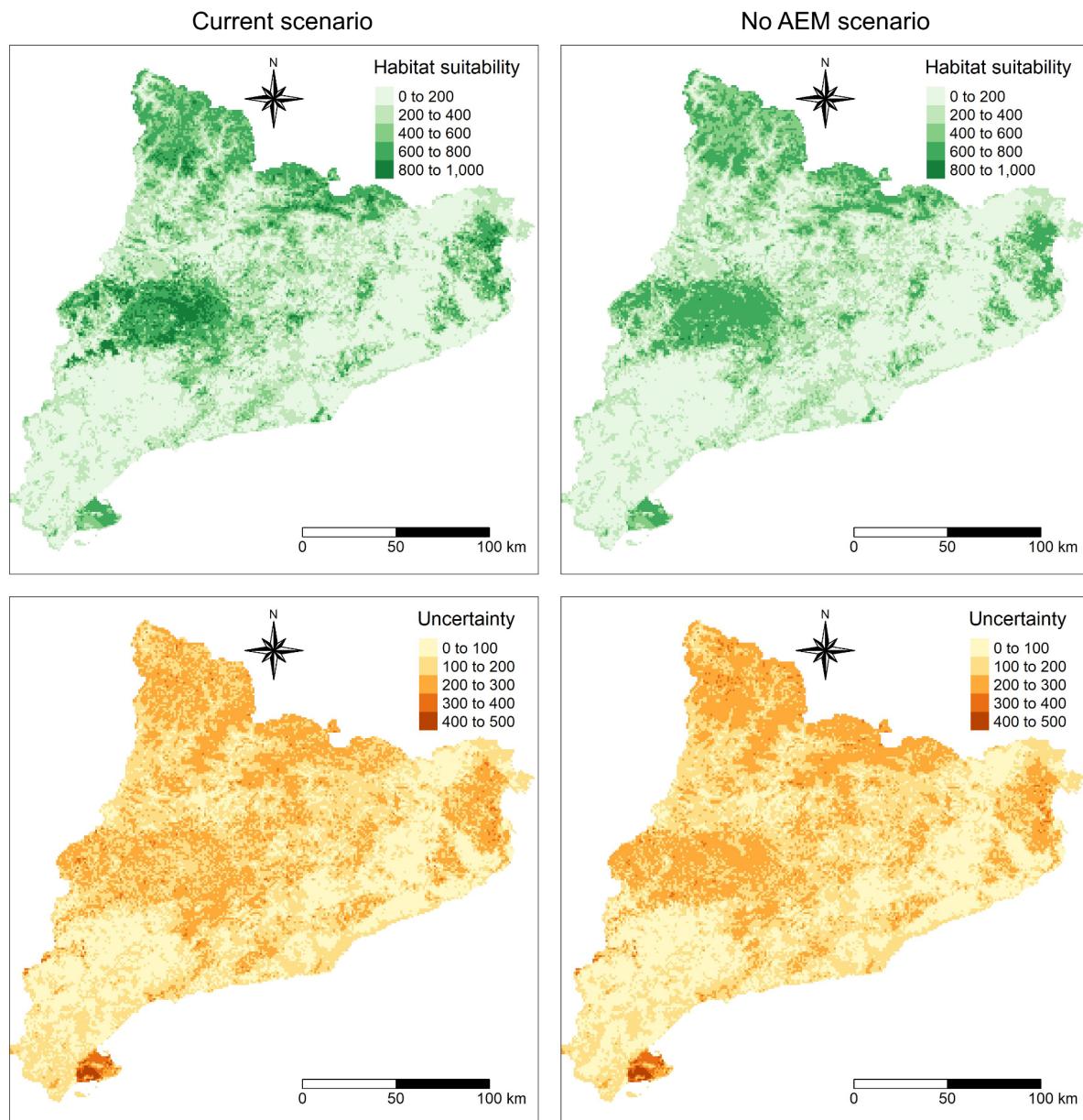


Figure 4: Modelled habitat suitability and related uncertainty maps for the skylark (*Alauda arvensis*) in Catalonia. The maps on the left refer to the current scenario, i.e. the land-use conditions as of 2019; the maps on the right refer to the “no AEM scenario”, in which all modelled AEM groups are removed from the landscape.

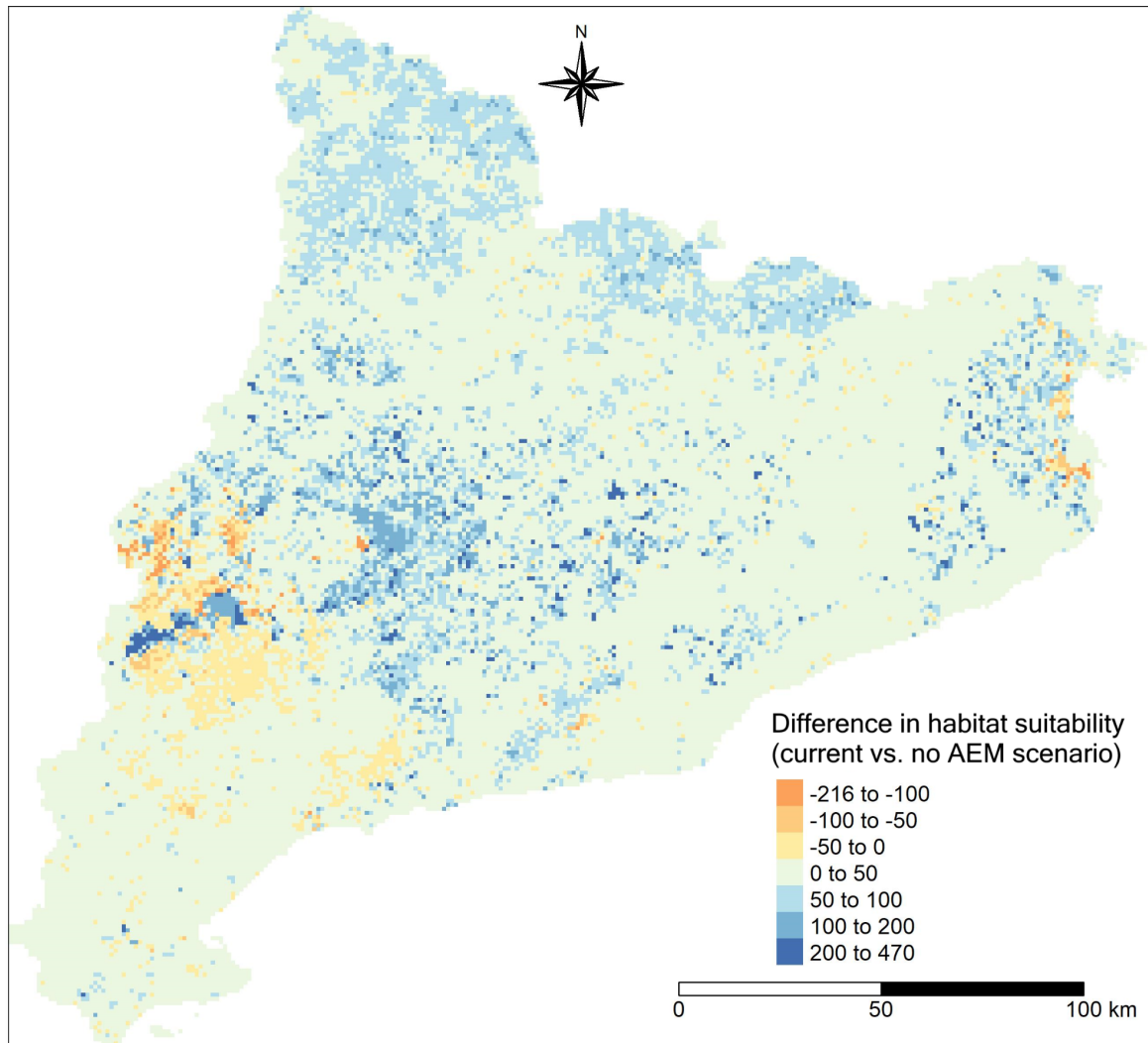


Figure 5: Difference in habitat suitability between the current and the no AEM scenario, for the skylark (*Alauda arvensis*) in Catalonia. Positive values (in blue) mark areas in which habitat suitability is higher when AEM are implemented, that is under current land-use conditions as of 2019. The opposite is true for areas with a negative change (in red).

3.2. Food and fodder

3.2.1. Model description

Authorship

Contact: Anne Paulus (anne.paulus@ufz.de), Predrag Lugonja (predrag.lugonja@biosense.rs), Katharina Schneider (katharina.schneider@ufz.de), Rosemary Wool (r.wool@leeds.ac.uk), Michael Beckmann (michael.beckmann@ufz.de)

Model name

Model of the effects of agri-environmental measures on food and fodder production.

Model objective

Main objective of the model is to estimate how the adoption of agri-environmental measures (AEM) affects the yield and production area of selected agricultural crops as well as economic output at the field and farm level. Figure 6 provides a conceptual overview of the model workflow.

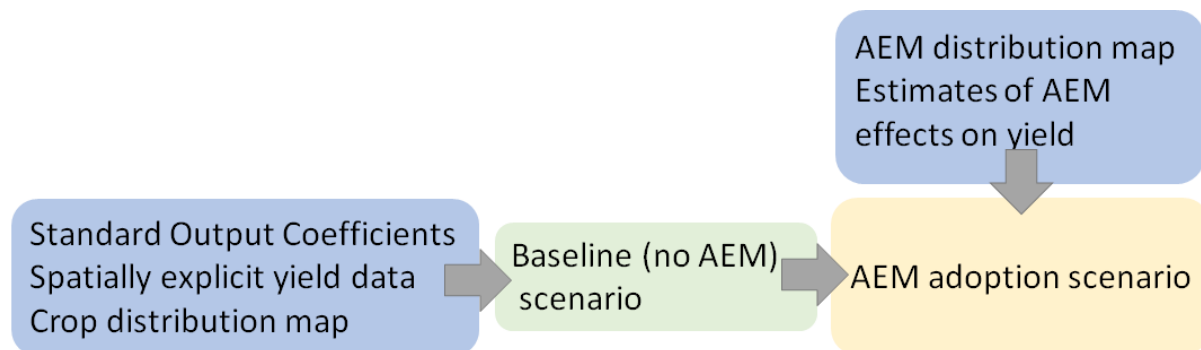


Figure 6: Schematic overview of the food and fodder model.

Model output

The model output consists of maps of crop production area, yield and standard output.

Data specifications

Geospatial information (e.g. as raster and shapefile data) on agricultural land-use, including management information like AEM adoption (cover crops, buffer areas/flower strips, land-use conversion, maintaining permanent grasslands, organic farming) and type of crops grown as well as spatially explicit yield data of agricultural crops and their standard output coefficients.

Assumptions

1. All relevant effects of the AEM on food and fodder production are included in the models,
2. Current AEM implementation levels do not affect the baseline yield and standard output,
3. Cover crop effects on yield depend only on climate, soil texture, catch crop and cover crop type,
4. Implementation of buffer areas and land-use conversion do not affect yield and standard output of neighbouring fields,
5. EUROSTAT and IACS/LPIS information on agricultural management is correct.

Algorithms and workflow

The general workflow of the food and fodder model is depicted in Figure 6. We obtained standard output coefficients (StOCs) of agricultural crops from EUROSTAT (2022) as an economic measure of agricultural production. A baseline yield map without AEM was produced using predictions created by the WOFOST model for arable land. Regional yield data for grassland were obtained from local data sources. These data were used as a weighting factor in order to account for spatial variation of StOCs. StOCs are published by EUROSTAT (2021) and represent the monetary value produced by cultivating a crop per hectare at a given time and location. We then used existing empirical data to estimate the

relative effect of AEM on crop yield. The results were then combined in order to produce case study maps of production area and yield of the selected crops.

WOFOST

WOFOST (WORLD FOOD STUDIES) is a simulation model developed at Wageningen University & Research for the quantitative analysis of the growth and production of annual field crops (Van Diepen et al., 1989). WOFOST is used in the European Mars crop yield forecasting system (de Wit et al., 2019). The WOFOST data used here were previously generated in the JRC study “Analysis of climate change impacts on EU agriculture by 2050” (Hristov et al., 2020). The WOFOST model was run on climate data. 8 climate models were used from 5 families and yield predictions were generated for two RCP scenarios, mid-range mitigation emission scenario (RCP4.5) and the high-end emission scenario (RCP8.5). We aggregated this data in the following way to create single yield maps for each scenario: first, we calculated the mean of each model's family, and then the median of aggregated results was used for final yield prediction. Yield predictions are generated for the following six crops: maize, sugar beet, wheat, sunflower, winter rapeseed, spring barley at a resolution of approx. 11km. WOFOST data were used as a baseline in all case studies, except for Spain, where agriculture is dominated by crop species not included in WOFOST.

Uncertainty analysis

The food and fodder model is largely based on two sources of information: i. the yield model, ii. information from IACS/LPIS and EUROSTAT. As there is no information of uncertainty about the latter, we assume that they are correct, so the uncertainty of our model can be calculated from the uncertainty of the crop yield model. As a measure for uncertainty of the WOFOST baseline model, we decided to use variance across the 8 climate models. To calculate uncertainty of the WOFOST model, we calculated variance of each pixel across years, since each pixel across 8 yield maps represents an independent random process. For comparison of uncertainty across years we calculated a histogram of variance for each year separately.

Model validation

The baseline yield model of arable crops was validated using regional yield statistics of each case study. The model was evaluated using the metrics R^2 and RMSE.

Software

Software: We used R version 4.0.2 (R Core Team 2020).

Code availability: the R code used for the preparation of the environmental variables and for fitting the models, together with a README file, is available here: <https://git.ufz.de/bestmap/bestmap-food-and-fodder>.

Linking the model outputs to indicators

The model results are not identical to, but can be linked to the following indicator (EUROSTAT 2022):

C.24 Agricultural factor income

Agricultural factor income represents the value generated by a farm business including all factors of production, which makes it a suitable indicator for evaluating the impact of

changes in subsidies like AEM on farm income. It is also used for the EU reporting on the United Nations' Sustainable Development Goals.

Model specifications for each case study are available in the model factsheet in the appendix.

3.2.2. Case study example

Mulde, DE

For the case study model of the Mulde river basin, annual yield data of the predominant arable crops (wheat, maize, barley, rapeseed, sugar beet) was obtained from WOFOST predictions (Hristov et al. 2020) and amended with regional grassland yield information from LfULG (2001). For all other crops, it was only possible to model changes in standard output. Cover crop effects on maize yield based on soil texture, main crop, cover crop, and climate were estimated according to Jian et al. (2020). We used the SoilHealthDatabase consisting of more than 200 original studies comparing crop yields with and without cover crops. For the effect of the maintaining grasslands AEM on food and fodder production, we took into consideration the reduction of grassland yield due to lower mowing frequency and fertilisation. Figure 7 shows the modelled standard output maps under the two scenarios (current implementation of AEM vs. no AEM). Crop-specific StOCs vary by several orders of magnitude, which masks the effect of AEM and leads to a similar appearance of the two maps. The effect becomes clearer when looking at the differences between the two scenarios shown in Figure 8. The largest reduction in standard output due to AEM is in the southern part of the CS, where maintaining permanent grassland schemes are common. In some fields, standard output is enhanced by AEM, which can be explained by a modelled yield increase due to cover crop implementation.

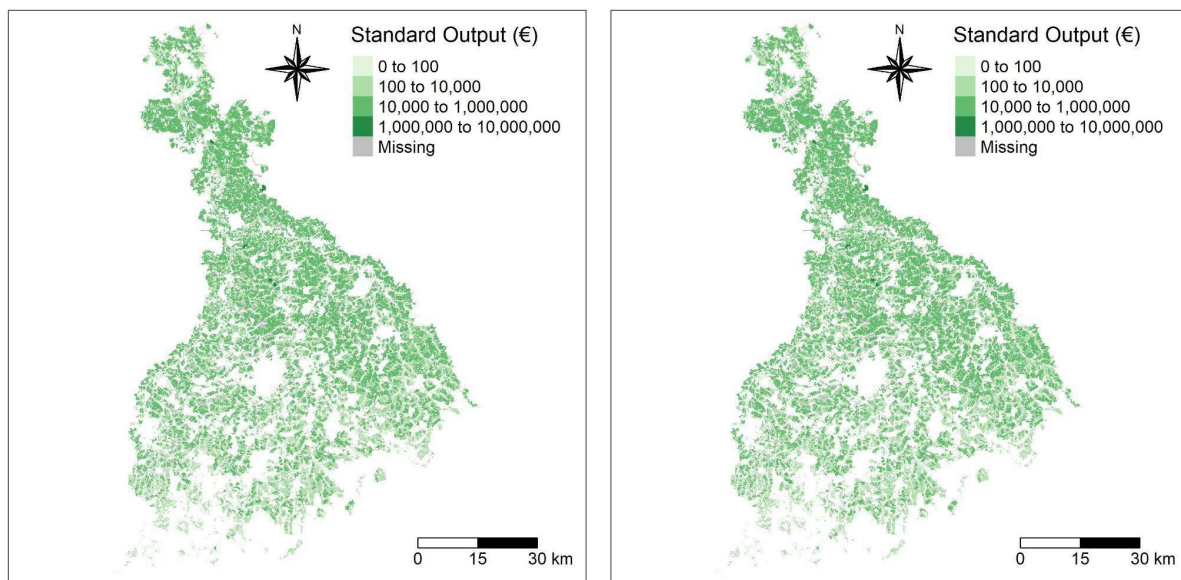


Figure 7: Modelled standard output (€) in the Mulde river basin. The map on the left refers to the current scenario, i.e. the land-use conditions as of 2019; the map on the right refers to the “no AEM scenario”.

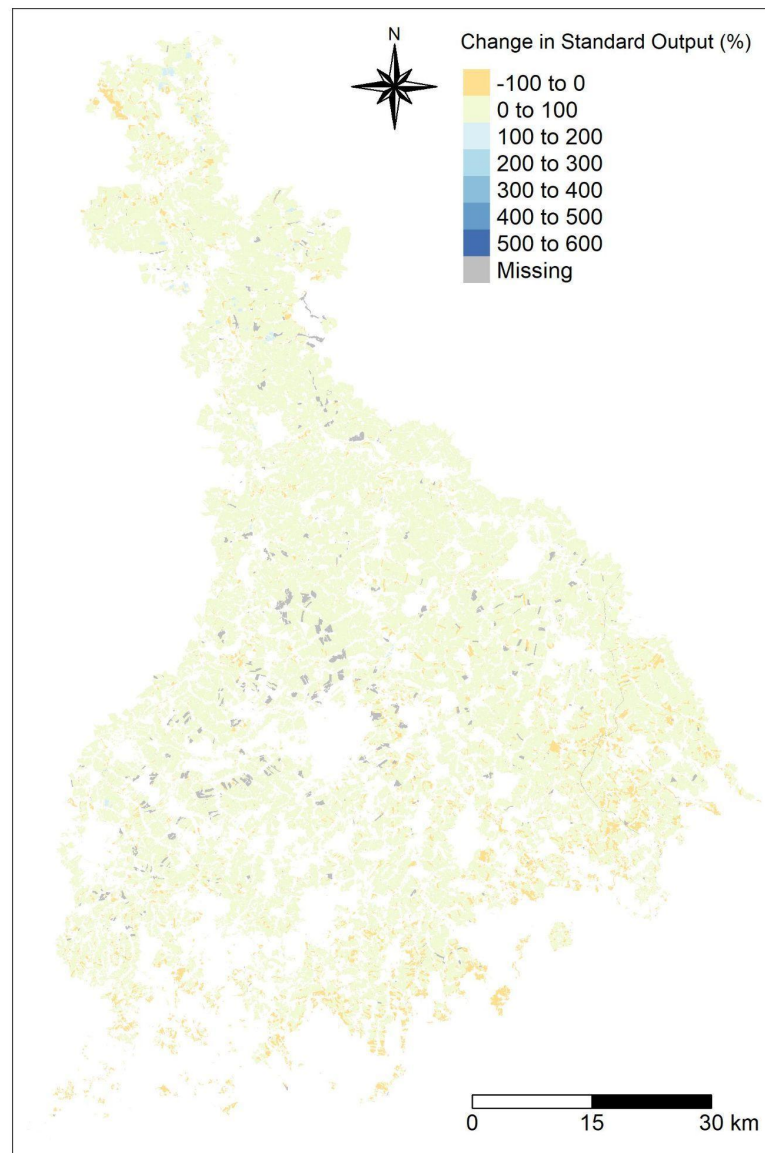


Figure 8: Difference in standard output (%) between the current and the no AEM scenario in the Mulde river basin. Positive values (in blue) mark areas in which standard output is equal or higher when AEM are implemented, that is under current land-use conditions as of 2019. The opposite is true for areas with a negative change (in red).

3.3. Carbon sequestration

3.3.1. Model description

Authorship

Contact: Fanny Langerwisch (fanny.langerwisch@upol.cz)

Model name

Model of the effect of agri-environmental measures on soil organic carbon (SOC).

Model objective

The main objective of the model is to estimate how the adoption of agri-environmental measures (AEM) affects soil carbon sequestration on field level / within landscapes (see Figure 9 for a conceptual workflow of the model).

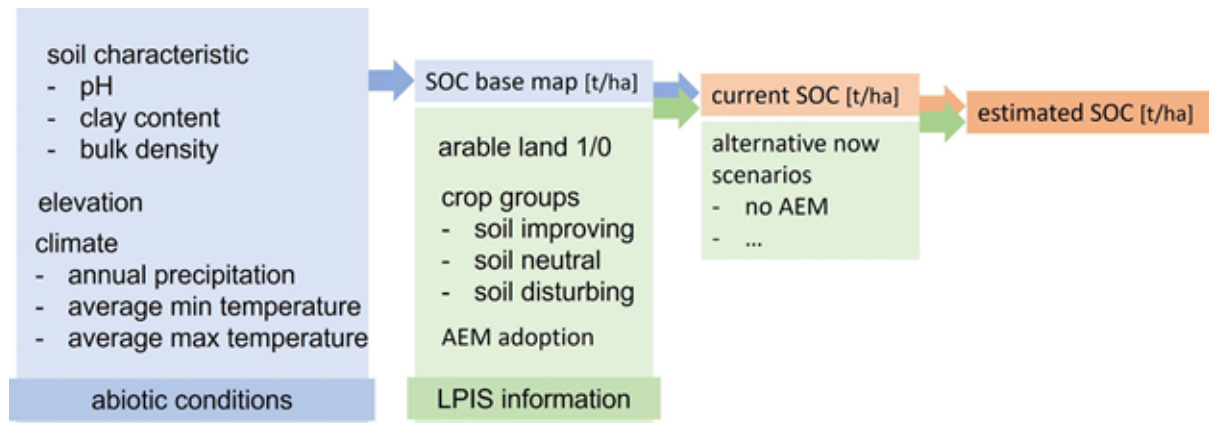


Figure 9: Conceptual figure of the workflow of the carbon model.

Model output

The model output consists of maps of soil organic carbon per field/parcel, under the current land-use patterns and AEM implementation and under alternative-now scenarios.

Data specifications

Response data type: soil organic carbon (SOC [t/ha]).

Predictor types: geospatial data (raster and polygons) on soil characteristics, climatic conditions, crops and adopted AEMs (agri-environmental schemes and ecological focus areas).

Hypotheses

We hypothesise that SOC is sensitive to the crop type and to the adoption of AEM. We also hypothesise that underlying SOC (SOC_{base}), which is only driven by abiotic factors (e.g. climate, clay content), is affected by the above-mentioned land-use and AEM interventions (SOC_{lu} and SOC_{curr} , respectively). To test our hypothesis we compared the simulated SOC under the current AEM implementation (SOC_{curr}) with a second scenario in which no AEM is implemented.

Assumptions

Model assumptions: (1) The soil organic carbon depends on abiotic conditions and is altered by land cover and land use. (2) Current amount of soil carbon is in equilibrium, i.e. the soil already contains organic carbon, there is no general building-up of soil organic carbon assumed. (3) There is no dependence of SOC on soil management (ploughing/mulching etc). (4) SOC is affected differently by different crop groups (soil-improving, soil-disturbing and neutral crops). (5) The rotation of each parcel over several years can be depicted by the crops rotated on all parcels per farm. This can be used to identify a 'pseudorotation', which indicates the coverage with soil-improving and soil-disturbing crops. (6) The effect of the

AEM ‘maintaining permanent grassland’, ‘buffer strips’ and ‘land-use conversion to permanent grassland’ are similar to the effect of growing ‘permanent grassland’ on the parcel.

Algorithms and workflow

We calculated the soil organic carbon base for each parcel/pixel only depending on abiotic conditions, such as climate and soil characteristics (clay, pH, bulk density, elevation, annual precipitation, average min. and max. temperature, see Eq.1).

$$\text{SOC}_{\text{base}} = -e^{(\text{intercept} + \text{elev} \times \text{c.elev} + \text{clay} \times \text{c.clay} + \text{pH} \times \text{c.pH} + \text{BD} \times \text{c.BD} + \text{prec} \times \text{c.prec} + \text{Tmin} \times \text{c.Tmin} + \text{Tmax} \times \text{c.Tmax})} \quad (\text{Eq.1})$$

The coefficients for this calculation (Table 1) were extracted from LUCAS observation points making use of a quasi-Poisson generalised linear model. Further information and data accessibility of the LUCAS data can be found at <http://esdac.jrc.ec.europa.eu/projects/lucas>. For our study, we included only the 8,554 points classified as arable, which were used also by Quemade et al. 2020.)

Table 1: Coefficients used in Eq.1 to calculate the SOC basemap.

Input variable	Coefficient	Value and significance
-	intercept	8.938178***
elevation (<i>elev</i>)	c.elev	-0.000077***
clay content (<i>clay</i>)	c.clay	-0.009685***
soil pH (<i>pH</i>)	c.pH	-0.022066***
bulk density (<i>BD</i>)	c.BD	-3.162275***
mean annual precipitation (<i>prec</i>)	c.prec	-0.000097***
mean maximal temperature (<i>Tmax</i>)	c.Tmax	-0.014182***
mean minimal temperature (<i>Tmin</i>)	c.Tmin	0.013269***

The quasi-Poisson-GLM led to an $R^2=0.902$. The deviance residuals were distributed the following: Min= -9.7610; 1Q= -0.6710; Median=0.0440; 3Q=0.7073, Max=10.5140.

In a second step, we used the baseline SOC (SOC_{base}) and adapted it according to the land use to calculate the SOC_{lu} . On arable parcels, we assumed that SOC is altered by different crops. We organised crops into three crop groups: (1) soil-disturbing crops, such as potatoes and sugar beet, which reduce the SOC, (2) soil-improving crops, such as legumes, which increase the SOC, and (3) neutral crops, which do not affect the SOC. This grouping was done for each case study separately. The parameters for the effects were extracted from the literature (Table 2). The parameters can be adapted to case study conditions. Additionally, we adapted the SOC (SOC_{lu} on permanent grassland) for parcels under permanent

grassland management, assuming an increase in SOC based on Poeplau & Don (2015). Also this parameter can be adapted locally. We assumed SOC to remain unaltered in the remaining parcels, i.e. non-arable and non-permanent grassland parcels.

The last step was the modification of SOC_{lu} depending on the currently applied AEM (SOC_{curr}) and alternative-now scenarios (SOC_{alt}). Here, we applied parameters for each of the following AEM groups: (1) cover crops, (2) organic farming, (3) maintaining permanent grassland, (4) buffer strips and land-use conversion (5) to permanent grassland and (6) to forest. The difference between SOC_{curr} and SOC_{alt} is the different distribution of AEM, where SOC_{curr} represents the current AEM adoption and SOC_{alt} any alternative AEM adoption. The parameters for this calculation were extracted from the literature (Table 2) and can be further adapted to local conditions. The parameters to calculate SOC_{lu} (p.lu.xxx) and SOC_{curr} and SOC_{alt} (p.aem.xxx) are listed in Table 2.

Calculation of SOC_{lu} and SOC_{curr} (as well as SOC_{alt}) with the following equations.

$$SOC_{lu} = SOC_{base} \times (1 + p.lu.xxx) \quad (Eq. 2)$$

$$SOC_{curr} = SOC_{lu} \times (1 + p.aem.xxx) \quad (Eq.3)$$

Eq.3 is applied to calculated SOC_{curr} as well as SOC_{alt} .

Table 2: Parameters used for the adaptation of the baseline SOC according to different land use and AEM application.

Parameter name	Value	Source
p.lu.soilimproving	0.35	Wu et al. 2016, Gregorich et al. 2001, Guan et al. 2016
p.lu.soildisturbing	-0.1	Goidts & van Wesemael 2007
p.lu.permgrass	0.45	Poeplau & Don 2015, Gregorich et al. 2001
p.aem.covercrops	0.1	Crystal-Ornelas et al. 2021, Poeplau & Don 2015, Abdalla et al. 2019
p.aem.organic	-0.05	Lorenz & Lal 2016, Mondelears et al. 2006, Gattinger et al. 2012
p.aem.maintgrass	0.45	Poeplau & Don 2015, Gregorich et al. 2001
p.aem.buffer	0.45	Poeplau & Don 2015, Gregorich et al. 2001
p.aem.luconvgrass	0.3	Poeplau & Don 2015, Ledo et al. 2020, Martens et al. 2003, Gregorich et al. 2001
p.aem.luconvforest	0.45	Poeplau & Don 2015, Gregorich et al. 2001, Martens et al. 2003

The resulting maps of SOC under different AEM implementation scenarios, including a “no AEM” scenario and several different AEM implementations (varying spatial arrangements of one or multiple AEM types) were used to estimate the effect of each agri-environmental measure.

Uncertainty analysis

We conducted an uncertainty analysis of the SOC basemap calculation (SOC_{base}), in which we changed the values of all input variables (see Table 1) by $\pm 5\%$ and $\pm 10\%$. The effect of changes in the bulk density (BD) was the highest, which is in line with our expectations and with empirical evidence since the coefficient for BD (c_{BD}) was the largest. The effect of variation in clay content and maximal temperature was small, while elevation, precipitation and minimal temperature had a negligible effect.

Additionally, we did a sensitivity analysis of the SOC_{lu} and SOC_{curr} by changing the parameters listed in Table 2.

Model validation

Validation of SOC base map (SOC_{base}) and current SOC (SOC_{curr}) was done with observations from SOILGRIDS 250m organic carbon stock. Case study specific validation is possible with regional data.

Software

R version 4.1.2 ‘Bird Hippie’ (2021-11-01) R Core Team (2021).

Code availability: the R code used for the preparation of the variables and for fitting the model is available here: <https://git.ufz.de/bestmap/bestmap-carbon-sequestration>

Linking the model outputs to indicators

The model results can be linked to the following policy indicators:

[C41 - Soil organic matter in arable land](#)

The indicator consists of 2 sub-indicators: i. the total estimate of organic carbon content in arable land; ii. the mean organic carbon content. The indicator is expressed as an estimate of the total SOC stocks in topsoil (0-20) of EU Member States. The mean SOC concentration per Member State is calculated for orientation purposes (European Commission 2021). The outputs of the carbon sequestration model can be linked to the first sub-indicator of the indicator C41.

Model specifications for each case study are available in the model factsheet in the appendix.

3.3.2. Case study example

South Moravia, CZ

The South Moravia case study is dominated by arable land in the lowlands and permanent grassland farms in the higher elevations (Figure 10). This is reflected by the distribution of SOC, which is influenced by cropping vs. permanent grassland (Figure 10). On about half of the parcels at least one AEM is adopted. The grouping of crops into soil-disturbing and soil-improving is shown in Table 3. All crops not included are referred to as 'neutral'. Barren parcels were classified as soil-disturbing.

Table 3: List of crops of each group in the case study.

Soil-improving crops	Alfalfa Bean Chickpea Clover Legume Lupine Pea
Soil-disturbing crops	Potato Radish Sugar beet Topinambur

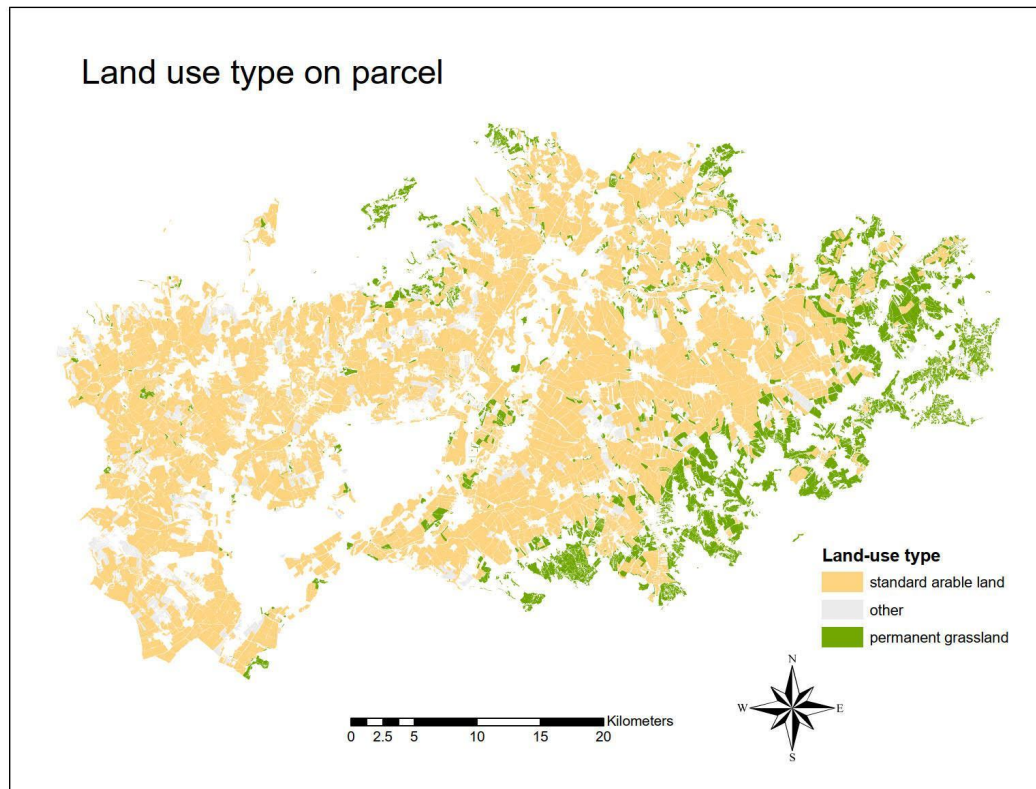


Figure 10: Distribution of the main land-use types - standard arable land and permanent grassland - in South Moravia.

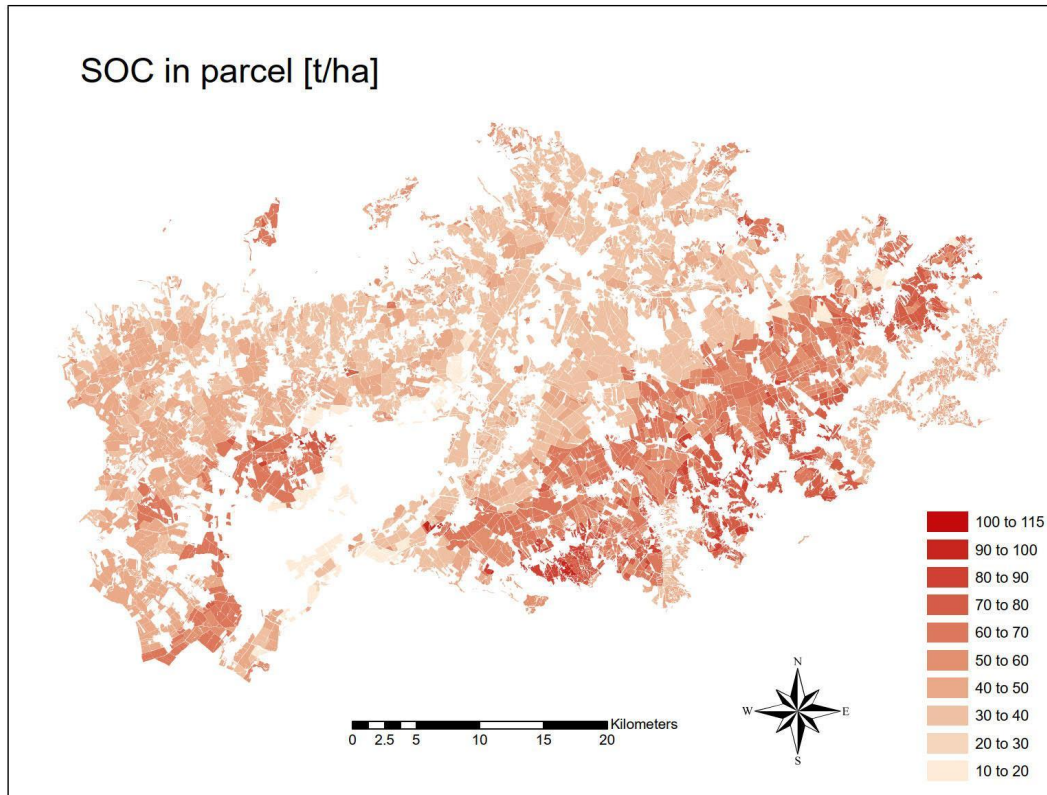


Figure 11: Estimated SOC_{curr} [t/ha] for each parcel in South Moravia.

Figure 12 shows the relative changes in SOC between the “no AEM” scenario (SOC_{alt}) and the current conditions (SOC_{curr}) (in terms of crops grown and applied AEM) as of 2019.

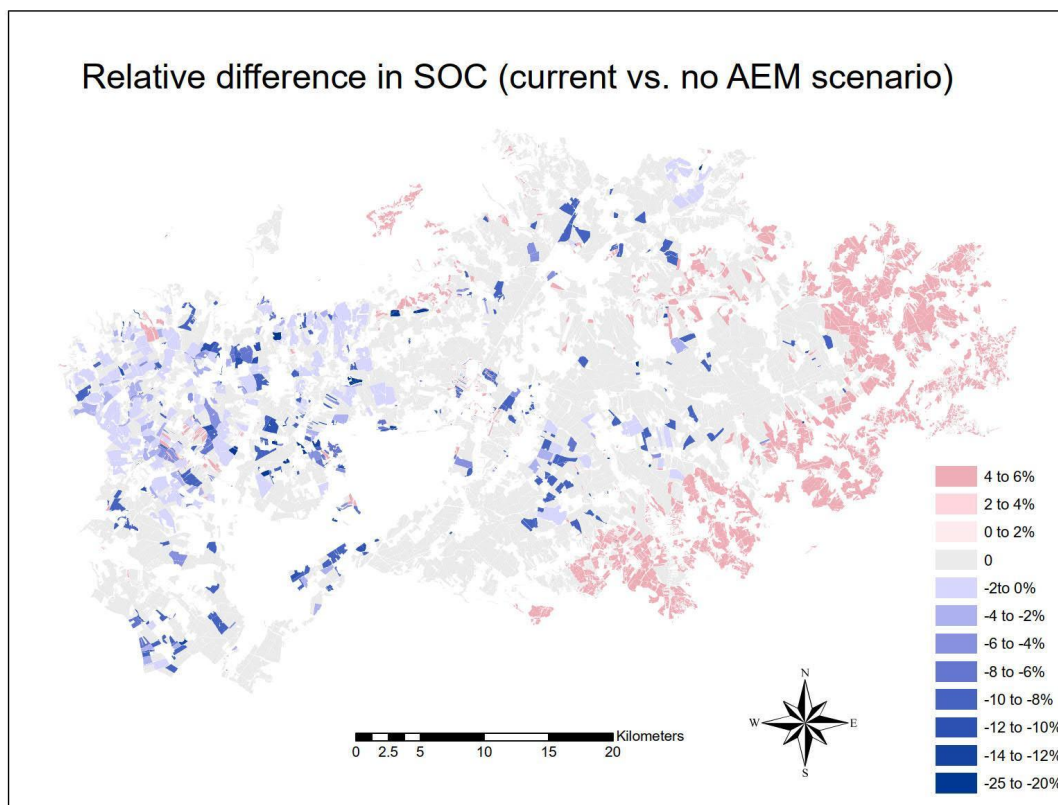


Figure 12: Relative changes in SOC [%] under the 'no AEM' scenario, compared to the current land-use conditions.

3.4. Water quality

3.4.1. Model description

Authorship

The model is authored by the Natural Capital Project: <https://naturalcapitalproject.stanford.edu/>. This instance of the model was run by: Dr. Arjan Gosal (a.gosal@leeds.ac.uk), Rosemary Wool (r.wool@leeds.ac.uk), Dr. Marek Bednář (marek.bednar@upol.cz) and Dr. Sanja Brdar (sanja.brdar@biosense.rs).

Model name

InVEST Nutrient Delivery Ratio: <https://naturalcapitalproject.stanford.edu/software/invest>

Model manual

A comprehensive manual is available online: <https://invest-userguide.readthedocs.io/en/latest/ndr.html>

Model objective

The InVEST Nutrient Delivery Model (NDR) is designed to map nutrient sources, from watershed to stream. It allows nutrient retention by natural vegetation in relation to surface water quality to be investigated (Sharp *et al.*, 2018).

Model processes

The following summary is abridged from the comprehensive [InVEST documentation](#) on the NDR model. The approach the NDR model utilises is one of simple mass balance by the movement of nutrients through space (see Figure 13). Rather than use details of the nutrient

cycle, the NDR model instead uses long-term, steady state flows through empirical relationships (Sharp *et al.*, 2018). Nutrient loads are associated with different land (or crop) types with nutrient delivery ratios computed for nutrient transport by surface flow (with the option for subsurface flow in the model). Surface flow is calculated using a delivery factor, which represents ability to transport nutrients without retention for downstream pixels and a topographic index (Sharp *et al.*, 2018).

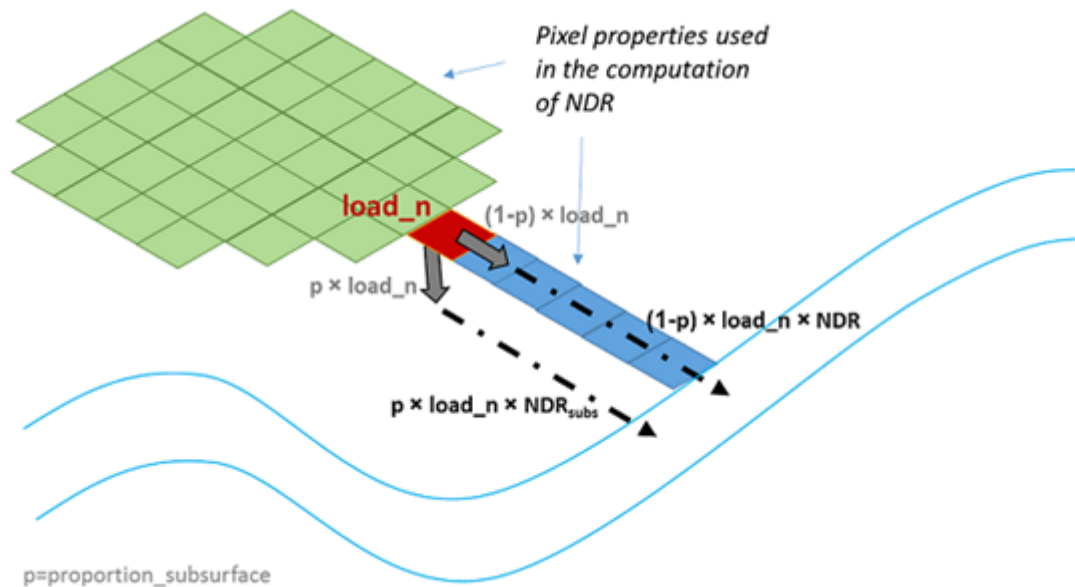


Figure 13: Conceptual representation of the nutrient delivery in the Nutrient Delivery Ratio model (source: Sharp *et al.*, 2018). The model is run assuming that the subsurface component is zero, as per Redhead *et al.* (2018)

Model output

The model provides spatial outputs. The first is a vector shapefile with the following attributes; the total nutrient loads in each watershed (i.e. the sum of the nutrient contribution from all land cover types), the total subsurface nutrient loads in each watershed, and the total nutrient export from each watershed. The second output is a raster tif file showing how much load from each pixel eventually reached the stream in kg/pixel. The model resolution of the output raster is the same resolution of the DEM provided as the input, and therefore this resolution will vary depending on the specific input data for different areas. The outputs of the model will be extracted at the farm-level in place of using the sub/watershed catchments that are outputted from the native model.

Data specifications

Geospatial information including digital elevation model (DEM), land use/land cover map (LCM), crop map, nutrient runoff proxy, watersheds delineated from a digital elevation model, and a biophysical table containing several different values on nutrients loading relating to each land use type (see Table 4).

Table 4: Description of Nutrient Delivery Model inputs.

Data type	Input	Description
Spatial	Digital elevation model (DEM)	Raster dataset with an elevation value for each pixel, given in metres

	Land use/land cover (LULC)	Raster of land use/land cover type for each pixel, where each unique integer represents a different land use/land cover class
	Nutrient runoff proxy	Raster representing the spatial variability in runoff potential, which in this case is annual precipitation
	Watersheds	Shapefile delineating the boundary of the watersheds within the case study area
Non-spatial	Biophysical table	A table containing information corresponding to each land use class in the LULC raster, which also includes each AEM class. The parameters include nitrogen/phosphorus load, maximum retention efficiency, the distance after which it is assumed that a patch of a particular LULC type retains nutrient at its maximum capacity, and the proportion of dissolved nutrients over the total amount of nutrients.

Assumptions

This model has high-sensitivity to inputs, therefore errors in the biophysical table have a large effect on predictions. This includes the outputs of the model being highly sensitive to the small number of input parameters.

Algorithms and workflow

See the model specification and details of the algorithm at: <https://invest-userguide.readthedocs.io/en/latest/ndr.html>

Model validation

This instance of the model is not validated, but has been validated in previous research for the UK: <https://www.sciencedirect.com/science/article/pii/S0048969717320909>

Uncertainty estimation

Uncertainty was ascertained using the results of Redhead et al (2018) study which validated the NDR model using regression models. We used the x solved trendline equation $x = (y-b)/m$ (where b is intercept, and m is slope). Intercept and slope values were taken for 25m resolution values, with the intercept being 0.31 for both N and P, and slope 0.67 and 0.49 for N and P respectively. We then calculated the Mean Absolute Percentage Error for each model instance.

Software

The Nutrient Delivery Ratio model as part of the InVEST Software Platform developed by the Natural Capital Project (Sharp *et al.*, 2018). The model was run using the GUI version of [InVEST](#) (version 3.9.0), though the steps can also be replicated using the InVEST Python package (version 3.9.2), which is outside the scope of this document (this additional method can be explored [here](#) and at the [Python Package Index: PyPi](#)). Many of the inputs are spatial in nature (see Table 4 and Model specifications section), these inputs were manually processed using GIS software, for example QGIS (<https://qgis.org/>).

Linking the model outputs to indicators

The outputs of this model (N and P export) are related to Gross Nutrient balance for nitrogen and phosphorus. The InVEST NDR model does not account for emissions into the atmosphere, and is limited to the retention in land/crop types to fresher water systems;

'pollution swapping' is not considered. Therefore this model contributes towards the gross calculation of nutrient balance, but does not have the function to calculate it independently.

Model settings

Apart from the spatial model inputs, there are a variety of model input values that were kept constant in the model unless specified elsewhere. These were set at values according to those from Redhead et al. (2018): Threshold Flow Accumulation (1000), Borselli k Parameter (2), Subsurface Critical Length (200), and Subsurface Maximum Retention Efficient (0.8).

Assessment

Validation has been carried out by Redhead et al. (2018) for the UK. The model was found to perform well for relative magnitude of nutrient export, though absolute values of modelled nutrient export showed large percentage differences from validation data (Redhead et al., 2018).

Model specifications for each case study are available in the model factsheet in the appendix.

3.4.2. Case study example

Humber, UK

Figure 14 shows modelled nitrogen export and Figure 15 modelled phosphorus export under the two scenarios for the Humber, UK. Model performance from validation by Redhead et al. (2018) showed that the absolute values from the InVEST NDR model should be treated with caution; though the model is useful in demonstrating relative differences (Redhead, et al. 2018). Current scenario Mean Absolute Percentage Error (MAPE) was 40.45 for N and 53.78 for P, and for the no AEM scenario MAPE was 32.92 for N and 50.80 for P. Change maps between both scenarios for both pollutants (Figures 16 and 17) show that the implementation of AEMs demonstrated a decrease in total exported pollutants.

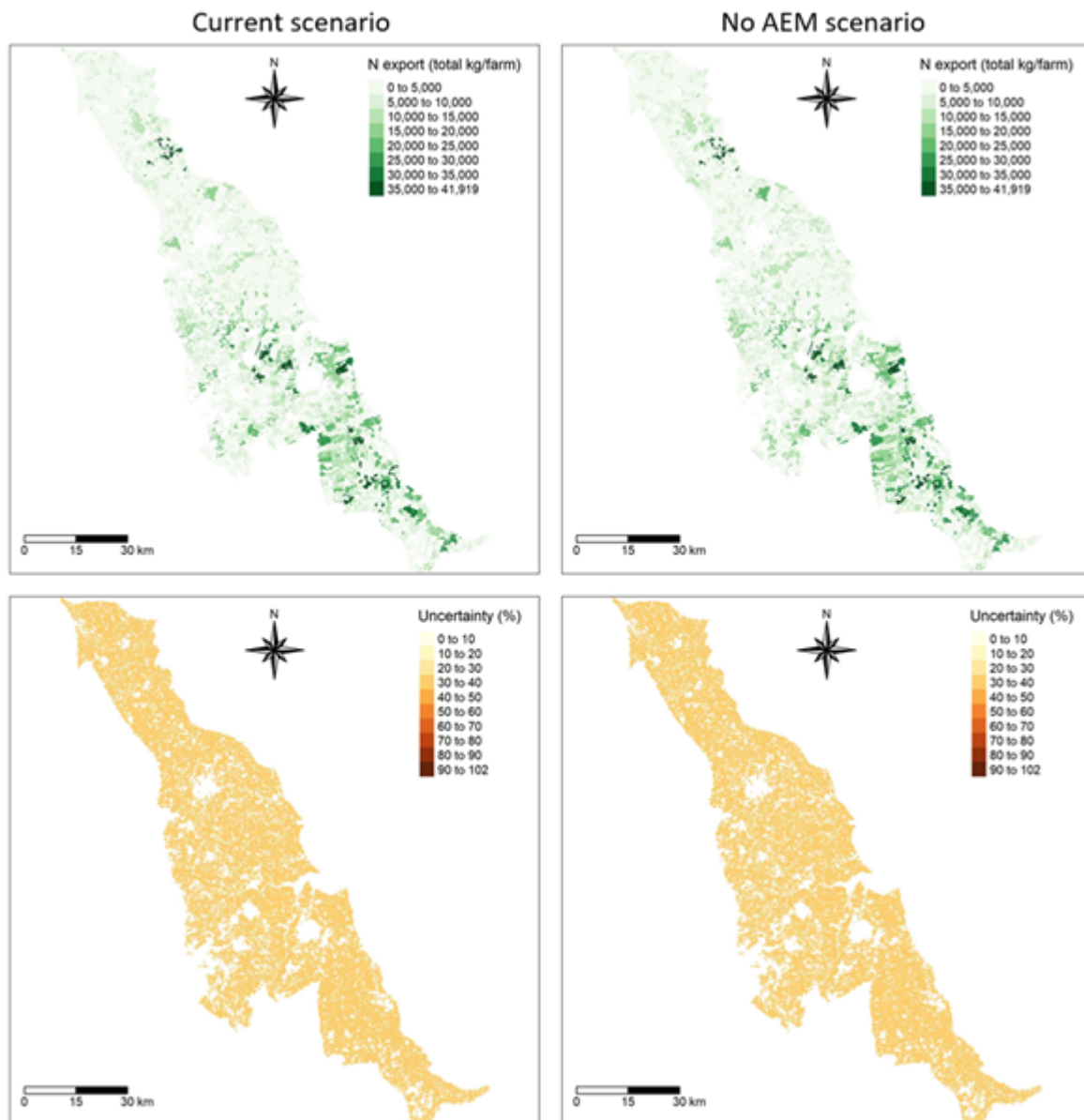


Figure 14: Modelled total nitrogen (N) export from farms to stream (kg/y) as a measure of N pollution from farms, with related uncertainty maps in the Humber, UK. The latter are calculated as percentage differences between modelled and validation regression corrected values (see uncertainty section earlier). Current scenario MAPE = 40.45, and No AEM scenario MAPE = 32.92. The maps on the left refer to the current scenario, i.e. the land-use conditions as of 2019; the maps on the right refer to the “no AEM scenario”, in which all modelled AEM groups described earlier are removed from the landscape.

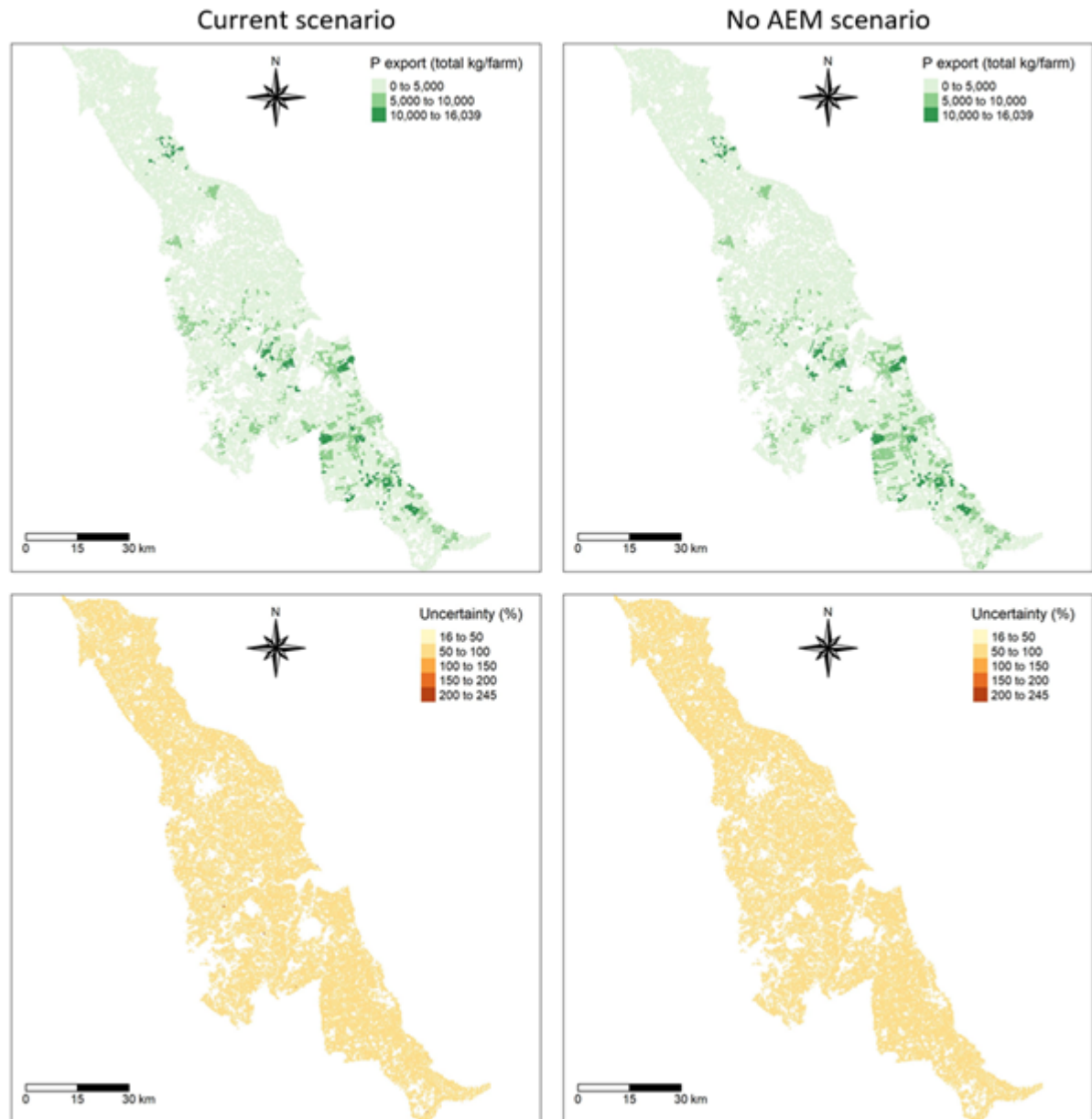


Figure 15: Modelled total phosphorus (P) export from farms to stream (kg/y) as a measure of P pollution from farms, with related uncertainty maps in the Humber, UK. The latter are calculated as percentage differences between modelled and validation regression corrected values (see uncertainty section earlier). Current scenario MAPE = 53.78, and No AEM scenario MAPE = 50.80. The maps on the left refer to the current scenario, i.e. the land-use conditions as of 2019; the maps on the right refer to the “no AEM scenario”, in which all modelled AEM groups described earlier are removed from the landscape.

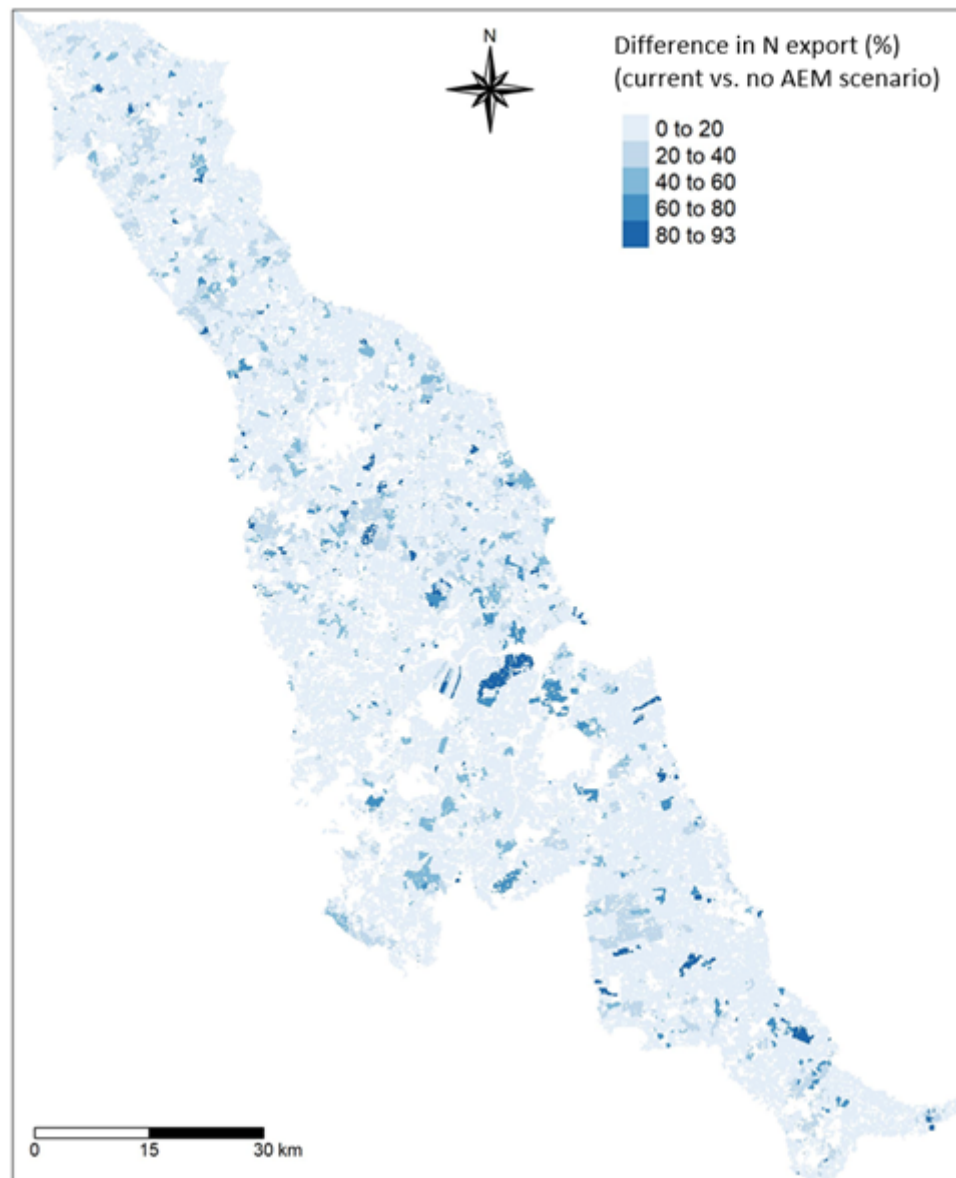


Figure 16: Difference in N export (%) between the current and the no AEM scenario in the Humber, UK. All values are positive and the darker blue mark areas in which N export is higher when AEM are not implemented.

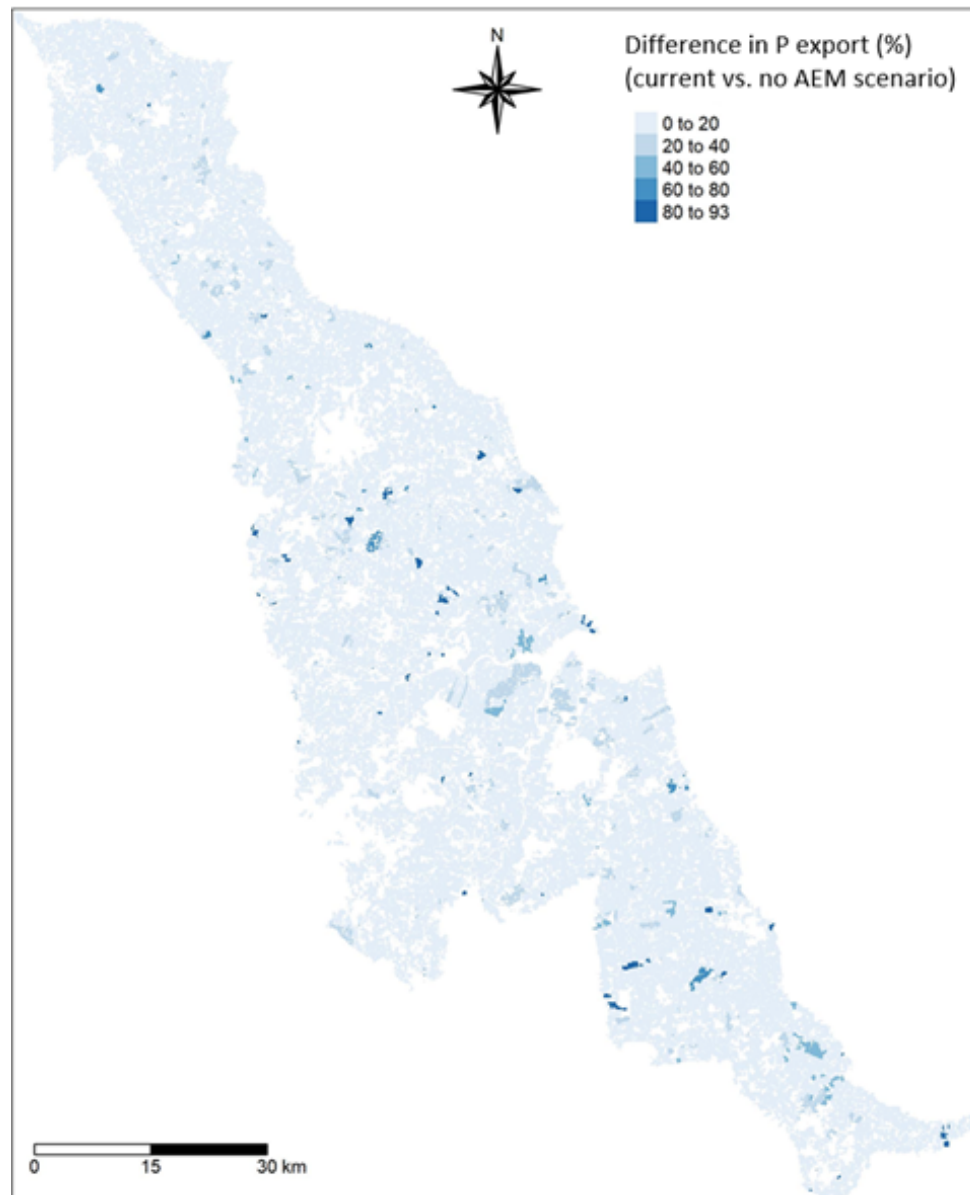


Figure 17: Difference in P export (%) between the current and the no AEM scenario in the Humber, UK. All values are positive and the darker blue mark areas in which P export is higher when AEM are not implemented.

3.5. Socio-economic effects

3.5.1. Model description

Authorship

Contact: *g.ziv@leeds.ac.uk

Authorship: George Breckenridge (model programming, analysis, writeup), Guy Ziv* (conceptual framing, analysis concept, data acquisition), Arjan Gosal (supervision), Anne Paulus (DEU data guidance, model interaction), Katharina Schneider (CZE data guidance, model interaction), Tomáš Václavík (CZE data/crop classification guidance), Stephanie Roilo (supervision).

Model name

Model of the socio-economic effects of the adoption of agri-environmental schemes.

Model objective

The main objective of the model is to estimate how the adoption of agri-environmental schemes (AES) affects the estimated total income per farm (per worker) in different case studies across Europe.

Model output

The model output comprises the estimated change in total income between adoption/non-adoption of AES scenarios, by calculating the change in estimated **Farm Net Value Added ('FNVA')** for a given year per farm. These results can then be aggregated.

Data specifications

For each BESTMAP case study region:

- 'IACS/LPIS' data containing field-level information on crop type, field area (.shp), AES uptake at group level of detail (i.e. 'cover crops' / 'maintaining grassland' etc.).
- Output data from BESTMAP food and fodder model containing farm-level estimated standard output values (in Euros) for overall income from crops, both for AES non-adoption scenario ('so') and, where applied, for AES adoption ('so_mod'). As stated, in turn this calculation used NUTS1-specific EUROSTAT (2021) standard output coefficients and scientific literature to achieve these estimates.
- FADN microdata on selected variables (mostly continuous and area-based) for 2017. Full input selection (to be filtered for all-0s/NaN columns, weighted by 'SYS02', then filtered for multicollinearity, then feature-selected using Lasso() regression model): ['SE005','SE025','SE030','SE035','SE041','SE042','SE046','SE050','SE054','SE055','SE065','SE071','SE073','SE074','SE075','AGE','TF8','SEX','REGION','ALTITUDE','ANC'].
- Expert judgement from agricultural academics on available AES schemes and their typical/distinct payment rates for the BESTMAP region, in Euros per ha per year, across these types/'groupings' of AES: 'cover crops', 'flower strips', 'maintaining grassland', 'converting arable land to grassland'.

- Expert judgement from agricultural academics on crop type classification in given local regions according to typical purposes of crops / crop classifications. Judgements are applied for AWU regression parameterization from 'IACS/LPIS' data.

Assumptions

In the calculation of FNVA it is assumed that other components do not change between the scenarios of AES adoption and AES non-adoption. It is assumed that all information from 'IACS/LPIS' data on crop land use and AES uptake is accurate/complete.

Algorithms and workflow

Farm Net Value Added (FNVA) is a new statistical definition of the indicator C.27 in the approved [Context and Indicators Impact guidelines](#) for the new Performance Monitoring and Evaluation Framework (PMEF) of the post-2020 EU Common Agricultural Policy (CAP), officially adopted in December 2021. It is absent from the older CMEF framework for CAP.

Farm Net Value Added (FNVA) is calculated by formula (European Commission, 2022: 54):

FNVA = Value of agricultural production + Pillar I and Pillar II payments + any national subsidies + VAT balance - intermediate consumption - farm taxes (excluding income taxes) - depreciation.

FNVA is standardised through Annual Work Units (AWU). FNVA is calculated per AWU *“in order to take into account the differences in the scale of farms and to obtain a better measure of the productivity of the agricultural workforce”* (European Commission, 2022: 54).

Our viable farm income model estimates the difference in Farm Net Value Added ('FNVA') between the scenarios of adoption / non-adoption of AES per farm in the European context.

The *net* contribution of AES adoption to FNVA is therefore deduced through calculating:

(Value of agricultural production + Pillar I and Pillar II payments + any national subsidies + VAT balance - intermediate consumption - farm taxes (excluding income taxes) - depreciation) with AES payments/yield changes

-

(Value of agricultural production + Pillar I and Pillar II payments + any national subsidies + VAT balance - intermediate consumption - farm taxes (excluding income taxes) - depreciation) without AES payments/yield changes.

Our estimation of FNVA is partial insofar as we do not incorporate FNVA components other than *Value of Agricultural Production* and *Pillar II payments*. We assume that other aspects do not change between the scenarios of AES adoption and AES non-adoption.

First, we take the output of the BESTMAP food and fodder model, which for a given BESTMAP case study region outputs a table of all unique farms and their associated modelled standard output values (in Euros). These are values rather than coefficients as they are understood here to represent the total modelled net income for an individual farm. These are calculated both for AES non-adoption ('so') and, where applied, for AES adoption ('so_mod'), with the modelling for AES adoption capturing the changes in crop coverage and respective yield implications in the calculations. This is the case though *only* on those farms with which AES is applied in real-life: otherwise, the value of 'so_mod' is always equal to the value for 'so'. These modelled estimations of the *Value of Agricultural Production* component of FNVA are derived from AES uptake information available in 'IACS/LPIS', as well as EUROSTAT (2021) data on NUTS1 Standard Output coefficients.

Second, the value of Pillar II payments is initially determined through research into local Agri-Environmental Schemes (AES) using expert knowledge by local agricultural researchers, in the case of the 5 BESTMAP Case Study regions (see Table 5 below). Difficulties were experienced in reconciling the complex agri-environment scheme policy landscape with this generalised schematic, although all values were based on expert judgement and/or statistical summarisation. We then estimate the modelled Pillar II payments due (AES) by summing up the areas of modelled AES adoption (at the field level from 'IACS/LPIS' data) multiplied by their researched payment rates per ha (Table 5).

Table 5: Data on AES payment rates per BESTMAP Case Study Region. Data Source: Consultation with subject/country experts by/within BESTMAP.

BESTMAP CS Region	Flower strips (inc. buffers) (/ha per annum)	Catch/cover crops (/ha per annum)	Maintaining Grassland (/ha per annum)	Conversion of arable land to grassland (/ha permanent)
UK	(AB8): €615.59	(SW6): €130.20	(GS6, ~GS2/GS9): €207.86	(SW7): €355.19
DE	(AL5c): €835.00	(AL4): €78.00	(GL5a): €330.00	-
CZ	(10.1.6): €591.00	- (Not as AES in CZ)	(10.1.4 Ošetřování travních porostů): €180.00	(10.1.5 Zatrávňování orné půdy): €400.00 (no permanent AES)
ES	-	(~AES_367): €95.92 (variable so split by crop group in model)	(~AES_363): €280.80 (~AES_368): €30.00	-
RS	~€662.00	~€287.00	~€136.00	~€551.00

Finally, we calculate an estimation for AWU from a model trained using FADN microdata. Our model for the socio-economic indicator uses FADN microdata to determine a linear regression model which can, for each given area, determine the variables from FADN which best account for the variance in farm labour as expressed through Annual Work Units (AWU). This FADN data is filtered to include only data from within NUTS2 and/or NUTS3 areas overlapping with the BESTMAP Case Study regions (see Ziv et al., 2020), unless the overlap was clearly not meaningful and therefore would have likely distorted the results more from including the NUTS region than from excluding it. With FADN data the weighting estimated by the 'SYS02' column representing 'farms represented' was used at all stages from collinearity analysis onwards to calculate appropriate relationships between variables in the FADN data. This was accounted for in practical terms by replicating the rows within the FADN table as many times as the 'rounded down' integer value cast from SYS02.

In the first instance, FADN columns with entirely 0.0 values / NaN values were removed from the analysis. Then, an algorithm was developed to automatically remove extreme levels of multicollinearity, so as to address the assumption that variables are truly independent. Variables were automatically removed if they had an absolute Pearson correlation coefficient ('r') greater than 0.8 with another independent variable and generated a lower relative R² value when modelled as a single input variable against SE010 (Total Labour in AWU) in a bivariate linear regression model. This process occurred for all (unique) sets of collinear variables identified in the [corr\(\) correlation matrix](#) until a list of unique 'variables to remove' were determined for that iteration. This entire process iterated until no unique sets of collinear variables remained. The value of this approach beyond automatically removing all variables with collinearities was that despite a higher computational demand, particularly

valuable explanatory variables could still remain in the model as (truly) independent entities so long as they only presented collinearities with less individually-explanatory input variables across the weighted FADN table.

For each case study area a [feature-selecting Lasso regression model](#) is then fitted which runs by aiming to reduce as many variable coefficients as possible to 0, leaving only significant features in the model. Continuous variables are [normalized using StandardScaler\(\)](#) and categorical variables are [encoded using the OneHotEncoder\(\) function](#) to ensure suitable incorporation into this first Lasso regression model. At this point, the selected variables from each case study were then input as Fixed Effects into a [Linear Mixed Effects Regression \(LMER\) Model](#), with selected categorical variables included as the declared Random Effects, in part to see if we can further improve the predictability of AWU (as measured through AIC). Although this was a worthwhile methodological exploration, it was ultimately determined that this farm income model would instead rely on the outputs of re-running a [statsmodel linear regression](#) using the feature-selected variables from the Lasso regression model output.

Having derived this statistical relationship to AWU from FADN variables, we can then return exclusively to data from 'IACS/LPIS' in order to build a socio-economic indicator through modelling change in Farm Net Value Added (FNVA) according to adoption/non-adoption of AES, as standardised through Annual Work Units (AWU). By taking, wherever pragmatically possible, variables of equivalent meaning from the 'IACS/LPIS' data to those selected in the FADN model for AWU, we are then able to use the estimated model for predicting AWU derived from FADN microdata and thenceforth deduce a more accurate estimate for AWU per farm in the 'IACS/LPIS' data across European places in order to complete our methodology for estimating (standardised) FNVA in both adoption scenarios. This estimate of AWU for standardisation was 'dynamic' insofar as it responded, in some instances, to changes in the adoption scenario when calculating proxy values from 'IACS/LPIS' to put into the AWU regression. As such, on a given individual farm, the estimated AWU value used to standardise estimations of FNVA was different according to if AES were being adopted.

Once an AWU-standardised value for the *Value of Agricultural Production* is therefore calculated for both adoption scenarios, the estimated percentage change in FNVA between AES non-adoption and AES adoption is calculated per farm. Tabular outputs from the model are at this point de-identified (assuming a sufficient sample of individual farms was input, e.g. $n \geq 10$) though they are also then typically aggregated as summary statistics to indicate the overall effect of AES adoption on farmer incomes across a given geographical region. All boxplot figures were generated using the *matplotlib* (Hunter, 2007) graphics environment in Python, with both *matplotlib* and *seaborn* (Waskom, 2021) libraries used for the histogram and scatterplot figures.

Model validation

Country-level EU data for validation assessments for farm income per AWU was identified to be available as C.25/C.26 in the old CAP CMEF framework, the closest available metric. These are currently available at:

1. <https://agridata.ec.europa.eu/extensions/IndicatorsSectorial/AgriFactorIncome.html> [Accessed 24/05/22]. C.25 in CMEF.
2. <https://agridata.ec.europa.eu/extensions/IndicatorsSectorial/AgriculturalEntrepreneurialIncome.html> [Accessed 24/05/22]. C.26 in CMEF.

Although a model validation exercise wasn't systematically conducted, using these statistics facilitates a qualitative evaluation of the model outputs, indicating that our model outputs in

the test case study are within the correct expected magnitude (~5 pre-decimal figures i.e. €10 000s) for income per AWU in late-2010s EU agricultural settings.

In some respects, it is actually unsurprising that our average *Value of Agricultural Production* estimate value would present disparities to the value contained here as on top of being a separate, new CAP indicator, not covered by the old CMEF indicator framework directly, our modelling also did not incorporate many of the stated components deducting from the total income figure in FNVA or similar metrics, including intermediate consumption, farm taxes and asset depreciation (European Commission, 2022: 54).

Data from FADN in Total labour output (SE010) can be used similarly to indicate reasonable bounds for estimating AWU at the farm level, with our model outputs appearing to roughly align, indicating efforts to estimate AWU using 'IACS/LPIS' data were acceptably accurate.

Uncertainty analysis

Uncertainty is relatively high for this farm income model, as it is a result of the outputs of the BESTMAP food and fodder model, as well as for being the outcome of the application of a linear regression from one dataset within the available ('best-fit') fields from another.

In the first instance the regression model for SE010 'Total labour input' (AWU) for CZE shows excellent ($R^2 > 0.85$) but nevertheless not perfect performance, despite best efforts to use a feature-selecting Lasso model to determine which variables should be included after excluding multicollinear columns. This is inevitable but clearly represents uncertainty and the model may be able to generate different levels of explainability in other European contexts.

The model specified below, from the Czech FADN region ($n = 3,350$ rows after weighting), produced an Adjusted R^2 value = 0.862, the same as its unadjusted R^2 value = 0.862:

$$SE010 = 0.7986 + 0.0097(SE005) + 0.1178(SE054) + 0.0212(SE071)$$

Here, the equal R^2 and Adjusted R^2 values (to 3 d.p.) and the large sample size indicate a relatively low risk of overfitting for a regional agricultural study.

In the application of this regression model to 'IACS/LPIS' data, there is inherent uncertainty introduced into the accuracy of the result, owing to the difficulty in accurately and consistently estimating an FADN category using 'IACS/LPIS' fields. In some cases values were unavailable, weren't readily available, or had uncertain degrees of crossover between categories and classifications.

As for measures to counter uncertainty, the uncertainty in the statistical model for AWU was countered through repeated, iterative efforts to improve the regression scores, including the Adjusted R^2 value. This included passing in a large number of both continuous and categorical variables, using feature-selection techniques, and experimenting with running more complicated models. In the case of classifications, avoiding unacceptable levels of uncertainty was helped through referencing the May 2019 European Commission (2019) Definitions for FADN wherever possible. Consulting regularly with local experts internal to BESTMAP also reduced uncertainties arising from classification issues between data sets, case study regions, and languages.

Software

Software: Python v3.7.11 (Python, 2018), using Geopandas 0.9.0 (Jordahl et al., 2021), sklearn 1.0.1 (cited as Pedregosa et al., 2011), matplotlib 3.4.3 (Hunter, 2007) and seaborn 0.11.2 (Waskom, 2021).

Code availability: Code to be made available via the UFZ GitLab repository.

Data availability: Data not publicly available or on request from authors. FADN microdata access available from European Commission DG Agri subject to specific request. 'IACS/LPIS' data access available from national and regional governments subject to specific request.

Linking the model outputs to indicators

The model results can be linked to the following policy indicator in European Commission (2022) CAP PMEF:

C.27 I.4 Supporting viable farm income / I.5 Contributing to territorial balance (p.54-56):
'Farm income by type of farming, region, by farm size, in areas facing natural and other specific constraints'.

Case study example: South Moravia, Czech Republic (FNVA; 2017)

Data specification: *South Moravia, Czech Republic (FNVA; 2017)*

The application of the socio-economic model to the BESTMAP case study region of South Moravia in Czech Republic used annual administrative data from 2017 at the field/farm scale. 'IACS/LPIS' data for South Moravia for 2015-2019 was sourced from the Ministry of Agriculture of the Czech Republic, though only 2017 data was used for consistency. FADN microdata for Czech Republic (FADN region 745) for 2017 was accessed from the Directorate-General for Agriculture and Rural Development at the European Commission.

As crop type and AES uptake were arranged in a complex way in the Czech 'IACS/LPIS' data, further pre-processing completed by the BESTMAP food and fodder model team was used in the implementation of the farm income algorithm. This involved the use of the *input file* to the food and fodder model, detailing crop use at the field-level (otherwise usually taken from the 'IACS/LPIS' file(s)), in addition to the routine use of the *output file* containing information on the ordinary and adjusted standard output values according to AES uptake.

Investigating biases: *South Moravia, Czech Republic (FNVA; 2017)*

Data from South Moravia posed challenges and presented potential biases. Firstly this was owing to the relatively high number of records output from the food and fodder model which were unable to determine standard output values for Czech farms. Unfortunately this meant that in 446 of the 1104 unique farms in South Moravia results for farm income could not be produced as the inputs were not available. In many other cases farms were not recorded as adopting AES in ground-truth data and therefore could not be represented in our results, which depend upon real distinction between the AES non-adoption and adoption scenarios within the input data format. As such, only 257 (23.28% to 2 d.p.) farms could be included.

As stated, such exclusions in the South Moravia case study occurred *in part* due to methodological choices and data issues in the food and fodder model, which was applied in the Czech Republic to ensure consistency between BESTMAP case studies. Firstly, the use of the WOFOST simulation predictions (Hristov et al., 2020) to generate yield predictions for six crops (maize, sugar beet, wheat, sunflower, winter rapeseed, spring barley), in addition to the Czech-specific ReSteP yield model for permanent and temporary grassland (VÚMOP, 2015), meant that whilst many crop types were catered for, many were also left without the yield information necessary for income modelling. Secondly, in the case of the Czech Republic, an abnormal number of crop entries in the EUROSTAT data on standard output

coefficients contained 0/NaN values which also prevented *Values of Agricultural Production* from being calculated with EUROSTAT (2021) coefficients.

To informally understand the biases these exclusions may introduce, the nature and spatial patterns of fields for farmers with no income estimation were examined in Python and GIS software. Firstly, a CSV file was created with the farm IDs of farms which were unable to be included in the final results. This generated a file which could be joined - as a delimited text layer - to the field-level South Moravia 'IACS/LPIS' shapefile in QGIS, with 'not null rows' highlighted for visual examination. It became immediately apparent that the majority of total field area did not belong to this set of excluded farm IDs, despite this set of IDs representing 76.72% of all farms in the South Moravia case study region. This initial impression was supported by statistical evidence that both the mean and median average field size was lower for excluded fields (4.38 ha, 0.61 ha respectively) than for all fields in the region (6.01 ha, 0.91 ha respectively), and that 66.77% (2 d.p.) of total field area in South Moravia was used in the final results. So, in conclusion, the fields attached to farmer IDs ('ID_UZ') whose income cannot be estimated represent in fact the minority of fields, as well as disproportionately representing smaller area fields. All this said, it is nevertheless true that a slim majority of fields in South Moravia were excluded from the results due to being associated with an excluded farmer: 53.84% (to 2 d.p.). Both the largest and the smallest fields were excluded from the analysis so the range of field sizes affected was as broad as theoretically possible. Returning to the findings of the visual inspection, it was clear that although many fields were scattered across the region, many also clustered together (as may be expected given fields are excluded on the basis of a common owner, and usually owned/managed locally in any case). Regions with higher than average presence of excluded fields were overlaid across an OpenStreetMap (2022) base layer which illustrated that clusters were not consistently found in urban centres. Although there was a degree of spatial grouping amongst *excluded* fields, the same could not be said for the remaining *included* fields, as they formed a larger part of the landscape, which was itself discontinuously represented across space by the vector shapefile fields in existence.

As such, it is concluded that it is more likely than otherwise that the biases introduced by these (involuntary) exclusions were disproportionately on groups of small holdings, and that they didn't prevent the majority of agricultural land (and for that matter, probably agricultural income) from being represented in the farm income analysis. The results of this farm income model application are therefore expected to be broadly representative of South Moravia. The code for this investigation into spatial biases is included in the main code file as an appendix.

Results: South Moravia, Czech Republic (FNVA; 2017)

Results for the demonstrative implementation of the BESTMAP socio-economic model are represented in Table 6, Figure 18, Figure 19 and Figure 20. They illustrate the FNVA value as standardised per Annual Work Unit (AWU) for South Moravia, Czech Republic, using 2017 data, for those farms (n = 257) for which income for both scenarios could be modelled.

The results indicate that the aggregate impact of AES adoption in this region is a major increase in net farm income, with a mean percent change of +67.72% (to 2 d.p.). This relates to mean average *Value of Agricultural Production* figures of €12,325.00 for non-adoption of AES, in comparison to €13,295.69 in the scenario of AES adoption. On average, therefore, it can be deduced that the income from AES subsidies estimated by this analysis is more than compensating sufficiently for the changes in land use and crop yield that are needed to fulfil, or a consequence of, agri-environment scheme requirements. Interestingly, the median average for non-adoption stands at the far lower level of €2,042.95, compared to €3,566.74 in the scenario of AES adoption.

The median average is many times closer to the minimum *Value of Agricultural Production* figures (€17.22, €33.14) than it is to the maximum figures which stood at €89,290.60 and €89,355.18 for non-adoption/adoption of AES respectively (see Table 6). A large range of values for the *Value of Agricultural Production* were predicted here, even within the single region of South Moravia, and despite the possible biases from excluding smaller holdings. Similarly, a large range of estimated percent changes in Farm Net Value Added (FNVA) are also predicted, ranging from a minimum value of -64.93% to a maximum value of +194.27%.

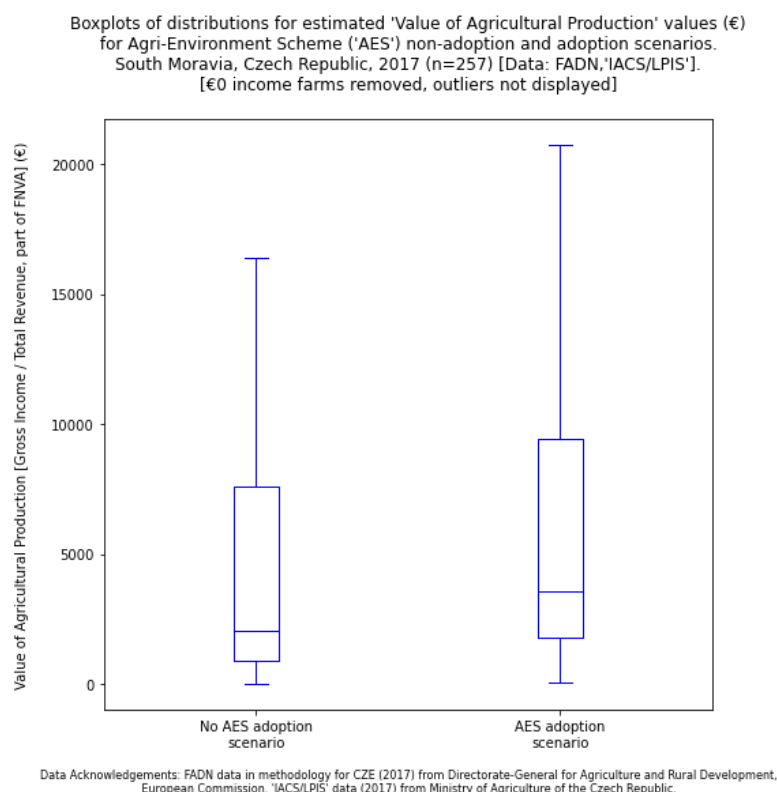
Given the *major* percentage increase, *both* in mean and median average terms, it was investigated whether unrealistic farm receipts were driving this summary statistic, as investigated by Figure 20. At various thresholds for inclusion on the basis of income levels in the scenario of AES non-adoption it was recorded the mean average value of estimated percent changes in FNVA, to examine this relationship between a selected sub-sample and aggregate results. Figure 20 reports results of the mean average FNVA change upon AES adoption statistic at the increasing thresholds of every €200 between €0 and €15,000. The results evidence a strong non-linear relationship between the size of the farm before AES adoption and the proportion of FNVA (income) increase reported overall (despite AES subsidy payments being calculated per ha). The mean percent change drops to below +30% once the lower half of the farms are excluded, as per the sequential Q1/Q2/Q3 grey lines shown. These results indicate that the effect of AES adoption on income is highly associated with levels of pre-AES adoption income, possibly due to similar levels of area being dedicated to the AES schemes irrespective of the size of the farm, which would naturally produce higher levels of proportionate income increase in farms with a smaller overall size.

Table 6: Aggregated summary statistics (all to 2 d.p.) for farm-level FNVA outputs, generated using [pandas.DataFrame.describe\(\)](#) (records with €0 for either AES scenarios removed), South Moravia, 2017.

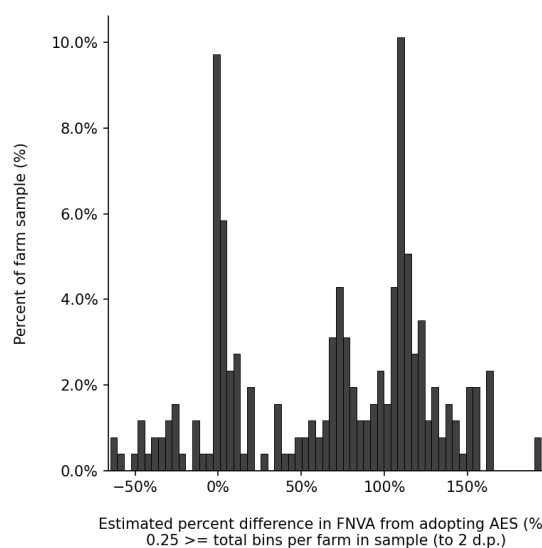
Summary statistics for 'Value of Agricultural Production' estimations in socio-economic model
South Moravia, Czech Republic, 2017 [Data: FADN, 'IACS/LPIS']
 [€0 income farms removed]

			Value of Agricultural Production (€)		Percent change
			No AES adoption	AES adoption	
summary	records	count	257	257	257
	average	mean	12325.00	13295.69	67.72
	variance	std	22604.38	22394.46	59.26
percentiles	min	0%	17.22	33.14	-64.93
	-	25%	864.13	1798.17	4.36
	median	50%	2042.95	3566.74	78.09
	-	75%	7608.46	9407.57	112.34
	max	100%	89290.60	89355.18	194.27

Data Acknowledgements: FADN data in methodology for ESP (2017) from Directorate-General for Agriculture and Rural Development, European Commission. 'IACS/LPIS' data (2017) is from Ministry of Agriculture of the Czech Republic.

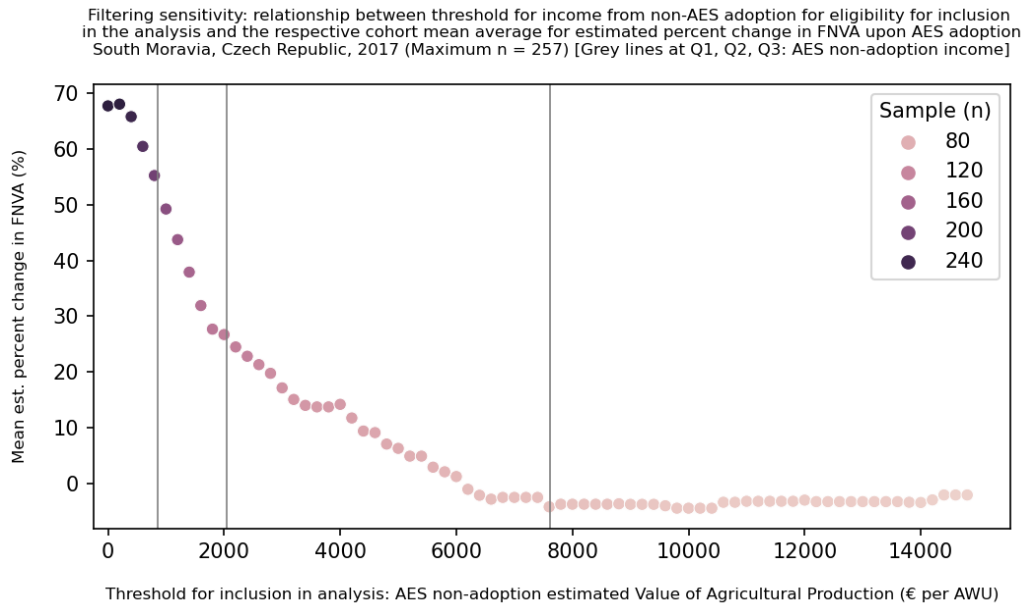
Figure 18: Boxplots of distributions for estimated FNVA, South Moravia, 2017.**Figure 19:** Histogram of distribution for farm-level *percentage difference* for FNVA between AES non-adoption and AES adoption, South Moravia, 2017.

Proportion of farm sample (n = 257) exhibiting (approximate) estimate percent difference in Farm Net Value Added ('FNVA', C.27 PMEF) from adopting AES. South Moravia, Czech Republic, 2017 [Data: FADN, 'IACS/LPIS']. [€0 income farms removed]



Data Acknowledgements: FADN data in methodology for CZE (2017) from Directorate-General for Agriculture and Rural Development, European Commission. 'IACS/LPIS' data (2017) from Ministry of Agriculture of the Czech Republic.

Figure 20: Scatterplot of relationship between sample inclusion threshold according to AES non-adoption income, and the cohort's respective mean average farm-level *percentage difference* for FNVA between AES non-adoption and AES adoption, South Moravia, 2017. [Data Acknowledgements: FADN for CZE (2017) from Directorate-General for Agriculture and Rural Development, European Commission. 'IACS/LPIS' data (2017) from Ministry of Agriculture of the Czech Republic.]



Specifications for other BESTMAP case study regions are currently under development and will in future be made available in the UFZ GitLab page (<https://git.ufz.de/>).

4. Obstacles and challenges

The first and major challenge that we encountered upon modelling agricultural policy impacts across several European countries was the significant access restrictions of the IACS/LPIS and the FADN datasets. Getting access to the IACS/LPIS and FADN data was a highly bureaucratic and time-consuming process, which delayed the start of the modelling tasks in several CS. Since the requests for IACS/LPIS data is still handled on a (sub)national level, the process had to be gone through multiple times and with different individual hold-ups and obstacles. While this lack of consistency and interoperability seems to have been acknowledged at EU level, e.g. through the funding of the Open-IACS Innovation Action (grant no 2018-EU-IA-0086; <https://open-iacs.eu/>), these initiatives have yet to bear fruit.

In addition, IACS/LPIS data in certain CSs are subject to strict data sharing agreements that prevent data sharing between project partners from different institutions and CSs. This meant that some modellers did not have access to data from other CSs and had to rely on other project staff for (pre-)processing of modelling input data based on IACS/LPIS. The interdependencies resulting from this situation posed an additional challenge for the timely provision of model results in all CSs. In addition to the difficulties at the CS level, requesting access to FADN data at the EU level was particularly difficult, resulting in delays to the development of the socio-economic model.

As planned from the beginning, the BESTMAP biodiversity and ES models were fitted on already available datasets, meaning that no fieldwork was performed nor additional data

collected for this purpose. We acknowledge that a tailored fieldwork or data collection, specifically designed to target fields and farms with/without AEM, would have allowed us a better, more robust assessment of AEM impacts on ESS and biodiversity; however, this was not possible within the resources available for the project. The search for high-quality, country or CS-level information to be used as input data for the models was thus also a tedious task, especially for models that heavily rely on parameters that have to be estimated from the literature (e.g. food and fodder model), that vary significantly across regions (e.g. water quality model), or for data that are collected and owned by third parties and are not freely available (e.g. biodiversity datasets). A major obstacle was the lack of area-based (i.e. field level) yield data, which is not systematically collected at the CS level or elsewhere. The ongoing war in Ukraine and the accompanying discussions on food security in Europe and elsewhere have clearly shown that the lack of centrally collected yield data is a major blind spot preventing research to develop alternative scenarios for agricultural production in the EU. Moreover, there is little scientific literature on the impact of some AEMs on yields, making this a priority topic for future research.

The different structure of the IACS/LPIS data in each CS meant that the models had to be adapted from CS to CS to accommodate the variable input data while providing comparable results (see “D1.3 Guidelines and protocols for harmonising activities in each CS” and “D3.1 Case study base layer dataset for each of the case studies” for how the data were collected, harmonised and stored for the modelling task).

5. Outlook

The biodiversity, ESS and socio-economic models are a central tool in the broader framework of the BESTMAP project. Indeed, there are several interdependencies between WP3 and the various work packages in the project. The results of the biophysical models provide the input data for many tasks in WP4, which includes a trade-off and synergy analysis across ESS, biodiversity and socio-economic outputs within and across CS. Differences in ESS, biodiversity and socio-economic outputs' intensities, derived from the models, will also be analysed across the various FSAs developed in WP3. WP4 is also responsible for mapping ESS/biodiversity/socioeconomic bundles into policy indicators, and relies on the spatially-explicit model results presented in this deliverable for it. The indicators will be visualised either via the interactive dashboard, in which different policy scenarios and their effects will be explored, or in other ways. Indeed, preliminary model results have already been presented in a first prototype of the BESTMAP dashboard in co-design sessions with stakeholders in each of the five CS. Moreover, the policy indicators will be upscaled from CS to European level based on the FSAs and the FADN data in WP5. The agent-based models will also be directly linked to the biophysical models, as the AEM adoption scenarios resulting from ABM models will be used as inputs for the biophysical models to directly estimate environmental impacts of farmers' decision-making.

The models of WP3 also feed directly into Task 5.1, and model results from each of the models at the CS level will feed into analysis at the European level (Task 5.2), that considers FSA and FADN data, and bioclimatic variables that are relevant to each particular ESS and biodiversity. This will enable predictions of ESS and biodiversity across the EU, together with an indicator of the confidence of those predictions based on a refined transferability analysis. Therefore, the EU-wide ESS results will be based on the model outputs from WP3.

6. Acknowledgements

We thank all data providers for the data provided to run the modelling tasks; these are listed in each of the models' factsheets.

7. References

Abdalla, M., Hastings, A., Cheng, K., Yue, Q., Chadwick, D., Espenberg, M., ... & Smith, P. (2019). A critical review of the impacts of cover crops on nitrogen leaching, net greenhouse gas balance and crop productivity. *Global change biology*, 25(8), 2530-2543.

Araújo, M. B., & New, M. (2007). Ensemble forecasting of species distributions. *Trends in ecology & evolution*, 22(1), 42-47.

Bryant, B. P., Borsuk, M. E., Hamel, P., Oleson, K. L., Schulp, C. J. E., & Willcock, S. (2018). Transparent and feasible uncertainty assessment adds value to applied ecosystem services modeling. *Ecosystem Services*, 33, 103-109.

Buisson, L., Thuiller, W., Casajus, N., Lek, S., & Grenouillet, G. (2010). Uncertainty in ensemble forecasting of species distribution. *Global Change Biology*, 16(4), 1145-1157.

Crystal-Ornelas, R., Thapa, R., & Tully, K. L. (2021). Soil organic carbon is affected by organic amendments, conservation tillage, and cover cropping in organic farming systems: A meta-analysis. *Agriculture, Ecosystems & Environment*, 312, 107356.

De Wit, A., Boogaard, H., Fumagalli, D., Janssen, S., Knapen, R., Kraalingen, D. van, Supit, I., Wijnjaart, R. van der and Diepen, K. van (2019): 25 years of the WOFOST cropping systems model. *Agricultural systems*, vol. 168, 154-167.

European Commission (2019): Definitions of Variables used in FADN standard results. COMMITTEE FOR THE FARM ACCOUNTANCY DATA NETWORK (FADN). Directorate-General for Agriculture and Rural Development, European Commission.

European Commission (2021). CMEF 2014-2020 - Context indicators (update December 2021)
https://ec.europa.eu/info/sites/default/files/food-farming-fisheries/key_policies/documents/context-indicator-fiches_en.pdf. Last accessed on 18th May 2022.

European Commission (2022): Context and Impact indicators. CAP Performance Monitoring and Evaluation Framework. Directorate-General for Agriculture and Rural Development, European Commission. Available at:
https://ec.europa.eu/info/sites/default/files/food-farming-fisheries/key_policies/documents/pmef-context-impact-indicators_en.pdf. Last accessed 27th May 2022.

EUROSTAT (2021): Standard output coefficients. Available at:
<https://ec.europa.eu/eurostat/web/agriculture/data/ancillary-data>. Last accessed 18th May 2022.

Eurostat (2022): Agricultural factor income per annual work unit (AWU) (source: Eurostat, DG AGRI) (sdg_02_20). ESMS Indicator Profile (ESMS-IP). Available at:
https://ec.europa.eu/eurostat/cache/metadata/en/sdg_02_20_esmsip2.htm. Last accessed 18th May 2022.

Fletcher, R., & Fortin, M. (2018). *Spatial ecology and conservation modeling*. Springer International Publishing.

Gattinger, A., Muller, A., Haeni, M., Skinner, C., Fliessbach, A., Buchmann, N., Mäder, P., Stolze, M., Smith, P., Scialabba, N.E.-H., Niggli, U. (2012). Enhanced top soil carbon stocks under organic farming. *Proc. Natl. Acad. Sci. USA*, 109 (2012), pp. 18226-18231.

Goidts, E., & van Wesemael, B. (2007). Regional assessment of soil organic carbon changes under agriculture in Southern Belgium (1955–2005). *Geoderma*, 141(3-4), 341-354.

Gregorich, E. G., Drury, C. F., & Baldock, J. A. (2001). Changes in soil carbon under long-term maize in monoculture and legume-based rotation. *Canadian journal of soil science*, 81(1), 21-31.

Hristov, J., Toreti, A., Perez Dominguez, I., Dentener, F., Fellmann, T., Elleby, C., Ceglar, A., Fumagalli, D., Niemeyer, S., Cerrani, I., Panarello, L. and Bratu, M. (2020): Analysis of climate change impacts on EU agriculture by 2050. EUR 30078 EN, Publications Office of the European Union, Luxembourg, ISBN 978-92-76-10617-3, doi:10.2760/121115, JRC119632.

Hunter, J. D. (2007): "Matplotlib: A 2D Graphics Environment". Computing in Science & Engineering, vol. 9, no. 3, pp. 90-95, doi: 10.1109/MCSE.2007.55.

Jordahl, K., Van den Bossche, J., Fleischmann, M., McBride, J., Wasserman, J., Gerard, J., et al. (2021): *geopandas/geopandas: v0.9.0*. <https://doi.org/10.5281/zenodo.4569086>.

Jian, J., Du, X., and Stewart, R.D. (2020): A database for global soil health assessment. *Sci Data*, vol. 7(16).

Ledo, A., Smith, P., Zerihun, A., Whitaker, J., Vicente-Vicente, J. L., Qin, Z., ... & Hillier, J. (2020). Changes in soil organic carbon under perennial crops. *Global change biology*, 26(7), 4158-4168.

Lorenz, K. and Lal, R. (2016). Chapter Three - Environmental Impact of Organic Agriculture, Editor(s): Sparks D. L., *Advances in Agronomy*, Academic Press, Volume 139, Pages 99-152.

Martens, D.A., Reedy, T.E. and Lewis, D.T. (2004), Soil organic carbon content and composition of 130-year crop, pasture and forest land-use managements. *Global Change Biology*, 10: 65-78.

Mondelaers, K., Aertsens, J. and Van Huylenbroeck, G. (2009), "A meta-analysis of the differences in environmental impacts between organic and conventional farming", *British Food Journal*, Vol. 111 No. 10, pp. 1098-1119.

OpenStreetMap (2022): OpenStreetMap: About. Available at: <https://www.openstreetmap.org/about>. Last accessed 27th May 2022.

Pedregosa, Fabian, Gaël Varoquaux, Alexandre Gramfort, Vincent Michel, Bertrand Thirion, Olivier Grisel, Mathieu Blondel et al. (2011): "Scikit-learn: Machine learning in Python." *the Journal of machine Learning research* 12: 2825-2830.

Poeplau, C., & Don, A. (2015). Carbon sequestration in agricultural soils via cultivation of cover crops—A meta-analysis. *Agriculture, Ecosystems & Environment*, 200, 33-41.

Python (2018): *Python Documentation contents*, v.3.7.13 <https://docs.python.org/3.7/contents.html>.

Quemada, M., Lassaletta, L., Leip, A., Jones, A., & Lugato, E. (2020). Integrated management for sustainable cropping systems: looking beyond the greenhouse balance at the field scale. *Global Change Biology*, 26(4), 2584-2598.

R Core Team (2020; 2021). R: A language and environment for statistical computing. R Foundation for Statistical Computing, Vienna, Austria. URL <https://www.R-project.org/>

Redhead, J. W., May, L., Oliver, T. H., Hamel, P., Sharp, R., & Bullock, J. M. (2018). National scale evaluation of the InVEST nutrient retention model in the United Kingdom. *Science of the Total Environment*, 610–611, 666–677. <https://doi.org/10.1016/j.scitotenv.2017.08.092>

LfULG (Sächsisches Landesamt für Umwelt, Landwirtschaft und Geologie) (2001). Ermittlung von Erträgen auf dem Grünland [Determination of yields on grassland]. Available at: <https://www.landwirtschaft.sachsen.de/download/Ertragsermittlung.pdf>. Last accessed 18th May 2022.

Senay, S. D., & Worner, S. P. (2019). Multi-scenario species distribution modeling. *Insects*, 10(3), 65.

Sharp, R., Tallis, H.T., Ricketts, T., Guerry, A.D., Wood, S.A., Chaplin-Kramer, R., Nelson, E., Ennaanay, D., Wolny, S., Olwero, N., Vigerstol, K., Pennington, D., Mendoza, G., Aukema, J., Foster, J., Forrest, J., Cameron, D., Arkema, K., Lonsdorf, E., Kennedy, C., Verutes, G., Kim, C.K., Guannel, G., Papenfus, M., Toft, J., Marsik, M., Bernhardt, J., Griffin, R., Glowinski, K., Chaumont, N., Perelman, A., Lacayo, M. Mandle, L., Hamel, P., Vogl, A.L., Rogers, L., Bierbower, W., Denu, D., and Douglass, J. (2018). InVEST +VERSION+ User's Guide. The Natural Capital Project, Stanford University, University of Minnesota, The Nature Conservancy, and World Wildlife Fund.

Thuiller, W., Georges, D., Engler, R., & Frank, B. (2019). Package “biomod2” Title Ensemble Platform for Species Distribution Modeling. CRAN, 1. https://r-forge.r-project.org/R/?group_id=302

Van Diepen, C. V., Wolf, J. V., Van Keulen, H., & Rappoldt, C. (1989). WOFOST: a simulation model of crop production. *Soil use and management*, 5(1), 16-24.

VÚMOP (2015): Trvalé travní porosty (TTP) [Permanent grassland]. Available at: [https://restep.vumop.cz/encyklopedie/index.php/Trval%C3%A9_travn%C3%AD_porosty_\(TTP\)](https://restep.vumop.cz/encyklopedie/index.php/Trval%C3%A9_travn%C3%AD_porosty_(TTP)).

Waskom, M. L. (2021). Seaborn: statistical data visualization. *Journal of Open Source Software*, 6(60), 3021. <https://doi.org/10.21105/joss.03021>

Watling, J. I., Brandt, L. A., Bucklin, D. N., Fujisaki, I., Mazzotti, F. J., Romanach, S. S., & Speroterra, C. (2015). Performance metrics and variance partitioning reveal sources of uncertainty in species distribution models. *Ecological Modelling*, 309, 48-59.

Wu, G.L., Liu, Y., Tian, F.P., and Shi, Z.H. (2016) Legumes Functional Group Promotes Soil Organic Carbon and Nitrogen Storage by Increasing Plant Diversity. *Land Degrad. Develop.*, 28: 1336– 1344.

Wüest, R. O., Zimmermann, N. E., Zurell, D., Alexander, J. M., Fritz, S. A., Hof, C., ... & Karger, D. N. (2020). Macroecology in the age of Big Data—Where to go from here?. *Journal of Biogeography*, 47(1), 1-12.

Wilkinson, M. D., Dumontier, M., Aalbersberg, I. J., Appleton, G., Axton, M., Baak, A., ... & Mons, B. (2016). The FAIR Guiding Principles for scientific data management and stewardship. *Scientific data*, 3(1), 1-9.

Ziv, G., Beckmann, M., Bullock, J., Cord, A., Delzeit, R., Domingo, C., et al. (2020). BESTMAP: behavioural, Ecological and Socio-economic Tools for Modelling Agricultural Policy. *Research Ideas and Outcomes*, 6, e52052. <https://doi.org/10.3897/rio.6.e52052>

Zurell, D., Franklin, J., König, C., Bouchet, P. J., Dormann, C. F., Elith, J., ... & Merow, C. (2020). A standard protocol for reporting species distribution models. *Ecography*, 43(9), 1261-1277. doi/full/10.1111/ecog.04960

Appendix

The appendix contains all the model factsheets for each of the biodiversity, ESS and socio-economic models developed in BESTMAP's WP3. The most recent version of each factsheet can be found in the BESTMAP GitLab (<https://git.ufz.de/>) in the respective model's repository.

Biodiversity model factsheet

BESTMAP biodiversity model

2022-05-10

The structure of this factsheet is largely based on the ODMAP (Overview, Data, Model, Assessment and Prediction) protocol developed by Zurell et al. 2020 [doi/full/10.1111/ecog.04960](https://doi.org/10.1111/ecog.04960)

Overview

Authorship

Contact: Stephanie Roilo (stephanie.roilo@tu-dresden.de) for the models in DE, CZ, ES and UK; Tijana Nikolic (tijana.nikolic@biosense.rs) for the models in RS; Tomas Vaclavik (tomas.vaclavik@upol.cz) for the models in CZ.

Model name

Species distribution model (SDM; Figure 1) for selected farmland bird species.

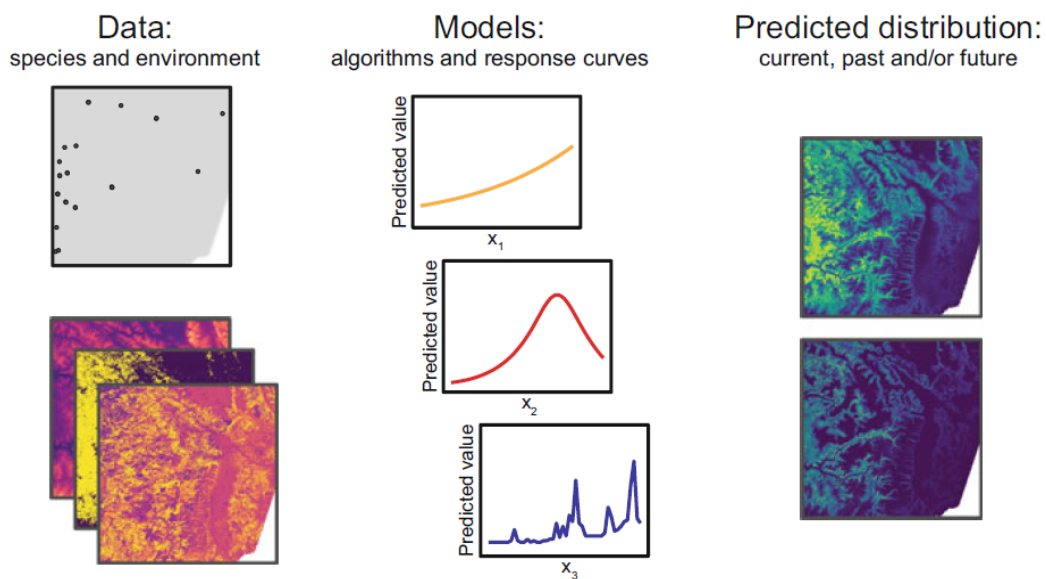


Figure 1: A general framework of species distribution models. Data on species location are linked to spatial data on the environment with quantitative models. Different model algorithms can vary considerably in the way they relate species responses to environmental

gradients. With estimated response curves, species distributions are mapped in space and/or time. Ensemble models combine several model algorithms to deliver more robust forecasts (source: Fletcher & Fortin 2018).

Model objective

Main objective of the model is to estimate how the adoption of Agri-Environment Measures (AEM, used here as an umbrella term for agri-environment schemes, ecological focus areas and organic farming) affects habitat suitability for a selected set of farmland bird species.

Model output

The model output consists of habitat suitability maps for the selected bird species.

Data specifications

Response data type: presence-only, georeferenced point occurrences of farmland birds.

Predictor types: geospatial (e.g. raster and shapefile data) information on climate, topography, anthropogenic disturbance, land cover and land-use, including land-use management information like AEM adoption extracted from the Integrated Administration and Control System (IACS) and Land Parcel Identification System (LPIS).

Assumptions

Model assumptions: 1. Species-environment equilibrium, 2. All relevant ecological drivers of farmland bird distributions are included in the models, 3. Bird dataset adequately covers fields with and without agri-environment measures.

Algorithms and workflow

Modelling techniques: we used ensemble SDMs to minimise the uncertainties arising from single algorithm models. The ensemble models were based on five modelling algorithms, namely generalised linear models and generalised additive models (GLM and GAM, regression-based methods), random forest, generalised boosting models, and maximum entropy (RF, GBM, and MAXENT; machine-learning methods) as implemented in the biomod2 package version 3.4.6 (Thuiller et al. 2019).

Model workflow: We fitted 10 repetitions for each model by randomly subdividing the dataset into 70% training data and 30% testing data. Each model run was evaluated via cross-validation. We used the Area Under the Receiver Operating Characteristics Curve (AUC), the True Skills Statistics (TSS), specificity and sensitivity as evaluation metrics (Fletcher & Fortin 2018). To obtain a relevant combination of several unbiased (i.e., with fair accuracy) models, only models with an AUC value ≥ 0.7 were retained, and the ensemble model was constructed for each species by computing the weighted average of all remaining models. The weights were based on the AUC scores of each model, so that better performing models had a higher influence in the final ensemble. The models were then projected onto the current (as of 2019) environmental and agricultural conditions to obtain habitat suitability maps for each bird species.

Model validation

Each model run was evaluated via cross-validation, and the average across the 10 runs was computed to assess the performance of the final model. We used AUC, TSS, specificity and sensitivity as evaluation metrics.

Uncertainty estimation

Ensemble SDMs were developed with the specific goal of minimising the uncertainty in estimating species distribution deriving from single algorithm models (Araújo & New 2007, Wüest et al. 2020). Indeed, among the many potential sources of uncertainty in SDMs, such as algorithms, environmental datasets, species presences, variable collinearity, etc., the choice of modelling algorithm is thought to be the greatest source of uncertainty in SDM performance and prediction maps (Watling et al. 2015, Wüest et al. 2020). We therefore produced uncertainty maps calculated as the standard deviation of the prediction maps deriving from the model algorithms included in the ensemble model (Buisson et al. 2010; Senai & Worner 2019). Such maps highlight the areas of highest disagreement across single algorithm predictions.

Software

Software: We used the biomod2 package version 3.4.6 (Thuiller et al., 2019) in R version 4.0.2 (R Core Team 2020).

Code availability: the R code used for the preparation of the environmental variables at multiple spatial scales (approach adopted in DE, CZ and RS), fitting the models and producing the uncertainty maps, together with a README file, is available here: <https://git.ufz.de/bestmap/bestmap-biodiversity>

Linking the model outputs to indicators

The model results can be linked to the following policy indicators:

[C.35/I.18 Farmland Bird Index](#) (FBI).

While the European Farmland Bird Indicator represents temporal trends of population sizes based on annual national bird surveys, we here aimed at developing an indicator that could detect the effects of AEM in a spatially-explicit way, and that could be compared across CS. We normalised all individual species' SDMs and we computed the average habitat suitability score across all modelled bird species. The output is an index of farmland birds' habitat suitability, with high (positive) values indicating highly suitable habitat, and low (negative) values indicating unsuitable habitat.

Model specifications in each case study

1) Mulde, DE

Location

Mulde River Basin, Saxony, Germany, which serves as one of the five BESTMAP case study regions.

Scale of Analysis

Spatial extent: 12.34771, 13.69364, 50.3809, 51.64169 (xmin, xmax, ymin, ymax, CRS=WGS84)

Spatial resolution: 20 m

Temporal extent: 2016 - 2019

Temporal resolution: year

Boundary: natural

Data

Biodiversity data

Species selection: We selected farmland bird species as those breeding in grassland, wet grassland, arable land, ruderal and fallow areas, according to the list of species occurring in Saxony (Blischke 2017). For the species for which no specific habitat information was available in Blischke (2017), we selected farmland species according to Busch et al. (2019). We excluded the common cuckoo (*Cuculus canorus*) and the mallard (*Anas platyrhynchos*) due to their parasitic and synanthropic behaviour, respectively, making them generalist species in terms of their breeding habitat selection. Lastly, we included in the analysis only those farmland species with a minimum number of 40 presence points after removal of replicates, i.e. multiple records in the same environmental raster cell. The final list of modelled species is shown in Table 1.1.

Ecological level: species

Data sources: Data is stored in the Saxon Central Species Database (Zentrale Artdatenbank, www.natur.sachsen.de/zentrale-artdatenbank-zena-sachsen-6905.html) and was shared with us upon request to the Saxon State Agency for Environment, Agriculture and Geology.

Sampling design: The database comprises observations from standardised monitoring projects (breeding bird monitoring, Natura2000 monitoring), monitoring activities of special interest groups and NGOs and opportunistic observations verified by the state agency ornithologists.

Sample size: number of presence points per species are reported in Table 1.1; we set the number of absence points as 10 times that of presence points for each species; with the exception of *Lanius collurio* for which the presence/absence ratio is 0.4.

Table 1.1: List of species included in the analyses and number of presence points used for modelling after filtering.

Species	Common name	Presence points
<i>Alauda arvensis</i>	Eurasian Skylark	79
<i>Anthus pratensis</i>	Meadow pipit	299
<i>Carduelis cannabina</i>	Common Linnet	55
<i>Charadrius dubius</i>	Little Ringed Plover	96
<i>Coturnix coturnix</i>	Common Quail	63
<i>Crex crex</i>	Corncrake	84
<i>Emberiza calandra</i>	Corn Bunting	90

<i>Emberiza citrinella</i>	Yellowhammer	164
<i>Gallinago gallinago</i>	Common Snipe	63
<i>Lanius collurio</i>	Red-backed Shrike	988
<i>Motacilla flava</i>	Blue-headed Yellow Wagtail	92
<i>Saxicola rubetra</i>	Whinchat	411
<i>Saxicola rubicola</i>	European Stonechat	205
<i>Sylvia communis</i>	Common Whitethroat	106
<i>Vanellus vanellus</i>	Northern Lapwing	41

Cleaning: We cleaned the dataset by removing incomplete (e.g. genus name with no species name) or incorrect taxonomical records. Based on the information on reproduction status, unit of observation (e.g. breeding pair, eggs, chicks, etc.), and behaviour (e.g. territorial behaviour, courtship, etc.), we filtered the dataset to retain only observations for which the breeding status was possible, probable or confirmed. Lastly, we included in the analysis only those farmland species with a minimum number of 40 presence points after removal of replicates, i.e. multiple records in the same environmental raster cell.

Absence data: As absence points, we used randomly selected observation points of other (farmland and non-farmland) bird species in the dataset, with a minimum distance to all presence points of 500 m.

Errors and biases: Due to its diverse sources, the observation data entails biases in the monitoring effort, which is higher in protected areas and close to cities, and in the species ratio, with rare species being monitored more intensively. The spatial uncertainty of the georeferenced observations is ≤ 100 m.

Predictor variables

Table 1.2: Explanatory variables used in the SDMs and sources of the original data.

Group	Variable (units)	Data source (original resolution)
Topography	Elevation (m)	DGM20, Staatsbetrieb Geobasisinformation und Vermessung Sachsen (20 m)
	Slope (°)	DGM20, Staatsbetrieb Geobasisinformation und Vermessung Sachsen (20 m)

Distance metrics	Distance from forest edge (m)	Copernicus High Resolution Layer (HRL) Forest type 2015 (20 m)
	Distance from highways (m)	OpenStreetMap 2020 (shapefile)
Land cover/use	Agricultural land-use diversity (Shannon's index)	IACS/LPIS 2016-2019 (shapefile) (SMEKUL 2020)
	Arable land (%)	IACS/LPIS 2016-2019 (shapefile) (SMEKUL 2020)
	Grassland cover (%)	Copernicus HRL Grassland status map 2015 (20 m)
	Small Woody Features (SWF) cover (%)	Copernicus HRL Small Woody Features 2015 (5 m)
	Urban cover (%)	APiC 2016 (Preidl et al. 2020) (20 m)
Agri-Environment Measures (AEM)	Buffer areas (%)	IACS/LPIS 2016-2019 (shapefile) (SMEKUL 2020)
	Cover crops (%)	IACS/LPIS 2016-2019 (shapefile) (SMEKUL 2020)
	Extensive grassland management (%)	IACS/LPIS 2016-2019 (shapefile) (SMEKUL 2020)
	Fallow land (%)	IACS/LPIS 2016-2019 (shapefile) (SMEKUL 2020)
	Organic farming (%)	IACS/LPIS 2016-2019 (shapefile) (SMEKUL 2020)

Predictor variables, data sources and their original spatial resolution and reference year are summarised in Table 1.2.

Coordinate reference system: EPSG:3035

Temporal resolution: Yearly resolution of IACS/LPIS data between 2016 and 2019; the other predictors were kept constant throughout the years.

Data processing: As elevation layer, we used the Digital Elevation Model of Saxony, (DGM20, Staatsbetrieb Geobasisinformation und Vermessung Sachsen, 2016). From this layer, we derived slope using the `terrain()` function from the raster package (Hijmans et al., 2020). To map land cover outside of agricultural fields, we used the Copernicus High Resolution Layers for Small Woody Features (SWF), Forest type product, Grassland status map, all available for the reference year 2015. Urban cover was extracted from the Sentinel-2a-based land cover map for 2016 by Preidl et al., 2020. All products were cropped and aligned to the same extent, disaggregated to 5 m resolution, and binary maps (0:absence, 1:presence) were produced for each land cover type. If binary maps overlapped (i.e. the same raster cell was covered by multiple land cover types), we masked the layers in the following hierarchical order: SWF (used as mask for all other layers due to its higher original resolution), grassland, forest, urban cover. From the forest cover layer we derived a

raster (5 m res.) of distance to forest edge, using the Proximity(Raster Distance) tool in QGIS version 3.10.11 (www.qgis.org). To account for anthropogenic disturbance, we included distance from highways to the environmental predictors. This was calculated at 5 m res. based on the OpenStreetMap highways shapefile (key:highway, value:motorway; www.openstreetmap.org), which we downloaded and rasterized. All layers were reprojected to the coordinate reference system EPSG:3035, cropped and aligned to the study area extent using the raster package (Hijmans et al., 2020) and the terra package (Hijmans et al., 2021) in R version 4.0.2 (R Core Team 2020). IACS/LPIS data for four consecutive years (2016-2019) were used in this study. While the IACS/LPIS data for the years of 2018 and 2019 held precise spatial information about the geometry and location of linear EFAs (field edges and buffer strips) within the field, the older datasets of 2016 and 2017 did not, and linear EFAs were linked to the entire field parcel. We therefore had to estimate the shape and location of 2016-2017 linear EFAs. If the same EFA scheme was applied also in 2018/2019, we assumed its geometry to stay constant, and used the precise spatial information of the 2018/2019 data. For all other fields, we assumed linear EFAs to be 1 m wide across the entire field perimeter. We chose a narrow width (1 m) to compensate for the total length (entire perimeter of the field parcel) of these features, which are usually applied on only one border of the field. From the IACS/LPIS data referring to the most recent year (2019), we calculated raster layers at 20 m resolution in which each raster cell value corresponded to the proportion of the given land cover/use type within circular windows with radii of 200, 500 and 1000 m. These rasters were used for projecting the models into the current AES and EFA adoption conditions, to obtain 20 m res. habitat suitability maps for each bird species.

Model

Variable pre-selection

Variable pre-selection: Explanatory variables were chosen to reflect environmental and habitat conditions likely to impact farmland birds' distributions at the field and landscape level. Climatic predictors, e.g. multiannual (1981-2010) total precipitation, minimum and maximum temperature (Deutscher Wetterdienst, opendata.dwd.de/climate_environment/CDC/grids_germany/multi_annual/), were initially included in the models, but due to their high correlation ($r > 0.7$) with elevation and their lower spatial resolution (1 km), we ultimately excluded them, thereby using elevation in the models, which roughly approximates the temperature and precipitation gradients in the study area.

Multicollinearity

Multicollinearity: To select the best scale for each variables and to exclude highly correlated variables from the same model, we fitted univariate linear models with binomial distribution for each explanatory variable and we ranked them by their Akaike Information Criterion corrected for small sample size (AICc) score. For each species, we then selected the best set of uncorrelated variables (i.e. with Spearman's correlation coefficient < 0.7) with the lowest AICc score.

Model settings

GLM: we used a binomial link function, and a stepwise backward selection was applied to select final models by removing unimportant variables, based on the Akaike Information Criterion (AIC). Interaction level was set to 0.

GAM: we used a binomial link function using the algorithm as implemented in the mgcv package (Wood, 2017), and the basis dimension of the smooth functions was set to $k = 5$ to avoid overfitting. Interaction level was set to 0.

MAXENT: the maximum number of iterations was set to 200 and the feature classes linear, quadratic and threshold were selected. The regularisation parameter β was set to -1 to allow for automatic setting, as the optimal value is likely to change across species (Elith et al., 2011).

RF: the number of trees was set to 500, the minimum size of terminal nodes was set to 5, and the number of variables randomly sampled as candidates at each split to 1.

GBM: we used the default settings (number of trees = 100, interaction depth parameter = 1, learning rate = 0.1, and subsampling fraction = 0.5) suggested in the gbm package (Greenwell et al., 2019).

Model estimates

Variable importance: Variable importance scores were obtained using the `get_variable_importance()` function in the biomod2 package (Thuiller et al., 2019) and were normalised, so that the sum of the importance scores of all variables in a model equals 100, to ensure comparability between variables and across species.

Assessment

Performance statistics

Performance on training data: AUC, TSS, sensitivity (true positive rate), specificity (true negative rate); see table 1.3 for the evaluation metrics of single models.

Table 1.3: Mean values of the evaluation metrics across the 10 model runs for each species-specific model.

Species	AUC	TSS	Sensitivity	Specificity
<i>Alauda arvensis</i>	0.89	0.67	0.86	0.81
<i>Anthus pratensis</i>	0.99	0.9	0.96	0.94
<i>Carduelis cannabina</i>	0.9	0.73	0.85	0.88
<i>Charadrius dubius</i>	0.93	0.75	0.85	0.90
<i>Coturnix coturnix</i>	0.94	0.77	0.87	0.90
<i>Crex crex</i>	0.97	0.87	0.93	0.94
<i>Emberiza calandra</i>	0.95	0.8	0.89	0.91
<i>Emberiza citrinella</i>	0.84	0.6	0.79	0.81
<i>Gallinago gallinago</i>	0.96	0.84	0.94	0.90
<i>Lanius collurio</i>	0.91	0.69	0.86	0.83
<i>Motacilla flava</i>	0.94	0.8	0.94	0.87
<i>Saxicola rubetra</i>	0.97	0.84	0.92	0.92
<i>Saxicola rubicola</i>	0.94	0.76	0.94	0.83

<i>Sylvia communis</i>	0.8	0.49	0.74	0.76
<i>Vanellus vanellus</i>	0.96	0.85	0.98	0.87

Plausibility check

Response shapes: The variable response plots were built with the *response.plot2()* function of the same package, and the standard deviation was calculated across the 10 model runs.

2) South Moravia, CZ

Location

South Moravia, Czech Republic, which serves as one of the five BESTMAP case study regions.

Scale of Analysis

Spatial extent: 16.893 17.919, 48.792, 49.189 (xmin, xmax, ymin, ymax; CRS= WGS84)

Spatial resolution: 10 m

Temporal extent: 2015 - 2019

Temporal resolution: year

Boundary: administrative

Data

Biodiversity data

Species selection: We selected farmland bird species according to the list used for the calculation of the European Farmland Bird Index, as in Gamero et al. (2016). We excluded species for which less than 40 presence points were available. The list of modelled species is shown in Table 2.1.

Ecological level: species

Data sources: Data was extracted from the official database of the Nature Conservation Agency of the Czech Republic ([Nálezová databáze ochrany přírody AOPK ČR](#), NDOP).

Sampling design: The database includes confirmed observations from standardised monitoring projects (breeding bird monitoring, Natura2000 monitoring), monitoring activities of special interest groups and NGOs and opportunistic observations verified by the database maintainers.

Sample size: number of presence points per species are reported in Table 2.1; we set the number of absence points as 10 times that of presence points for each species; if this number exceeded the total available absence points after the distance filtering, we used all available points in the dataset.

Table 2.1: List of species included in the analyses and number of presence points used for modelling after filtering.

Species	Common name	Presence points
---------	-------------	-----------------

<i>Alauda arvensis</i>	Eurasian Skylark	90
<i>Anthus pratensis</i>	Meadow Pipit	62
<i>Carduelis cannabina</i>	Common Linnet	73
<i>Ciconia ciconia</i>	White Stork	313
<i>Corvus frugilegus</i>	Rook	66
<i>Emberiza calandra</i>	Corn Bunting	57
<i>Emberiza citrinella</i>	Yellowhammer	228
<i>Falco tinnunculus</i>	Common Kestrel	181
<i>Galerida cristata</i>	Crested Lark	241
<i>Hirundo rustica</i>	Barn Swallow	350
<i>Lanius collurio</i>	Red-backed Shrike	347
<i>Motacilla flava</i>	Blue-headed Yellow Wagtail	126
<i>Passer montanus</i>	Eurasian Tree Sparrow	176
<i>Perdix perdix</i>	Grey Partridge	190
<i>Saxicola rubetra</i>	Whinchat	69
<i>Saxicola rubicola</i>	European Stonechat	195
<i>Serinus serinus</i>	European Serin	73
<i>Streptopelia turtur</i>	European Turtle Dove	134
<i>Sturnus vulgaris</i>	Common Starling	237

<i>Sylvia communis</i>	Common Whitethroat	52
<i>Upupa epops</i>	Eurasian Hoopoe	89
<i>Vanellus vanellus</i>	Northern Lapwing	216

Cleaning: The dataset included only records verified by the Nature Conservation Agency of the Czech Republic. We excluded species with less than 40 presence points.

Absence data: As absence points, we used randomly selected observation points of other farmland bird species in the dataset, with a minimum distance to all presence points of 500 m.

Errors and biases: The observation data entails biases in the monitoring effort, which is higher in protected areas and close to cities and road infrastructures.

Predictor variables

Table 2.2: Explanatory variables used in the SDMs and sources of the original data.

Group	Variable (units)	Data source (original resolution)
Topography	Elevation (m)	4th generation digital relief model of the Czech Republic (DMR 4G) (5 m) (Czech Office for Surveying, Mapping and Cadastre 2020 https://www.cuzk.cz/English/Home.aspx)
	Slope (°)	4th generation digital relief model of the Czech Republic (DMR 4G) (5 m) (Czech Office for Surveying, Mapping and Cadastre 2020)
Distance metrics	Distance from forest edge (m)	S2GLC Europe 2017 (10 m) (Malinowski et al. 2020) - classes 82 and 83 Broadleaf and coniferous tree cover
	Distance from highways and primary roads (m)	OpenStreetMap 2020 (shapefile)
Land cover/use	Agricultural land-use diversity (Shannon's index)	IACS/LPIS 2015-2019 (shapefile) (Ministry of Agriculture of the Czech Republic 2020)
	Arable land (%)	IACS/LPIS 2015-2019 (shapefile) (Ministry of Agriculture of the Czech Republic 2020)
	Grassland cover (%)	S2GLC Europe 2017 (10 m) (Malinowski et al. 2020)- class 102 Herbaceous vegetation
	Small Woody Features (SWF) cover (%)	Copernicus HRL Small Woody Features 2015 (5 m)

	Urban cover (%)	S2GLC Europe 2017 (10 m) (Malinowski et al. 2020) - class 62 Artificial surfaces and constructions
Agri-Environment Measures (AEM)	Buffer areas (%)	IACS/LPIS 2015-2019 (shapefile) (Ministry of Agriculture of the Czech Republic 2020)
	Extensive grassland management (%)	IACS/LPIS 2015-2019 (shapefile) (Ministry of Agriculture of the Czech Republic 2020)
	Land use conversion to grassland (%)	IACS/LPIS 2015-2019 (shapefile) (Ministry of Agriculture of the Czech Republic 2020)
	Organic and integrated farming (%)	IACS/LPIS 2015-2019 (shapefile) (Ministry of Agriculture of the Czech Republic 2020)

Predictor variables, data sources and their original spatial resolution and reference year are summarised in Table 2.2.

Coordinate reference system: EPSG:3035

Temporal resolution: Yearly resolution of IACS/LPIS data between 2015 and 2019; the other predictors were kept constant throughout the years.

Data processing: As elevation layer, we used the 4th generation digital relief model of the Czech Republic (DMR 4G) (Czech Office for Surveying, Mapping and Cadastre 2020). From this layer, we derived slope using the slope() function from the terra package (Hijmans et al., 2021). To map land cover outside of agricultural fields, we used the Land Cover Map of Europe 2017 from the S2GLC project (Malinowski et al., 2020) and the Copernicus High Resolution Layers for Small Woody Features (SWF) for the reference year 2015. All products were cropped and aligned to the same extent, disaggregated to 5 m resolution, and binary maps (0:absence, 1:presence) were produced for each land cover type. If binary maps overlapped (i.e. the same raster cell was covered by multiple land cover types), we used the SWF layer as mask for all other layers due to its higher original resolution. From the forest cover layer we derived a raster (5 m res.) of distance to forest edge, using the Proximity(Raster Distance) tool in QGIS version 3.10.11 (www.qgis.org). To account for anthropogenic disturbance, we included distance from highways and primary roads to the environmental predictors. This was calculated at 5 m res. based on the OpenStreetMap highways shapefile (key:highway, value:primary; www.openstreetmap.org), which we downloaded and rasterized. All layers were reprojected to the coordinate reference system EPSG:3035, cropped and aligned to the study area extent using the raster package (Hijmans et al., 2020) and the terra package (Hijmans et al., 2021) in R version 4.0.2 (R Core Team 2020). IACS/LPIS data for five consecutive years (2015-2019), provided by the Ministry of Agriculture of the Czech Republic, were used in this study to compute the proportion of arable land and of different AES, as well as the agricultural land-use diversity index. The Czech IACS/LPIS data hold information on all grown crops within each field parcel, but no spatial information on the distribution of the crops within the parcel is given. This implied some approximation in the calculation of the agricultural land-use diversity index. From the IACS/LPIS data referring to the most recent year (2019), we calculated raster layers at 10 m resolution in which each raster cell value corresponded to the proportion of the given land cover/use type within circular windows with radii of 200, 500 and 1000 m. These rasters were used for projecting the models into the current AES adoption conditions, to obtain 10 m res. habitat suitability maps for each bird species.

Model

Variable pre-selection

Variable pre-selection: Explanatory variables were chosen to reflect environmental and habitat conditions likely to impact farmland birds' distributions at the field and landscape level. We used elevation in the models, which roughly approximates the temperature and precipitation gradients in the study area, and allowed us to model at much higher spatial resolution.

Multicollinearity

Multicollinearity: To select the best scale for each variables and to exclude highly correlated variables from the same model, we fitted univariate linear models with binomial distribution for each explanatory variable and we ranked them by their Akaike Information Criterion corrected for small sample size (AICc) score. For each species, we then selected the best set of uncorrelated variables (i.e. with Spearman's correlation coefficient < 0.7) with the lowest AICc score.

Model settings

GLM: we used a binomial link function, and a stepwise backward selection was applied to select final models by removing unimportant variables, based on the Akaike Information Criterion (AIC). Interaction level was set to 0.

GAM: we used a binomial link function using the algorithm as implemented in the *mgcv* package (Wood, 2017), and the basis dimension of the smooth functions was set to $k = 5$ to avoid overfitting. Interaction level was set to 0.

MAXENT: the maximum number of iterations was set to 200 and the feature classes linear, quadratic and threshold were selected. The regularisation parameter β was set to -1 to allow for automatic setting, as the optimal value is likely to change across species (Elith et al., 2011).

RF: the number of trees was set to 500, the minimum size of terminal nodes was set to 5, and the number of variables randomly sampled as candidates at each split to 1.

GBM: we used the default settings (number of trees = 100, interaction depth parameter = 1, learning rate = 0.1, and subsampling fraction = 0.5) suggested in the *gbm* package (Greenwell et al., 2019).

Model estimates

Variable importance: Variable importance scores were obtained using the *get_variable_importance()* function in the *biomod2* package (Thuiller et al., 2019) and were normalised, so that the sum of the importance scores of all variables in a model equals 100, to ensure comparability between variables and across species.

Assessment

Performance statistics

Performance on training data: AUC, TSS, sensitivity (true positive rate), specificity (true negative rate); see table 2.3 for the evaluation metrics of single models.

Table 2.3: Mean values of the evaluation metrics across the 10 model runs for each species-specific model.

Species	AUC	TSS	Sensitivity	Specificity
<i>Alauda arvensis</i>	0.81	0.53	0.74	0.79
<i>Anthus pratensis</i>	0.79	0.51	0.68	0.83
<i>Carduelis cannabina</i>	0.82	0.53	0.76	0.78
<i>Ciconia ciconia</i>	0.77	0.42	0.74	0.69
<i>Corvus frugilegus</i>	0.82	0.54	0.74	0.81
<i>Emberiza calandra</i>	0.95	0.88	0.93	0.95
<i>Emberiza citrinella</i>	0.88	0.64	0.86	0.78
<i>Falco tinnunculus</i>	0.79	0.47	0.71	0.77
<i>Galerida cristata</i>	0.97	0.85	0.93	0.93
<i>Lanius collurio</i>	0.80	0.47	0.75	0.73
<i>Hirundo rustica</i>	0.83	0.53	0.77	0.75
<i>Motacilla flava</i>	0.90	0.65	0.82	0.84
<i>Passer montanus</i>	0.88	0.65	0.88	0.77
<i>Perdix perdix</i>	0.89	0.66	0.85	0.81
<i>Saxicola rubetra</i>	0.76	0.45	0.76	0.70
<i>Saxicola rubicola</i>	0.75	0.41	0.67	0.74
<i>Serinus serinus</i>	0.85	0.61	0.83	0.79
<i>Streptopelia turtur</i>	0.85	0.61	0.75	0.86
<i>Sturnus vulgaris</i>	0.87	0.60	0.82	0.78
<i>Sylvia communis</i>	0.84	0.60	0.87	0.73
<i>Upupa epops</i>	0.84	0.59	0.70	0.89
<i>Vanellus vanellus</i>	0.89	0.64	0.78	0.86

Plausibility check

Response shapes: The variable response plots were built with the *response.plot2()* function of the same package, and the standard deviation was calculated across the 10 model runs.

3) Catalonia, ES

Location

Catalonia, Spain, which serves as one of the five BESTMAP case study regions.

Scale of Analysis

Spatial extent: 0.1557295, 3.338699, 40.51405, 42.8691 (xmin, xmax, ymin, ymax; CRS=WGS84)

Spatial resolution: 1 km

Temporal extent: 2019

Temporal resolution: year

Boundary: administrative

Data

Biodiversity data

Species selection: We selected farmland bird species according to the list used for the calculation of the European Farmland Bird Index, as in Gamero et al. (2016), and we complemented it with the species of the Spanish Farmland Bird Index, as in Traba & Morales (2019). We excluded species for which less than 40 presence points were available. The list of modelled species is shown in Table 3.1.

Ecological level: species

Data sources: the bird data was downloaded from GBIF.org on 23 August 2021 (GBIF Occurrence Download <https://doi.org/10.15468/dl.9svutg>), and is owned by the Catalan Ornithological Institute ([Institut Català d'Ornitologia](https://www.institut-catala-d-ornitologia.cat/)).

Sampling design: The database, curated by the Catalan Ornithological Institute, includes observations collected through the portal www.ornitho.cat, a website that allows citizens to store and share field observations of some groups of animals (<https://www.gbif.org/publisher/ada19a05-4216-44c7-aa4f-6e7177bcb0ac>). The data is uploaded in the GBIF repository in gridded format, at 1x1 km resolution.

Sample size: number of presence points per species are reported in Table 3.1; we set the number of absence points as 10 times that of presence points for each species; if this number exceeded the total available absence points after the distance filtering, we used all available points in the dataset.

Table 3.1: List of species included in the analyses and number of presence points used for modelling after filtering.

Species	Common name	Presence points
<i>Alauda arvensis</i>	Eurasian Skylark	463
<i>Alectoris rufa</i>	Red-legged Partridge	708
<i>Anthus campestris</i>	Tawny Pipit	111
<i>Anthus pratensis</i>	Meadow Pipit	668

<i>Athene noctua</i>	Little Owl	417
<i>Bubulcus ibis</i>	Cattle Egret	508
<i>Carduelis carduelis</i>	European Goldfinch	1733
<i>Ciconia ciconia</i>	White Stork	417
<i>Cisticola juncidis</i>	Zitting Cisticola	634
<i>Coturnix coturnix</i>	Common Quail	329
<i>Emberiza calandra</i>	Corn Bunting	696
<i>Emberiza cirrus</i>	Cirl Bunting	1152
<i>Emberiza citrinella</i>	Yellowhammer	145
<i>Emberiza hortulana</i>	Ortolan Bunting	74
<i>Falco tinnunculus</i>	Common Kestrel	1561
<i>Galerida cristata</i>	Crested Lark	850
<i>Galerida theklae</i>	Thekla's Lark	132
<i>Hirundo rustica</i>	Barn Swallow	1677
<i>Lanius collurio</i>	Red-backed Shrike	269
<i>Lanius senator</i>	Woodchat Shrike	493
<i>Linaria cannabina</i>	Common Linnet	919
<i>Melanocorypha calandra</i>	Calandra Lark	114
<i>Merops apiaster</i>	European Bee-eater	1118

<i>Motacilla flava</i>	Blue-headed Yellow Wagtail	425
<i>Oenanthe hispanica</i>	Western black-eared Wheatear	115
<i>Passer domesticus</i>	House Sparrow	1651
<i>Passer montanus</i>	Eurasian Tree Sparrow	691
<i>Petronia petronia</i>	Rock Sparrow	390
<i>Pica pica</i>	Eurasian Magpie	1472
<i>Saxicola rubetra</i>	Whinchat	370
<i>Saxicola rubicola</i>	European Stonechat	1020
<i>Serinus serinus</i>	European Serin	1742
<i>Streptopelia turtur</i>	European Turtle Dove	487
<i>Sturnus unicolor</i>	Spotless Starling	458
<i>Sturnus vulgaris</i>	Common Starling	1315
<i>Sylvia communis</i>	Common Whitethroat	335
<i>Upupa epops</i>	Eurasian Hoopoe	1247
<i>Vanellus vanellus</i>	Northern Lapwing	201

Cleaning: We excluded species with less than 40 presence points.

Absence data: As absence points, we used randomly selected observation points of other farmland bird species in the dataset, with a minimum distance to all presence points of 5 km.

Errors and biases: The observation data is based on a citizen science project (www.ornitho.cat), and may thus entail biases in terms of monitoring effort, e.g. with higher coverage in and around populated areas.

Predictor variables

Table 3.2: Explanatory variables used in the SDMs and sources of the original data.

Group	Variable (units)	Data source (original resolution)
Topography	Elevation (m)	Copernicus EU-DEM v1.1 (25 m)
Climate	Maximum temperature between April and July	CHELSA Climatologies 1981-2010 V2.1, tasmax_04 - 07 (1 km) (Karger et al. 2020)
	Precipitation sum between April and July	CHELSA Climatologies 1981-2010 V2.1, pr_04 - 07 (1 km) (Karger et al. 2020)
Land cover/use	Land cover diversity (Shannon´s index)	IACS/LPIS 2019 (shapefile) (Generalitat de Catalunya-Ministry of Agriculture, Livestock, Fisheries and Food-Department of Rural Department 2020)
	Arable land (%)	IACS/LPIS 2019 (shapefile) (Generalitat de Catalunya-Ministry of Agriculture, Livestock, Fisheries and Food-Department of Rural Department 2020)
	Forest cover (%)	IACS/LPIS 2019 (shapefile) (Generalitat de Catalunya-Ministry of Agriculture, Livestock, Fisheries and Food-Department of Rural Department 2020)
	Grassland cover (%)	IACS/LPIS 2019 (shapefile) (Generalitat de Catalunya-Ministry of Agriculture, Livestock, Fisheries and Food-Department of Rural Department 2020)
	Orchards, nuts and fruit plantations cover (%)	IACS/LPIS 2019 (shapefile) (Generalitat de Catalunya-Ministry of Agriculture, Livestock, Fisheries and Food-Department of Rural Department 2020)
	Small Woody Features (SWF) cover (%)	Copernicus HRL Small Woody Features 2015 (5 m)
	Urban cover (%)	IACS/LPIS 2019 (shapefile) (Generalitat de Catalunya-Ministry of Agriculture, Livestock, Fisheries and Food-Department of Rural Department 2020)
	(Mixed) Vineyards cover (%)	IACS/LPIS 2019 (shapefile) (Generalitat de Catalunya-Ministry of Agriculture, Livestock, Fisheries and Food-Department of Rural Department 2020)

Agri-Environment Measures (AEM)	Cover crops, as part of integrated production management (%)	IACS/LPIS 2019 (shapefile) (Generalitat de Catalunya-Ministry of Agriculture, Livestock, Fisheries and Food-Department of Rural Department 2020)
	Extensive grassland management (%)	IACS/LPIS 2019 (shapefile) (Generalitat de Catalunya-Ministry of Agriculture, Livestock, Fisheries and Food-Department of Rural Department 2020)
	Fallow land (%)	IACS/LPIS 2019 (shapefile) (Generalitat de Catalunya-Ministry of Agriculture, Livestock, Fisheries and Food-Department of Rural Department 2020)
	Organic farming, including organic livestock and alternative systems to chemical control (%)	IACS/LPIS 2019 (shapefile) (Generalitat de Catalunya-Ministry of Agriculture, Livestock, Fisheries and Food-Department of Rural Department 2020)

Predictor variables, data sources and their original spatial resolution and reference year are summarised in Table 3.2.

Coordinate reference system: EPSG:3035

Temporal resolution: models were developed based on the IACS/LPIS data relative to the year of 2019; the reference year of the other environmental layers are listed in table 3.2.

Data processing: As the bird data was in gridded format, we used the bird monitoring grid provided by the Catalan Ornithological Institute as a blueprint for the preparation of all other environmental layers. We intersected the bird monitoring grid with the IACS/LPIS 2019 layer and calculated the proportion of cover, within each 1x1 km grid cells, for the different land cover classes and AES groups (Table 3.2), using the *sf* package (Pebesma 2018). We then rasterized each of the computed variables using the *terra* package (Hijmans et al., 2021). We downloaded the Copernicus High Resolution Layers for Small Woody Features (SWF) for the reference year 2015, extracted the proportion of SWF cover within each grid cell, and rasterized it. We used the Copernicus EU-DEM v1.1 as elevation layer, which was reprojected to the same extent and resolution of the other previously prepared layers. We downloaded the CHELSA climatologies (Karger et al. 2020) layers for maximum temperature and precipitation sum for the months April to July, and we computed the maximum temperature values and the sum of precipitation across the 4 months. All layers were reprojected to the coordinate reference system EPSG:3035, cropped and aligned to the study area extent using the *terra* package (Hijmans et al., 2021) in R version 4.1.1 (R Core Team 2020).

Model

Variable pre-selection

Variable pre-selection: Explanatory variables were chosen to reflect environmental and habitat conditions likely to impact farmland birds' distributions at the field and landscape level.

Multicollinearity

Multicollinearity: To exclude highly correlated variables from the same model, we fitted univariate linear models with binomial distribution for each explanatory variable and we ranked them by their Akaike Information Criterion corrected for small sample size (AICc) score. For each species, we then selected the best set of uncorrelated variables (i.e. with Spearman's correlation coefficient < 0.7) with the lowest AICc score.

Model settings

GLM: we used a binomial link function, and a stepwise backward selection was applied to select final models by removing unimportant variables, based on the Akaike Information Criterion (AIC). Interaction level was set to 0.

GAM: we used a binomial link function using the algorithm as implemented in the mgcv package (Wood, 2017), and the basis dimension of the smooth functions was set to $k = 5$ to avoid overfitting. Interaction level was set to 0.

MAXENT: the maximum number of iterations was set to 200 and the feature classes linear, quadratic and threshold were selected. The regularisation parameter β was set to -1 to allow for automatic setting, as the optimal value is likely to change across species (Elith et al., 2011).

RF: the number of trees was set to 500, the minimum size of terminal nodes was set to 5, and the number of variables randomly sampled as candidates at each split to 1.

GBM: we used the default settings (number of trees = 100, interaction depth parameter = 1, learning rate = 0.1, and subsampling fraction = 0.5) suggested in the gbm package (Greenwell et al., 2019).

Model estimates

Variable importance: Variable importance scores were obtained using the `get_variable_importance()` function in the biomod2 package (Thuiller et al., 2019) and were normalised, so that the sum of the importance scores of all variables in a model equals 100, to ensure comparability between variables and across species.

Assessment

Performance statistics

Performance on training data: AUC, TSS, sensitivity (true positive rate), specificity (true negative rate); see table 3.3 for the evaluation metrics of single models.

Table 3.3: Mean values of the evaluation metrics across the 10 model runs for each species-specific model.

Species	AUC	TSS	Sensitivity	Specificity
<i>Alauda arvensis</i>	0.82	0.51	0.75	0.77
<i>Alectoris rufa</i>	0.78	0.41	0.66	0.76
<i>Anthus campestris</i>	0.78	0.47	0.74	0.73
<i>Anthus pratensis</i>	0.86	0.59	0.77	0.83

<i>Athene noctua</i>	0.90	0.68	0.81	0.87
<i>Bubulcus ibis</i>	0.95	0.78	0.92	0.86
<i>Carduelis carduelis</i>	0.84	0.55	0.75	0.81
<i>Ciconia ciconia</i>	0.94	0.77	0.87	0.91
<i>Cisticola juncidis</i>	0.95	0.76	0.88	0.89
<i>Coturnix coturnix</i>	0.89	0.65	0.83	0.82
<i>Emberiza calandra</i>	0.89	0.64	0.81	0.83
<i>Emberiza cirrus</i>	0.87	0.62	0.83	0.79
<i>Emberiza citrinella</i>	0.88	0.66	0.79	0.87
<i>Emberiza hortulana</i>	0.76	0.48	0.67	0.81
<i>Falco tinnunculus</i>	0.83	0.52	0.72	0.81
<i>Galerida cristata</i>	0.94	0.73	0.87	0.86
<i>Galerida theklae</i>	0.94	0.76	0.87	0.90
<i>Hirundo rustica</i>	0.85	0.56	0.71	0.85
<i>Lanius collurio</i>	0.96	0.82	0.88	0.95
<i>Lanius senator</i>	0.83	0.51	0.80	0.71
<i>Linaria cannabina</i>	0.74	0.37	0.59	0.78
<i>Melanocorypha calandra</i>	0.99	0.95	1.00	0.95
<i>Merops apiaster</i>	0.86	0.55	0.68	0.87
<i>Motacilla flava</i>	0.89	0.65	0.81	0.84
<i>Oenanthe hispanica</i>	0.83	0.56	0.78	0.78
<i>Passer domesticus</i>	0.93	0.70	0.83	0.87
<i>Passer montanus</i>	0.93	0.74	0.86	0.88
<i>Petronia petronia</i>	0.83	0.54	0.82	0.73
<i>Pica pica</i>	0.94	0.77	0.88	0.90
<i>Saxicola rubetra</i>	0.81	0.50	0.80	0.70
<i>Saxicola rubicola</i>	0.78	0.43	0.72	0.72
<i>Serinus serinus</i>	0.88	0.62	0.83	0.79

<i>Streptopelia turtur</i>	0.81	0.48	0.82	0.66
<i>Sturnus unicolor</i>	0.88	0.61	0.82	0.79
<i>Sturnus vulgaris</i>	0.92	0.72	0.87	0.85
<i>Sylvia communis</i>	0.80	0.49	0.71	0.79
<i>Upupa epops</i>	0.89	0.64	0.82	0.83
<i>Vanellus vanellus</i>	0.93	0.73	0.83	0.90

Plausibility check

Response shapes: The variable response plots were built with the *response.plot2()* function of the same package, and the standard deviation was calculated across the 10 model runs.

4) Bačka, RS

Location

Bačka region, Serbia, which serves as one of the five BESTMAP case study regions.

Scale of Analysis

Spatial extent: 18.8194, 20.31623, 45.13434, 46.18879 (xmin, xmax, ymin, ymax; CRS=WGS84)

Spatial resolution: 10 m

Temporal extent: 2015-2019

Temporal resolution: year

Boundary: administrative

Data

Biodiversity data

Species selection: We selected farmland bird species by using a two step approach: first, we checked the list of farmland species used for the calculation of the European Farmland Bird Index, as in Gamero et al. (2016) and in a second step from that list, in communication with species expert from University of Novi Sad we selected species that rely on open grassland habitat distribution for its foraging and reproduction in our study area. Additionally, we used data on small mammal grassland specialists whose life cycle is strongly attained to open grassland habitats. The final list of modelled species is shown in Table 4.1.

Ecological level: species

Data sources: The Bird Protection and Study Society of Serbia provided us with the data for selected bird species; we used in-house (BioSense) data on small mammal grassland specialists.

Sampling design: The database includes confirmed observations from standardised monitoring projects (breeding bird monitoring, Natura2000 monitoring), and monitoring activities of researchers verified by the species experts at University of Novi Sad.

Sample size: number of presence points per species are reported in Table 4.1; we set the number of absence points as 10 times that of presence points for each species, randomly distributed across study area.

Table 4.1: List of species included in the analyses and number of presence points used for modelling after filtering.

Species	Common name	Presence points
<i>Anthus campestris</i>	Tawny Pipit	53
<i>Lanius minor</i>	Lesser Grey Shrike	50
<i>Vanellus vanellus</i>	Northern Lapwing	299
<i>Spermophilus citellus</i>	European Ground Squirrel	76

Cleaning: The dataset included only records verified by local experts. We excluded species with less than 40 presence points.

Absence data: As absence points, we used randomly selected observation points with a minimum distance to all presence points of 500 m.

Errors and biases: The observation data entails biases in the monitoring effort, which is higher in protected areas or within ecological network and road infrastructures.

Predictor variables

Table 4.2: Explanatory variables used in the SDMs and sources of the original data.

Group	Variable (units)	Data source (original resolution)
Topography	Elevation (m)	ALOS World 3D-30m (AW3D30) Version 3.2/3.1 (30m) ALOS@EORC Homepage (jaxa.jp)
	Slope (°) and aspect	Derived from ALOS World 3D-30m (AW3D30) Version 3.2/3.1 (30m) ALOS@EORC Homepage (jaxa.jp)
Distance metrics	Distance from forest edge (m)	Copernicus HRL Forest Type 2018 (10m) Status Maps — Copernicus Land Monitoring Service
	Distance from highways (m)	OpenStreetMap 2020 (shapefile)

	Distance from Water and wetness areas (m)	Copernicus Water & Wetness 2018 (10m) Water & Wetness 2018 — Copernicus Land Monitoring Service
Land cover/use	Agricultural land-use diversity (Shannon's index)	BioSense in-house crop distribution map 2013-2020 (10 m)
	Arable land (%)	BioSense in-house file (shapefile)
	Grassland cover and grassland cover change (%)	Copernicus HRL Grassland 2015 (20m) and 2018 (10m) Status Maps — Copernicus Land Monitoring Service Copernicus HRL Grassland change 2015-2018 (20m) Change Maps — Copernicus Land Monitoring Service
	Small Woody Features (SWF) cover (%)	Copernicus HRL Small Woody Features 2015 (5m) Small Woody Features — Copernicus Land Monitoring Service
	Urban cover (%)	Copernicus European Settlement Map 2012, release 2017 ESM 2012 - Release 2017 — Copernicus Land Monitoring Service
Surrogates for Agri-Environment Measures (AEM)	Linear elements (%)	BioSense in-house file derived from sentinel images available for the pick of vegetation season in the CS area 2019 (10 m)
	Extensive grassland management - grassland maintenance (%)	Provincial Institute for Nature Protection 2016-2019 (shapefile)
	Fallow land (%)	BioSense in-house file derived from crop diversity maps 2019 (10 m)
	Organic farming (%)	BioSense in-house file (shapefile)

Predictor variables, data sources and their original spatial resolution and reference year are summarised in Table 4.2.

Coordinate reference system: EPSG:3035

Temporal resolution: Yearly resolution of grassland 2015 and 2018; the other predictors were kept constant throughout the years.

Data processing: As an elevation layer, we used the Digital Elevation Model ALOS World 3D-30m (AW3D30) Version 3.2/3.1 (30m) [ALOS@EORC Homepage \(jaxa.jp\)](#). From this layer, we derived slope and aspect using the terrain() function from the raster package (Hijmans et al., 2020). To map land cover outside of agricultural fields, we used the Copernicus High Resolution Layers for Small Woody Features (SWF), Forest type product, Grassland status map, all available for the reference year 2015, and grasslands for reference years 2015 and 2018 in which percentage of grassland pixels varied. Urban cover was extracted from the Copernicus European Settlement Map 2017. All products were cropped and aligned to the same extent, disaggregated to 10 m resolution, and binary maps

(0:absence, 1:presence) were produced for each land cover type. If binary maps overlapped (i.e. the same raster cell was covered by multiple land cover types), we masked the layers in the following hierarchical order: SWF (used as mask for all other layers due to its higher original resolution), grassland, forest, urban cover. From the forest cover layer and water and wetness we derived a raster (10 m res.) of distance to forest edge, using the Proximity(Raster Distance) tool in QGIS version 3.10.11 (www.qgis.org). To account for anthropogenic disturbance, we included distance from highways to the environmental predictors. This was calculated at 10 m res. based on the OpenStreetMap highways shapefile (key:highway; primary, secondary and trunk, code: 5111; 5113; 5114 and 5112; www.openstreetmap.org), which we downloaded and rasterized. All layers were reprojected to the coordinate reference system EPSG:3035, cropped and aligned to the study area extent using the raster package (Hijmans et al., 2020) and the terra package (Hijmans et al., 2021) in R version 4.0.2 (R Core Team 2020). For developing the linear elements layer we used available Sentinel 2 images and Google engine, and used NDVI time series to detect permanent vegetation along roads and arable fields in the study area. We developed the fallow land layer in the agricultural zone by using crop cover distribution data (2015-2019) and, by applying an algorithm for plugin detection, we calculated areas where in 3 consecutive years no plugin activity was detected. The developed binary files were masked with grassland maintenance and grassland maps. In a final step, all the pixels from SWF, grassland, forest, linear elements, and fallow land binary maps were once again masked from urban areas. We rasterized the shapefile of organic farms and the grasslands maintenance files in QGIS version 3.10.11 (www.qgis.org) and developed 10 m resolution binary layers. From the linear elements, grassland maintenance, fallow land and organic farming data referring to the most recent year (2019), we calculated raster layers at 10 m resolution in which each raster cell value corresponded to the proportion of the given land cover/use type within circular windows with radii of 200, 500 and 1000 m. These rasters were used for projecting the models into the current conditions of AES “surrogates”, to obtain 10 m res. habitat suitability maps for each selected species.

Model

Variable pre-selection

Variable pre-selection: Explanatory variables were chosen to reflect environmental and habitat conditions likely to impact farmland species' distributions at the field and landscape level.

Multicollinearity

Multicollinearity: To select the best scale for each variables and to exclude highly correlated variables from the same model, we fitted univariate linear models with binomial distribution for each explanatory variable and we ranked them by their Akaike Information Criterion corrected for small sample size (AICc) score. For each species, we then selected the best set of uncorrelated variables (i.e. with Spearman's correlation coefficient < 0.7) with the lowest AICc score.

Model settings

GLM: we used a binomial link function, and a stepwise backward selection was applied to select final models by removing unimportant variables, based on the Akaike Information Criterion (AIC). Interaction level was set to 0.

GAM: we used a binomial link function using the algorithm as implemented in the mgcv package (Wood, 2017), and the basis dimension of the smooth functions was set to $k = 5$ to avoid overfitting. Interaction level was set to 0.

MAXENT: the maximum number of iterations was set to 200 and the feature classes linear, quadratic and threshold were selected. The regularisation parameter β was set to -1 to allow for automatic setting, as the optimal value is likely to change across species (Elith et al., 2011).

RF: the number of trees was set to 500, the minimum size of terminal nodes was set to 5, and the number of variables randomly sampled as candidates at each split to 1.

GBM: we used the default settings (number of trees = 100, interaction depth parameter = 1, learning rate = 0.1, and subsampling fraction = 0.5) suggested in the gbm package (Greenwell et al., 2019).

Model estimates

Variable importance: Variable importance scores were obtained using the `get_variable_importance()` function in the biomod2 package (Thuiller et al., 2019) and were normalised, so that the sum of the importance scores of all variables in a model equals 100, to ensure comparability between variables and across species.

Assessment

Performance statistics

Performance on training data: AUC, TSS, sensitivity (true positive rate), specificity (true negative rate); see table 4.3 for the evaluation metrics of single models.

Table 4.3: Mean values of the evaluation metrics across the 10 model runs for each species-specific model.

Species	AUC	TSS	Sensitivity	Specificity
<i>Anthus campestris</i>	0.83	0.60	0.78	0.83
<i>Lanius minor</i>	0.81	0.53	0.84	0.70
<i>Vanellus vanellus</i>	0.79	0.49	0.74	0.75
<i>Spermophilus citellus</i>	0.96	0.89	0.97	0.92

Plausibility check

Response shapes: The variable response plots were built with the `response.plot2()` function of the same package, and the standard deviation was calculated across the 10 model runs.

5) Humber, UK

Location

Humber River Basin, United Kingdom, which serves as one of the five BESTMAP case study regions.

Scale of Analysis

Spatial extent: -1.723979, 0.1374987, 53.05964, 54.46706 (xmin, xmax, ymin, ymax; CRS=WGS84)

Spatial resolution: 1 km

Temporal extent: 2019

Temporal resolution: year

Boundary: natural

Data

Biodiversity data

Species selection: We selected farmland bird species according to the list used for the calculation of the European Farmland Bird Index, as in Gamero et al. (2016). We excluded species for which less than 30 presence points were available. We used a lower threshold compared to the one (40 presence points) used in other CS because of the coarser spatial resolution (1 km) of the UK models compared to e.g. DE and CZ models, and to the relatively small extent of the CS. The list of modelled species is shown in Table 5.1; species highlighted in red were not included in the calculation of the indicator due to low model performance (i.e. whenever more than half of the algorithms had AUC < 0.7, hindering the setup of a robust ensemble model).

Ecological level: species

Data sources: the bird data was requested for the selected species to the British Trust for Ornithology (BTO). The data was collected as part of the breeding bird survey of the BTO. To increase the number of observations and the spatial coverage of the dataset, additional bird observations from the National Biodiversity Network (NBN) Atlas (<https://nbnatlas.org>, accessed on Fri Dec 17 12:46:47 UTC 2021) for the year of 2019. The NBN Atlas records were further filtered to only retain observations considered correct, with spatial uncertainty < 708 m, and for which the listed data provider was the BTO.

Sampling design: The bird data is part of the UK breeding bird survey, a standardised annual bird count on randomly-located 1-km sites (more information can be found here <https://www.bto.org/our-science/projects/bbs>). The NBN Atlas dataset is a collection of records from multiple sources (we only retained datasets from the BTO), deriving from diverse monitoring schemes; more information can be found here <https://nbnatlas.org/about-nbn-atlas/>.

Sample size: number of presence points per species are reported in Table 5.1; for each modelled species we used all available absence points, e.g. all location points of surveyed grid squares where the focal species was not recorded.

Table 5.1: List of species included in the analyses and number of presence points used for modelling after filtering. For the species marked in red, model performance was too low to produce reliable results, and are thus removed from the multispecies indicator.

Species	Common name	Presence points
<i>Alauda arvensis</i>	Eurasian Skylark	70
<i>Alectoris rufa</i>	Red-legged Partridge	32
<i>Corvus frugilegus</i>	Rook	62

<i>Emberiza citrinella</i>	Yellowhammer	62
<i>Falco tinnunculus</i>	Common Kestrel	41
<i>Hirundo rustica</i>	Barn Swallow	77
<i>Linaria cannabina</i>	Common Linnet	59
<i>Passer montanus</i>	Eurasian Tree Sparrow	37
<i>Sturnus vulgaris</i>	Common Starling	80
<i>Sylvia communis</i>	Common Whitethroat	65
<i>Vanellus vanellus</i>	Northern Lapwing	45

Cleaning: We excluded species with less than 30 presence points.

Absence data: As absence points, we used all other monitored grid squares (from the UK Ordnance survey grid at 1 km) in which the focal species was not found.

Errors and biases: data from standardised monitoring schemes such as the breeding bird monitoring of the BTO are collected by skilled volunteers and are not spatially biased towards more populated area, like other citizen science monitoring programs; nonetheless, the number of monitored grid per year within the Humber catchment is rather small, which affects the performance of our models.

Predictor variables

Table 5.2: Explanatory variables used in the SDMs and sources of the original data.

Group	Variable (units)	Data source (original resolution)
Topography	Elevation (m)	Copernicus EU-DEM v1.1 (25 m)
Climate	Maximum temperature between April and July	CHELSA Climatologies 1981-2010 V2.1, tasmx_04 - 07 (1 km) (Karger et al. 2020)
	Precipitation sum between April and July	CHELSA Climatologies 1981-2010 V2.1, pr_04 - 07 (1 km) (Karger et al. 2020)
Land cover/use	Land cover diversity (Shannon's index)	Copernicus HRL Small Woody Features 2015 (5 m) and S2GLC Europe 2017 (10 m) (Malinowski et al. 2020)

	Arable land (%)	S2GLC Europe 2017 (10 m) (Malinowski et al. 2020)- class 73 Cultivated areas
	Forest cover (%)	S2GLC Europe 2017 (10 m) (Malinowski et al. 2020)- classes 82 and 83 Broadleaf tree cover and coniferous tree cover
	Grassland cover (%)	S2GLC Europe 2017 (10 m) (Malinowski et al. 2020)- class 102 Herbaceous vegetation
	Small Woody Features (SWF) cover (%)	Copernicus HRL Small Woody Features 2015 (5 m)
	Urban cover (%)	S2GLC Europe 2017 (10 m) (Malinowski et al. 2020) - class 62 Artificial surfaces and constructions
Agri-Environment Measures (AEM)	Buffer strips/areas (%)	IACS/LPIS 2019 (shapefile) (Rural Payments Agency, 2020)
	Cover crops (%)	IACS/LPIS 2019 (shapefile) (Rural Payments Agency, 2020)
	Extensive grassland management (%)	IACS/LPIS 2019 (shapefile) (Rural Payments Agency, 2020)
	Fallow land (%)	IACS/LPIS 2019 (shapefile) (Rural Payments Agency, 2020)

Predictor variables, data sources and their original spatial resolution and reference year are summarised in Table 5.2.

Coordinate reference system: EPSG:3035

Temporal resolution: models were developed based on the IACS/LPIS relative to the year of 2019; the reference years of the other environmental layers are listed in table 5.2.

Data processing: As the bird data was in gridded format, we used the ordnance survey national grid as a blueprint for the preparation of all other environmental layers. We intersected the bird monitoring grid with the IACS/LPIS 2019 layer and calculated the proportion of cover, within each 1 km grid cells, for the different AES groups, using the sf package (Pebesma 2018). We then rasterized each of the computed variables using the terra package (Hijmans et al., 2021). Similarly, we downloaded the Copernicus High Resolution Layers for Small Woody Features (SWF) for the reference year 2015, extracted the proportion of SWF cover within each grid cell, and rasterized it. We applied the same approach for the other land cover classes (e.g. forest, grassland, etc.) using the S2GLC Europe 2017 (Malinowski et al. 2020) land cover raster, which we previously masked with the SWF layer. We downloaded the CHELSA climatologies (Karger et al. 2020) layers for maximum temperature and precipitation sum for the months April to July, and we computed the maximum temperature values and the sum of precipitation across the 4 months. We used the elevation layer EU-DEM v1.1 from Copernicus, which we aggregated to 1 km resolution. All layers were reprojected to the coordinate reference system EPSG:3035, cropped and aligned to the study area extent using the terra package (Hijmans et al., 2021) in R version 4.1.1 (R Core Team 2020).

Model

Variable pre-selection

Variable pre-selection: Explanatory variables were chosen to reflect environmental and habitat conditions likely to impact farmland birds' distributions at the field and landscape level. Some AES groups (e.g. organic farming, land-use conversion to grassland, land-use conversion to forest) could not be included in the model as only limited (i.e. only 4 monitored squares) bird data was available from the farms/area where these schemes were applied.

Multicollinearity

Multicollinearity: To exclude highly correlated variables from the same model, we fitted univariate linear models with binomial distribution for each explanatory variable and we ranked them by their Akaike Information Criterion corrected for small sample size (AICc) score. For each species, we then selected the best set of uncorrelated variables (i.e. with Spearman's correlation coefficient < 0.7) with the lowest AICc score.

Model settings

GLM: we used a binomial link function, and a stepwise backward selection was applied to select final models by removing unimportant variables, based on the Akaike Information Criterion (AIC). Interaction level was set to 0.

GAM: we used a binomial link function using the algorithm as implemented in the *mgcv* package (Wood, 2017), and the basis dimension of the smooth functions was set to $k = 3$ to avoid overfitting. Interaction level was set to 0.

MAXENT: the maximum number of iterations was set to 200 and the feature classes linear, quadratic and threshold were selected. The regularisation parameter β was set to -1 to allow for automatic setting, as the optimal value is likely to change across species (Elith et al., 2011).

RF: the number of trees was set to 500, the minimum size of terminal nodes was set to 5, and the number of variables randomly sampled as candidates at each split to 1.

GBM: we used the default settings (number of trees = 100, interaction depth parameter = 1, learning rate = 0.1, and subsampling fraction = 0.5) suggested in the *gbm* package (Greenwell et al., 2019).

Model estimates

Variable importance: Variable importance scores were obtained using the *get_variable_importance()* function in the *biomod2* package (Thuiller et al., 2019) and were normalised, so that the sum of the importance scores of all variables in a model equals 100, to ensure comparability between variables and across species.

Assessment

Performance statistics

Performance on training data: AUC, TSS, sensitivity (true positive rate), specificity (true negative rate); see table 5.3 for the evaluation metrics of single models.

Table 5.3: Mean values of the evaluation metrics across the 10 model runs for each species-specific model. For four species, several single algorithm models had AUC scores lower than 0.7, and hence no ensemble model was produced.

Species	AUC	TSS	Sensitivity	Specificity
<i>Alauda arvensis</i>	0.78	0.51	0.81	0.69
<i>Alectoris rufa</i>	no ensemble model produced			
<i>Corvus frugilegus</i>	0.77	0.55	0.85	0.70
<i>Emberiza citrinella</i>	0.83	0.59	0.83	0.77
<i>Falco tinnunculus</i>	no ensemble model produced			
<i>Hirundo rustica</i>	0.77	0.48	0.86	0.62
<i>Linaria cannabina</i>	0.76	0.75	0.70	0.45
<i>Passer montanus</i>	0.79	0.53	0.83	0.71
<i>Sturnus vulgaris</i>	no ensemble model produced			
<i>Sylvia communis</i>	0.75	0.65	0.82	0.46
<i>Vanellus vanellus</i>	no ensemble model produced			

Plausibility check

Response shapes: The variable response plots were built with the *response.plot2()* function of the same package, and the standard deviation was calculated across the 10 model runs.

References:

- Araújo, M. B., & New, M. (2007). Ensemble forecasting of species distributions. *Trends in ecology & evolution*, 22(1), 42-47.
- Blischke, H. (2017). In Sachsen auftretende Vogelarten 2.0, Sächsisches Landesamt für Umwelt, Landwirtschaft und Geologie www.uvp-verbund.de/documents/ingrid-group_ige-iplug-sn/9BE35011-E4E8-43B3-A778-27CAC8FDCF43/%C3%9Cbersicht%20Vogelarten.pdf
- Broyer, J., Curtet, L., & Chazal, R. (2014). How to improve agri-environment schemes to achieve meadow bird conservation in Europe? A case study in the Saône valley, France. *Journal of Ornithology*, 155(1), 145–155. <https://doi.org/10.1007/s10336-013-0996-6>
- Buisson, L., Thuiller, W., Casajus, N., Lek, S., & Grenouillet, G. (2010). Uncertainty in ensemble forecasting of species distribution. *Global Change Biology*, 16(4), 1145-1157.
- Busch, M., Katzenberger, J., Trautmann, S., Gerlach, B., Dröschmeister, R., & Sudfeldt, C. (2019). Drivers of population change in common farmland birds in Germany. *Bird Conservation International*, 1980. Fletcher, R. and Fortin, M., 2018. *Spatial ecology and conservation modeling*. Springer International Publishing.
- Elith, J., Phillips, S. J., Hastie, T., Dudík, M., Chee, Y. E., & Yates, C. J. (2011). A statistical explanation of MaxEnt for ecologists. *Diversity and Distributions*, 17(1), 43–57. <https://doi.org/10.1111/j.1472-4642.2010.00725.x>

Fletcher, R., & Fortin, M. (2018). *Spatial ecology and conservation modeling*. Springer International Publishing.

Gamero, A., Brotons, L., Brunner, A., Foppen, R., Fornasari, L., Gregory, R. D., ... & Voříšek, P. (2017). Tracking progress toward EU biodiversity strategy targets: EU policy effects in preserving its common farmland birds. *Conservation Letters*, 10(4), 395-402.

Generalitat de Catalunya-Ministry of Agriculture, Livestock, Fisheries and Food-Department of Rural Department (2020). SIGPAC data, https://governobert.gencat.cat/ca/dades_obertes/inici

Greenwell, B., Boehmke, B., & Cunningham, J. (2019). Package “gbm” - Generalized Boosted Regression Models. *CRAN Repository*, 39. <https://cran.r-project.org/web/packages/gbm/gbm.pdf%0Ahttps://github.com/gbm-developers/gbm>

Hijmans, R. J. (2021). raster: Geographic Data Analysis and Modeling. R package version 3.4-13. <https://CRAN.R-project.org/package=raster>

Hijmans R. J. (2021). terra: Spatial Data Analysis. R package version 1.3-22. <https://CRAN.R-project.org/package=terra>

Karger, D. N.; Dabaghchian, B.; Lange, S.; Thuiller, W.; Zimmermann, N. E.; Graham, C. H. (2020). High resolution climate data for Europe. *EnviDat*. doi:10.16904/envidat.150.

Malinowski, R., Lewiński, S., Rybicki, M., Gromny, E., Jenerowicz, M., Krupiński, M., ... & Schauer, P. (2020). Automated production of a land cover/use map of Europe based on Sentinel-2 imagery. *Remote Sensing*, 12(21), 3523.

Iturbide, M., Bedia, J., Herrera, S., del Hierro, O., Pinto, M., & Gutiérrez, J. M. (2015). A framework for species distribution modelling. Supplementary material. *Ecological Modelling*, 312, 166–174.

Pebesma, E. (2018). Simple Features for R: Standardized Support for Spatial Vector Data. *The R Journal* 10 (1), 439-446, <https://doi.org/10.32614/RJ-2018-009>

Preidl, S., Lange, M., & Doktor, D. (2020). Introducing APiC for regionalised land cover mapping on the national scale using Sentinel-2A imagery. *Remote Sensing of Environment*, 240(April 2019), 111673. <https://doi.org/10.1016/j.rse.2020.111673>

R Core Team (2020). R: A language and environment for statistical computing. R Foundation for Statistical Computing, Vienna, Austria. URL <https://www.R-project.org/>

Senay, S. D., & Worner, S. P. (2019). Multi-scenario species distribution modeling. *Insects*, 10(3), 65.

Staatsbetrieb Geobasisinformation und Vermessung Sachsen, 2016, Digitale Geländemodell (DGM20) für den Freistaat Sachsen, www.geodaten.sachsen.de/downloadbereich-dgm25-4162.html

SMEKUL (2020) Integriertes Verwaltungs- und Kontrollsystem (InVeKoS) 2016-2019, Sächsisches Staatsministerium für Energie, Klimaschutz, Umwelt und Landwirtschaft.

Thuiller, W., Georges, D., Engler, R., & Frank, B. (2019). Package “biomod2” Title Ensemble Platform for Species Distribution Modeling. *CRAN*, 1. https://r-forge.r-project.org/R/?group_id=302

Traba, J., & Morales, M. B. (2019). The decline of farmland birds in Spain is strongly associated to the loss of fallowland. *Scientific reports*, 9(1), 1-6.

Watling, J. I., Brandt, L. A., Bucklin, D. N., Fujisaki, I., Mazzotti, F. J., Romanach, S. S., & Speroterra, C. (2015). Performance metrics and variance partitioning reveal sources of uncertainty in species distribution models. *Ecological Modelling*, 309, 48-59.

Wood, S. N. (2017). Package ‘mgcv’ - Generalized additive models: An introduction with R, second edition. In *Generalized Additive Models: An Introduction with R, Second Edition*. <https://doi.org/10.1201/9781315370279>

Wüest, R. O., Zimmermann, N. E., Zurell, D., Alexander, J. M., Fritz, S. A., Hof, C., ... & Karger, D. N. (2020). Macroecology in the age of Big Data—Where to go from here?. *Journal of Biogeography*, 47(1), 1-12.

Zurell, D., Franklin, J., König, C., Bouchet, P. J., Dormann, C. F., Elith, J., ... & Merow, C. (2020). A standard protocol for reporting species distribution models. *Ecography*, 43(9), 1261-1277. <https://doi.org/10.1111/ecog.04960>

Food and fodder model factsheet

BESTMAP food & fodder model

2022-05-16

The structure of this factsheet is largely based on the ODMAP (Overview, Data, Model, Assessment and Prediction) protocol developed by Zurell et al. 2020 [doi/full/10.1111/ecog.04960](https://doi.org/10.1111/ecog.04960)

Overview

Authorship

Contact: Anne Paulus (anne.paulus@ufz.de), Predrag Lugonja (predrag.lugonja@biosense.rs), Katharina Schneider (katharina.schneider@ufz.de), Rosemary Wool (r.wool@leeds.ac.uk), Michael Beckmann (michael.beckmann@ufz.de).

Model name

Model of the effects of agri-environmental measures on food and fodder production.

Model objective

Main objective of the model is to estimate how the adoption of agri-environmental measures (AEM) affects yield and production area of selected agricultural crops as well as economic output at the field and farm level. Figure 1 provides a conceptual overview of the model workflow.

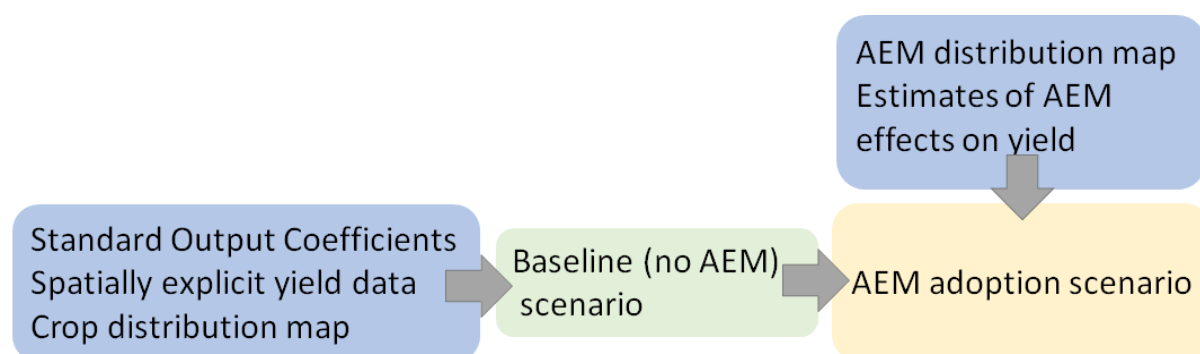


Figure 1: Schematic overview of the food and fodder model.

Model output

The model output consists of maps of crop production area, yield and standard output.

Data specifications

Geospatial information (e.g. as raster and shapefile data) on agricultural land-use, including management information like AEM adoption (cover crops, buffer areas/flower strips, land-use conversion, maintaining permanent grasslands) and type of crops grown as well as spatially explicit yield data of agricultural crops and their standard output coefficients.

Assumptions

1. All relevant effects of the AEM on food and fodder production are included in the models,
2. Current AEM implementation levels do not affect the baseline yield and standard output,
3. Cover crop effects on yield depends only on climate, soil texture, catch crop and cover crop type,
4. Implementation of buffer areas and land-use conversion do not affect yield and standard output of neighbouring fields,
5. EUROSTAT and IACS/LPIS information on agricultural management is correct.

Algorithms and workflow

The general workflow of the food and fodder model is depicted in Figure 1. We obtained standard output coefficients of agricultural crops from EUROSTAT (2022) as an economic measure of agricultural production. A baseline yield map without AEM was produced using predictions created by the WOFOST model for arable land. Regional yield data for grassland was obtained from local data sources. These data were used as a weighting factor in order to account for spatial variation of standard output coefficients (SOC). SOC are published by EUROSTAT (2021) and represent the monetary value produced by cultivating a crop per hectare at a given time and location. We then used existing empirical data to estimate the relative effect of AEM on crop yield. The results were then combined in order to produce case study maps of production area and yield of the selected crops.

WOFOST

WOFOST (WORld FOod STudies) is a simulation model developed at Wageningen University & Research for the quantitative analysis of the growth and production of annual field crops (Van Diepen et al., 1989). WOFOST is used in the European Mars crop yield forecasting system (de Wit et al., 2019). The WOFOST data used here were previously generated in the JRC study “Analysis of climate change impacts on EU agriculture by 2050” (Hristov et al., 2020). The WOFOST model was run on climate data. 8 climate models were used from 5 families and yield predictions were generated for two RCP scenarios, mid-range mitigation emission scenario (RCP4.5) and the high-end emission scenario (RCP8.5). We aggregate this data in the following way to create single yield maps for each scenario: first, we calculated the mean of each model's family, and then the median of aggregated results was used for final yield prediction. Yield predictions are generated for the following six crops: maize, sugar beet, wheat, sunflower, winter rapeseed, spring barley at a resolution of appr. 11km. WOFOST data were used as a baseline in all case studies, except for Spain, where agriculture is dominated by crop species not included in WOFOST.

Uncertainty analysis

The food and fodder model is largely based on two sources of information: i. the yield model, ii. information from IACS/LPIS and EUROSTAT. As there is no information of uncertainty about the latter, we assume that they are correct, so the uncertainty of our model can be calculated from the uncertainty of the crop yield model. As a measure for uncertainty of the WOFOST baseline model, we decided to use variance across the 8 climate models. To calculate uncertainty of the WOFOST model, we calculated variance of each pixel across years, since each pixel across 8 yield maps represents an independent random process. For comparison of uncertainty across years we calculated a histogram of variance for each year separately.

Model validation

The baseline yield model of arable crops was validated using regional yield statistics of each case study. The model was evaluated using the metrics R^2 and RMSE.

Software

Software: We used R version 4.0.2 (R Core Team 2020).

Code availability: the R code used for the preparation of the environmental variables and for fitting the models, together with a README file, is available here: <https://git.ufz.de/bestmap/bestmap-food-and-fodder>.

Linking the model outputs to indicators

The model results are not identical to, but can be linked to the following indicator (EUROSTAT 2022):

[C.24 Agricultural factor income](#)

Agricultural factor income represents the value generated by a farm business including all factors of production, which makes it a suitable indicator for evaluating the impact of changes in subsidies like AEM on farm income. It is also used for the EU reporting on the United Nations' Sustainable Development Goals.

Model specifications in each case study

1) Mulde, DE

Location

Mulde River Basin, Saxony, Germany, which serves as one of the five BESTMAP case study regions.

Scale of Analysis

Spatial extent: 12.34771, 13.69364, 50.3809, 51.64169 (xmin, xmax, ymin, ymax, CRS=WGS84)

Spatial resolution: field scale

Temporal extent: 2016 - 2019

Temporal resolution: year

Boundary: natural

Data

Spatially explicit information on agriculture in the Mulde case study region was obtained from the InVeKoS database, which is part of the EU-wide Integrated Administration and Control System (IACS) (SMEKUL, 2020). The InVeKoS dataset used in this study consists of pseudonymised information on farm business, crop type and AEM implemented at the field parcel level for the years 2016-2019. Standard output coefficients at NUTS2 level were obtained from EUROSTAT (2021). The coefficients were multiplied by field parcel area in order to obtain the standard output per parcel. Where available, yield data were used in order to spatially weight the standard output within each NUTS2 region. At this aim, annual yield data of the predominant arable crops (wheat, maize, barley, rapeseed, sugar beet) was obtained from WOFOST predictions (Hristov et al., 2020) and amended with grassland yield information from LfULG (2001). In order to model cover crop effects, we compiled information on Koeppen-Geiger climate zone, soil texture, and cover crop type applied per field. The effect of flower strips on crop yield was estimated based on the findings of Albrecht et al. (2020). Relative changes in grassland yield induced by AEM aimed at maintaining permanent grasslands were implemented based on yield data from Kesting & Riehl (2014). For land use conversion and buffer areas, we accounted for changes in the cultivation area of the respective crop.

Model

Grassland yield

Grassland yield of non-AEM fields was assumed to depend on grassland type and biophysical site conditions. We used yield estimates for temporary grassland, meadows, pastures, and mowed pastures by LfULG (2001) for the different agricultural structure areas (ASA) of the case study. ASA have been defined by LfULG (2012) as regions of similar agri-environmental characteristics.

Cover crops

Cover crop effects based on soil texture, main crop, cover crop, and climate were estimated according to Jian et al. (2020). We used the SoilHealthDatabase consisting of more than 200 original studies comparing crop yields with and without cover crops. For each observation, the response ratio was calculated as the natural logarithm of the quotient of the yield with and without cover crops. Then, we calculated grouped mean response ratios aggregating all observations by the climate zone of the experiment location (A, B, C, D according to Koppen-Geiger classification), soil texture (coarse, medium, fine), cash crop (vegetables, soybean, wheat, maize, corn-soybean-wheat rotation, corn-soybean rotation, others), and cover crop (grasses, legumes, others). The percent yield change induced by cover crop cultivation was derived from the mean response ratio (RR) using the following equation:

$$Yield\ Effect\ (\%) = (exp(RR) - 1) * 100$$

In the German case study, cover crop effects were only modelled for maize as the subsequent cash crop as this was the predominant cropping sequence and soybean and vegetables are not commonly grown crops in the region. An overview of the inputs and outputs of the model is given in Table 1.

Table 1: Overview of the data used to model cover crops effects on maize yields in the Mulde. N: Number of observations, RR: response ratio, SD: standard deviation, SE: standard error, CV: coefficient of variation, C: temperate climate zone according to Koeppen-Geiger.

Climate Zone	Soil Texture	Cash Crop	Cover Crop	N	RR	SD	SE	CV (%)	Yield Effect (%)
C	coarse	Maize	Grass	18	0.007	0.068	0.016	976.178	0.696
			others	128	0.758	0.718	0.063	94.68	113.412
	medium		Grass	36	0.043	0.269	0.045	631.778	4.343
			others	59	0.155	0.472	0.061	304.086	16.799

Maintaining permanent grasslands

For the effect of the maintaining permanent grasslands AEM on food and fodder production, we took into consideration the reduction of grassland yield due to lower mowing frequency and fertilisation. According to findings from Kesting & Riehl (2014), we defined the fodder yield of grassland fields with AEM to be 58% of the yield of non-AEM fields.

Buffer areas and fallow land

Buffer areas, flower strips and fallow land are unproductive types of land use, thus affecting cultivation area and total production rather than crop yield per area. Based on the meta-analysis by Albrecht et al. (2020) showing ambiguous and partly negligible effects of flower strips on crop yields, we assumed no effect of buffer areas on yields of adjacent fields. When removing the buffer areas in the no AEM scenario, we assumed that the respective fields would yield the median standard output coefficient of the fields of the same farm.

Land-use conversion

Land-use conversion from agricultural to non-agricultural land as well as conversion from arable to permanent grassland was considered as a change of cultivation area.

Assessment

Performance statistics

The baseline yield model of arable crops was validated using annual yield statistics at the NUTS3 level (DESTATIS, 2016-2019). Table 2 lists the coefficients of determination (R^2) and root means square errors (RMSE, dt/ha) of each year.

Table 2: Overview of the agreement of the WOFOST baseline yield model with yield statistics. R^2 : coefficient of determination, RMSE: root mean square error [dt/ha].

Year	R^2	RMSE
2019	0.13	126.59
2018	0.008	134.33
2017	0.19	124.54
2016	0.49	114.79

Uncertainty analysis

For the uncertainty analysis of the cover crop model, we computed the number of observations, standard deviation, standard error and coefficient of variation of the response ratios per group (Table 1). In 3 of the 4 groups, the standard deviation was larger than the mean response ratio, resulting in coefficients of variation well above 100%. This indicates a high uncertainty of the predictions.

2) South Moravia, CZ

Location

South Moravia, Czech Republic, which serves as one of the five BESTMAP case study regions.

Scale of Analysis

Spatial extent: 16.893 17.919, 48.792, 49.189 (xmin, xmax, ymin, ymax; CRS= WGS84)

Spatial resolution: field scale

Temporal extent: 2015 - 2019

Temporal resolution: year

Boundary: administrative

Data

Spatially explicit information on agriculture in the case study region was received from the Ministry of Agriculture of the Czech Republic (MZ) in January 2020. The IACS/LPIS dataset used in this study consists of pseudonymised information on farm business, crop type and AEM implemented at the field parcel level for the years 2015-2019. Additionally, information on EFA (Ecological Focus Areas) implemented at the field parcel level received by the MZ in February 2022 was added to each year. Standard output coefficients at NUTS1 level were obtained from EUROSTAT (2021). The coefficients were multiplied by field parcel area in order to obtain the standard output per parcel. Where available, yield data were used in order to spatially weight the standard output. Annual yield data of the predominant arable crops (wheat, maize, barley, rapeseed, sugar beet, sunflower) was obtained from WOFOST predictions (Hristov et al., 2020) and amended with grassland yield estimations received by the Research Institute of Soil and Water Conservation (VÚMOP) in March 2022. The grassland yield data (TTP) was created by the Czech University of Life Sciences Prague (CZU) and VÚMOP as part of the project ReStEP (Regional Sustainable Energy Policy) in 2014 (VÚMOP, 2015). The data contains grassland yield predictions for three scenarios of nitrogen input (0, 60 and 120 kg per hectare) for all czech BPEJ (rated soil-ecological units). BPEJ data was obtained in March 2022 (SPÚ, 2022). We used the grassland yield estimations to implement relative changes in grassland yield induced by AEM aimed at maintaining grasslands. In order to model cover crop effects, we compiled information on the Koeppen-Geiger climate zone and soil texture per field parcel. The IACS/LPIS data does not provide information on cover crop types, therefore this could not be considered in the analysis. The effect of flower strips on crop yield was estimated based on the findings of Albrecht et al. (2020). For land-use conversion and buffer areas, we accounted for changes in cultivation area of the respective crop.

Model

Grassland yield

Grassland yields were estimated based on model results from the project ReStEP (CZU & VÚMOP, 2014). Based on calculations performed by the online plant process calculator (KTBL, 2022), we used the scenario of 120 kg of nitrogen input per hectare for grassland yields of non-AEM fields. Based on findings by Dellar et al. (2019), yields of temporary grasslands in continental Europe are expected to be twice that of permanent grasslands.

Cover crops

The two types of cover crops in the Czech Republic are i. mixture of at least two allowed crop types, and ii. undersowing of clover and grasses. They can be used in two temporal versions: summer cover crops are sown until 31 July and left on field until 24 September; winter cover crops are sown until 06 September and left on field until 31 October (SZIF, 2016). The EFA dataset only provides information on whether cover crops were used on a field or not, but it does not specify the type or temporal version of the cover crop. In the Czech case study, cover crop effects were only modelled for maize and wheat as the subsequent cash crops as these were the predominant cropping sequences.

Maintaining permanent grasslands

The effects of maintaining permanent grasslands AEM were estimated based on the allowed maximum of nitrogen input for each measure. Nitrogen inputs include nitrogen fertilisation and N input by livestock. In total no more than 160 kg N/ha/year are permitted. AEM with no further nitrogen input restrictions are assigned to the scenario of 120 kg nitrogen input per hectare from the grassland yield estimations, AEM with livestock and no allowed N fertilisation are assigned to the scenario of 60 kg nitrogen input per hectare and AEM with no livestock and no allowed N fertilisation are assigned to the scenario of 0 kg nitrogen input per hectare.

Buffer areas and fallow land

Buffer areas, flower strips and fallow land are unproductive land uses, thus affecting cultivation area and total production rather than crop yield per area. Based on the meta-analysis by Albrecht et al. (2020) showing ambiguous and partly negligible effects of flower strips on crop yields, we assumed no effect of buffer areas on yields of adjacent fields.

Land-use conversion

Land-use conversion from agricultural to non-agricultural land as well as conversion from arable to permanent grassland was considered as a change in cultivation area.

Organic farming

The effect of organic farming on yield of crops and pastures was estimated based on a review of scientific literature. Meta-analyses by Seufert et al. (2012) and Ponisio et al. (2015) have shown that organic farming yields are on average 80% of conventional yields on a global scale. According to the Czech Ministry of Agriculture, organic farming yields mostly range between 50 and 75% of conventional yields (MZ, 2021). The yield gaps are different for different crops like cereals (56-72%), legumes (70%), potatoes (59%), oil crops (27%) and fodder crops (44%) (MZ, 2019). Redlichová et al. (2021) confirm these findings from a monetary perspective, estimating production of cereals and oilseeds under organic management to be on average 53% of that in conventional farming. Based on this evidence we estimated organic yields to be 36.5% lower than conventional yields for all crops except cereals (36%), legumes (30%), potatoes (41%), oil crops (73%) and fodder crops (56%).

3) Catalonia, ES

Location

Catalonia, Spain, which serves as one of the five BESTMAP case study regions.

Scale of Analysis

Spatial extent: 0.1557295, 3.338699, 40.51405, 42.8691 (xmin, xmax, ymin, ymax; CRS=WGS84)

Spatial resolution: field scale

Temporal extent: 2015-2019

Temporal resolution: year

Boundary: administrative

Data

Spatially explicit information on agriculture in the case study region was obtained from Generalitat de Catalunya-Ministry of Agriculture, Livestock, Fisheries and Food-Department of Rural Department (2020). The IACS/LPIS dataset used in this study consists of pseudonymised information on farm business, crop type and AEM implemented at the field parcel level for the years 2015-2019. Annual yield data of the predominant crops at the municipality level was also provided by Generalitat de Catalunya-Ministry of Agriculture, Livestock, Fisheries and Food-Department of Rural Department (2020).

In order to model cover crop effects, the effect of flower strips on crop yield was estimated based on the findings of Albrecht et al. (2020). For land-use conversion, we accounted for changes in cultivation area of the respective crop.

Model

Cover crops/Integrated farming

Cover crops are mainly applied as part of integrated farming practices in olive plantations and orchards. We assumed that this practice does not change crop yield as studies have shown that yields of integrated farming do not deviate from those of conventional farming (Katayama et al., 2019; Morugán-Coronado et al., 2020).

Maintaining permanent grasslands

The AEM directed at maintaining permanent grasslands in the Spanish case study do not prescribe any management restrictions. Instead they are designed in a way to encourage farmers to keep grasslands in production and prevent woody plant encroachment. Therefore we assumed that the yield of these parcels is equal to grassland parcels without an AEM.

Buffer areas and fallow land

Buffer areas, flower strips and fallow land are unproductive types of land use, thus affecting cultivation area and total production rather than crop yield per area. Based on the meta-analysis by Albrecht et al. (2020) showing ambiguous and partly negligible effects of flower strips on crop yields, we assumed no effect of buffer areas on yields of adjacent fields.

Organic farming

The effect of organic farming on yield of crops and pastures was estimated based on a review of scientific literature. Meta-analyses have shown that organic yields are typically lower than conventional ones but with a high variation among crops and study locations. De Ponti et al. (2012), Ponisio et al. (2015), and Smith et al. (2019) all found that organic yields are on average about 80% of conventional yields, both globally and in Mediterranean Europe. Seufert et al. (2012) reported a 75% yield of organic compared to conventional agriculture, however, the gap is notably smaller regarding developed countries (80%) and fruit cultivation (97%). In Spain, organic yields are generally lower than conventional ones but with a few exceptions (e.g. rainfed fruit trees) (Alonso & Guzmán, 2010). Taking into account this evidence, we estimated the yield of organic crops to be 20% lower compared to their conventional counterparts except for tree species where we assumed organic yields to be equal.

4) Humber, U.K.

Location

Humber River Basin, United Kingdom, which serves as one of the five BESTMAP case study regions.

Scale of Analysis

Spatial extent: xmin: 418008.24, ymin: 353867.54, xmax: 542556.68, ymax: 507394.51

Spatial resolution: field scale

Temporal extent: 2015 – 2019

Temporal resolution: year

Boundary: natural

Data

Spatially explicit information on agriculture in the Humber case study region was obtained from the Rural Payments Agency (RPA) of the UK Department for Environment, Food and Rural Affairs. The IACS/LPIS dataset used in this study consists of pseudonymised information on farm business, crop type and AEM implementation at the field parcel level for the years 2015 to 2019. Standard output coefficients at NUTS1 level were obtained from EUROSTAT (2021). The coefficients were multiplied by field parcel area in order to obtain the standard output per parcel. Where available, yield data were used in order to spatially weight the standard output. Annual yield data of the predominant arable crops (maize, sugar beet, wheat, sunflower, winter rapeseed, spring barley, permanent grassland and temporary grassland) was obtained from WOFOST predictions (Hristov et al., 2020) and amended with grassland yield estimations from the literature (Qi et al., 2017; Morrison et al., 1980; Williams et al., 2003). To model the effect of maintaining permanent grassland AEMs, data was taken from the Agriculture and Horticulture Development Board (AHDB) that represented yield change depending on three scenarios of nitrogen input. The effect of flower strips on crop yield was estimated based on the findings of Albrecht et al. (2020). For land-use conversion and buffer areas, we accounted for changes in cultivation area of the respective crop.

Model

Grassland yield

Grassland yields were estimated based on literature (Qi et al., 2017; Morrison et al., 1980; Williams et al., 2003). Qi et al. (2007) and Williams et al. (2003) values were based on an average fertiliser input. Morrison et al. (1980) values were the overall mean of yield at 21 lowland locations in England and Wales. Means were then taken for both permanent and temporary grassland.

Cover crops

On fields featuring catch and cover crops farmers are allowed to use any percentage of a sown mix as long as there is a visible mix of at least two different crops (a minimum of one cereal and one non-cereal): barley, oats and rye as cereal crops; phacelia, vetch, mustard, radish and lucerne as non-cereal crops. However, the datasets used for identifying cover crops only provided information on whether cover crops were present on a field or not, and how much land they occupied, but no information on the species of cover crop was available, therefore we did not model this AEM group.

Maintaining permanent grasslands

The effect of the maintaining permanent grassland AEM on food and fodder production is associated with the lower fertilisation rates. As a result, on land that employs this AEM there is a reduction in yield. Data from the Agriculture and Horticulture Development Board (AHDB) focused on the yields from low-input perennial ryegrass, which is a commonly used grass species in the UK. The yields derived from three scenarios of nitrogen application levels, including 100, 200 and 400 kg N/ha. In the UK, we expect this land without the AEM to have a nitrogen level of 92.4 kg N/ha (Redhead et al., 2018). With the AEM employed, the nitrogen application rate is limited to a max. of 50 kg N/ha. Using the data from AHDB, we therefore calculated the difference in yield as a result of the change in nitrogen levels. At a rate of 100 kg N/ha, a yield of 5 t/ha was produced. Therefore, at 92.4 kg N/ha a yield of 4.62 t/ha is expected, and at 50 kg N/ha a yield of 2.5 t/ha is achieved, meaning the yield of grassland fields with AEM is 45.89% of the yield of non-AEM fields.

Buffer areas

Buffer areas, flower strips and fallow land are unproductive land uses, thus affecting cultivation area and total production rather than crop yield per area. Based on the meta-analysis by Albrecht et al. (2020) showing ambiguous and partly negligible effects of flower strips on crop yields, we assumed no effect of buffer areas on yields of adjacent fields.

Land-use conversion

Land-use conversion from agricultural to non-agricultural land as well as conversion from arable to permanent grassland was considered as a change of cultivation area.

5) Bačka, RS

Location

Bačka Region, Serbia, which serves as one of the five BESTMAP case study regions.

Scale of Analysis

Spatial extent: 18.8194, 20.31623, 45.13434, 46.18879 (xmin, xmax, ymin, ymax; CRS= WGS84)

Spatial resolution: field scale

Temporal extent: 2015 – 2019

Temporal resolution: year

Boundary: administrative

Data

We compiled geospatial (e.g. raster and shapefile data) information on agricultural land-use, including “surrogate” management information since AEM do not currently exist in Serbia (maintaining grasslands, buffer areas/flower strips, fallow land, organic farming) and type of crops grown as well as spatially explicit yield data of agricultural crops and their standard output coefficients.

Land-use data were extracted from the Copernicus portal. AEM “surrogates” were developed and generated in-house from the available online information, Sentinel 2 data and spatial information from Institute of Nature Conservation of Vojvodina Province (PZZP, 2021). The type of crops grown in Bačka CS was extracted from the BioSense database AgroSens (<https://agrosens.rs/>) and yields data from the Statistical Office of the Republic of Serbia (RZS, 2021).

Serbia does not have IACS/LPIS data. As a substitute for IACS/LPIS data, we used data from the AgorSens platform (<https://agrosens.rs/>). Agrosens was developed by the BioSense Institute in order to provide to farmers and agricultural companies in monitoring the growth of crops and planning of the agricultural activities.

By merging data from different years, we identified 11000 parcels of 734 farmers that cover an area of 2200 km², which is in total 27% of the entire Bačka region. For the parcels for which we did not have information for consecutive years, we assigned values from an in-house crop classification (wheat, corn, soyabean, corn and sunflower) database that BioSens generates for each year since 2013 (Lugonja, 2019.). The analysis was thus limited to these five crops, which cover over 93% of parcels in the Bačka region (Census of Agriculture 2012).

Standard output coefficients are not available for Serbia. To fill the gap, during preparation of the Farming System Archetypes (FSAs) for RS (see deliverable D3.5 - Farming System Archetypes for each CS) standard output coefficients were calculated for the Backa region for 2013, based on yield and price data from the Statistical Office of the Republic of Serbia (RZS, 2021).

Model

Assumptions for Bačka CS

Model assumptions: 1. All relevant effects of the AEM “surrogate” are included in the models, 2. Current state and distribution of AEM “surrogate” do not affect baseline yield and standard output, 3. Organic farming effect on yield only depends on climate, soil texture and crop type, 4. Presence of buffer areas, fallow land and maintaining grasslands do not affect yield and standard output of neighbouring fields.

Grassland yield

Grassland yield of non-AEM fields was assumed to depend on grassland type and biophysical site conditions. We used yield estimates for permanent grasslands and pastures by the Institute of

Nature Conservation of Vojvodina Province (Vasin et al., 2010) for the different agricultural areas in Vojvodina. Means were then taken for meadows and pastures.

Maintaining permanent grasslands

The “surrogate” for the maintaining permanent grasslands AEM was derived from the Nature Conservation of Vojvodina Province data (PZZP, 2021). These areas were designed in a way to encourage farmers to keep open grassland and pasture, prevent vegetation succession towards woody encroachment and disable land-use conversion. Also, there is non-fertilization practice in Bačka, and in Serbia as a whole, for meadows and pastures. We assumed that the yield of these parcels is equal to grasslands of non-surrogate-AEM fields.

Buffer areas

Linear elements were used as AEM “surrogates”. They were derived from Sentinel 2 images (which were available for the peak of the vegetation season in 2019) and processed on Google engine. An NDVI time series was generated, and a threshold selected to detect permanent vegetation locations along roads and arable fields in the Bačka CS region. Identified areas were then used as “surrogates” for buffer areas and flower strips in arable fields. The “surrogate” file for fallow land was developed within the agricultural field zones from Sentinel 2 images by developing and applying an in-house algorithm for ploughing detection. We determined areas where in three consecutive years no ploughing activity was detected. The developed binary files were masked with permanent grassland maintenance and grassland maps.

Organic farming

The effect of organic farming on yield of crops and pastures was estimated based on a review of scientific literature. Meta-analyses have shown that organic yields are typically lower than conventional ones but with a high variation among crops and study locations. De Ponti et al. (2012), Ponisio et al. (2015), and Smith et al. (2019) all found that organic yields are on average about 80% of conventional yields. Seufert et al. (2012) reported a 75% yield of organic compared to conventional agriculture, however, the gap is notably smaller regarding developed countries (80%) and fruit cultivation (97%). In Serbia, organic yields are generally lower than conventional ones in the range of 10-40% (Mirecki, 2011). Considering the published data, we estimated the yield of organic crops to be 20% lower compared to their conventional counterparts.

References:

Albrecht, M., Kleijn, D., Williams, N.M., Tschumi, M., Blaauw, B.R., Bommarco, R., Campbell, A.J., Dainese, M., Drummond, F.A., Entling, M.H., Ganser, D., Arjen de Groot, G., Goulson, D., Grab, H., Hamilton, H., Herzog, F., Isaacs, R., Jacot, K., Jeanneret, P., Jonsson, M., Knop, E., Kremen, C., Landis, D.A., Loeb, G.M., Marini, L., McKerchar, M., Morandin, L., Pfister, S.C., Potts, S.G., Rundlöf, M., Sardiñas, H., Sciligo, A., Thies, C., Tschamntke, T., Venturini, E., Veromann, E., Vollhardt, I.M., Wäckers, F., Ward, K., Westbury, D.B., Wilby, A., Woltz, M., Wratten, S. and Sutter, L. (2020): The effectiveness of flower strips and hedgerows on pest control, pollination services and crop yield: a quantitative synthesis. *Ecol. Lett.*, vol. 23, 1488-1498. <https://doi.org/10.1111/ele.13576>.

Alonso, A.M. and Guzmán, G.J. (2010): Comparison of the Efficiency and Use of Energy in Organic and Conventional Farming in Spanish Agricultural Systems. *Journal of Sustainable Agriculture*, vol. 34(3), 312-338. <https://doi.org/10.1080/10440041003613362>.

Census of Agriculture 2012—Agriculture in the Republic of Serbia, Volume 1, Statistical Office of the Republic of Serbia, Belgrade (2013). Available at: <https://www.stat.gov.rs/en-us/oblasti/poljoprivreda-sumarstvo-i-ribarstvo/popis-poljoprivrede/>

CZU and VÚMOP (2014): Potenciální výnos trvale travních porostů (TTP) [Potential yield of permanent grassland (TTP)]. Available at: <https://metadata.vumop.cz/en/record/basic/53f3474e-a714-41bd-b7cf-08c87f000001>.

Dellar, M., Topp, C., Pardo, G., del Prado, A., Fitton, N., Holmes, D., Banos, G. and Wall, E. (2019): Empirical and dynamic approaches for modelling the yield and N content of European grasslands. *Environmental Modelling & Software*, vol. 122, 104562. <https://doi.org/10.1016/j.envsoft.2019.104562>.

De Ponti, T., Rijk, B. and Ittersum, M.K. van (2012): The crop yield gap between organic and conventional agriculture. *Agricultural Systems*, vol. 108(C), 1-9. <https://doi.org/10.1016/j.agsy.2011.12.004>.

DESTATIS (Statistisches Bundesamt) (2016-2019): Erträge ausgewählter landwirtschaftlicher Feldfrüchte - Jahressumme - regionale Tiefe: Kreise und krfr. Städte [Yields of selected agricultural crops - annual total - regional depth: administrative districts and independent cities]. Available at: <https://www.regionalstatistik.de/genesis/online?operation=statistic&levelindex=0&levelid=1637223269322&code=41241&option=table&info=on#abreadcrumb>.

DESTATIS (Statistisches Bundesamt) (2021): 41241-01-03-4: Erträge ausgewählter landwirtschaftlicher Feldfrüchte - Jahressumme - regionale Tiefe: Kreise und krfr. Städte [Yields of selected agricultural crops - annual total - regional depth: administrative districts and independent cities]. Available at: <https://www.regionalstatistik.de/genesis/online?operation=table&code=41241-01-03-4&bypass=true&levelindex=1&levelid=1633957779441#abreadcrumb>.

De Wit, A., Boogaard, H., Fumagalli, D., Janssen, S., Knapen, R., Kraalingen, D. van, Supit, I., Wijnagaart, R. van der and Diepen, K. van (2019): 25 years of the WOFOST cropping systems model. *Agricultural systems*, vol. 168, 154-167. <https://doi.org/10.1016/j.agsy.2018.06.018>.

Diepen, C.A. van, Wolf, J. and Keulen, H. van (1989). WOFOST: a simulation model of crop production. *Soil Use and Management*, vol. 5, 16-24. <https://doi.org/10.1111/j.1475-2743.1989.tb00755.x>.

EUROSTAT (2021): Standard output coefficients. Available at: <https://ec.europa.eu/eurostat/web/agriculture/data/ancillary-data>.

EUROSTAT (2022): Agricultural factor income per annual work unit (AWU) (source: Eurostat, DG AGRI) (sdg_02_20). ESMS Indicator Profile (ESMS-IP). Available at: https://ec.europa.eu/eurostat/cache/metadata/en/sdg_02_20_esmsip2.htm.

Generalitat de Catalunya-Ministry of Agriculture, Livestock, Fisheries and Food-Department of Rural Department (2020): SIGPAC data. https://governobert.gencat.cat/ca/dades_obertes/inici.

Hristov, J., Toreti, A., Perez Dominguez, I., Dentener, F., Fellmann, T., Elleby, C., Ceglar, A., Fumagalli, D., Niemeyer, S., Cerrani, I., Panarello, L. and Bratu, M. (2020): Analysis of climate change impacts on EU agriculture by 2050. EUR 30078 EN, Publications Office of the European Union, Luxembourg, ISBN 978-92-76-10617-3, doi:10.2760/121115, JRC119632.

Jian, J., Du, X., and Stewart, R.D. (2020): A database for global soil health assessment. *Sci Data*, vol. 7(16). <https://doi.org/10.1038/s41597-020-0356-3>.

Katayama, N., Bouam, I., Koshida, C. and Baba, Y.G. (2019): Biodiversity and yield under different land-use types in orchard/vineyard landscapes: A meta-analysis. *Biological Conservation*, vol. 229, 125–133. doi:10.1016/j.biocon.2018.11.020.

Kesting, S. and Riehl, G. (2014): Abschätzung des Grünlandertrages in Sachsen [Estimation of the grassland yield in Saxony]. Available at: https://www.lfl.bayern.de/mam/cms07/ipz/dateien/aggf_2014_kesting_riehl.pdf.

KTBL (2022): Online Verfahrensrechner des Kuratorium für Technik und Bauwesen in der Landwirtschaft [Online calculator of Association for Technology and Structures in Agriculture]. Available at: <http://daten.ktbl.de/vrpfanze/home.action>.

LfULG (Sächsisches Landesamt für Umwelt, Landwirtschaft und Geologie) (2001): Ermittlung von Erträgen auf dem Grünland [Determination of yields on grassland]. Available at: <https://www.landwirtschaft.sachsen.de/download/Ertragsermittlung.pdf>.

LfULG (Sächsisches Landesamt für Umwelt, Landwirtschaft und Geologie) (2012): Die Agrarstrukturgebiete in Sachsen - Zusammenstellung standörtlicher Bedingungen für die Landwirtschaft und Flächennutzung [The agricultural structure areas in Saxony - compilation of local conditions for agriculture and land use]. Available at: https://www.landwirtschaft.sachsen.de/download/RAWIS_Natuerliche_Bedingungen_ASG.pdf.

Lugonja, P., Brdar, S., Simović, I., Mimić, G., Palamarchuk, Y., Sofiev, M. and Šikoparija, B. (2019): Integration of in situ and satellite data for top-down mapping of Ambrosia infection level. *Remote Sensing of Environment*, vol. 235, 111455.

Mirecki, N., Wehinger, T., Repic, P. and Jakilč, M. (2011): Priručnik za organsku proizvodnju – za osoblje savjetodavne službe [Handbook for organic production - for personnel of the advisory service]. Biotehnički fakultet, Podgorica. ISBN 978-9940-606-00-8 COBISS.CG-ID 19270928.

Morrison, J., Jackson, M.V. and Sparrow, P.E. (1980): The response of perennial ryegrass to fertilizer nitrogen in relation to climate and soil. Report of the joint ADAS/GRI grassland manuring trial-GM. 20. Tech. Rep. 27, The Grassland Research Institute, Hurley, 95 p.

Morugán-Coronado, A., Linares, C., Gómez-López, M.D., Faz, Á. and Zornoza, R. (2020): The impact of intercropping, tillage and fertilizer type on soil and crop yield in fruit orchards under Mediterranean conditions: A meta-analysis of field studies. *Agricultural Systems*, vol. 178, 102736, ISSN 0308-521X, <https://doi.org/10.1016/j.agsy.2019.102736>.

MZ (Ministerstvo zemědělství) (2019): ROČENKA 2018 Ekologické zemědělství v České republice / YEARBOOK 2018 Organic Farming in the Czech Republic. 57 - 73. Available at: https://eagri.cz/public/web/file/643739/Rocenka_ekologickeho_zemedelstvi_2018_WEB.pdf.

MZ (Ministerstvo zemědělství) (2021): AKČNÍ PLÁN ČR pro rozvoj ekologického zemědělství v letech 2021–2027 [ACTION PLAN of the Czech Republic for the development of organic agriculture in 2021-2027]. Available at: https://eagri.cz/public/web/file/681755/Akcni_plan_CR_2021_2027.pdf.

Ponisio, L.C., M'Gonigle, L.K., Mace, K.C., Palomino, J., de Valpine, P. and Kremen, C. (2015): Diversification practices reduce organic to conventional yield gap. *Proc. R. Soc. B*. 2822014139620141396.

PZZP (2021): Institute for Nature Conservation of Voivodina Province. Available at: <https://pzzp.rs/en/>

Qi, A., Murray, P. J. and Richter, G. M. (2017): Modelling productivity and resource use efficiency for grassland ecosystems in the UK. *European Journal of Agronomy*, vol. 89, 148-158.

R Core Team (2020): R: A language and environment for statistical computing. R Foundation for Statistical Computing, Vienna, Austria. Available at: <https://www.R-project.org/>.

Redlichová, R., Chmelíková, G., Blažková, I., Svobodová, E. and Vanderpuje, I.N. (2021): Organic Food Needs More Land and Direct Energy to Be Produced Compared to Food from Conventional Farming: Empirical Evidence from the Czech Republic. *Agriculture*, vol. 11(9), 813. <https://doi.org/10.3390/agriculture11090813>.

RZS (2021): Crop production. Available at: <https://data.stat.gov.rs/Home/Result/130102?languageCode=en-US>

Seufert, V., Ramankutty, N. and Foley, J.A. (2012): Comparing the yields of organic and conventional agriculture. *Nature*, vol. 485, 229–232. <https://doi.org/10.1038/nature11069>.

SMEKUL (Sächsisches Staatsministerium für Energie, Klimaschutz, Umwelt und Landwirtschaft) (2020): InVeKoS Sachsen 2016-2019.

Smith, O.M., Cohen, A.L., Rieser, C.J., Davis, A.G, Taylor, J.M., Adesanya, A.W., Jones, M.S., Meier, A.R., Reganold, J.P., Orpet, R.J., Northfield, T.D. and Crowder, D.W. (2019): Organic Farming Provides Reliable Environmental Benefits but Increases Variability in Crop Yields: A Global Meta-Analysis. *Frontiers in Sustainable Food Systems*, vol. 3, 82. <https://doi.org/10.3389/fsufs.2019.00082>.

SPÚ (2022): Celostátní databáze BPEJ. Available at: <https://www.spucr.cz/bpej/celostatni-database-bpej>.

SZIF (Státní zemědělský intervenční fond) (2016): INFORMACE PRO ŽADATELE - SZP 2016. PLATBA NA ZEMĚDĚLSKÉ POSTUPY PŘÍZNIVÉ PRO KLIMA A ŽIVOTNÍ PROSTŘEDÍ (GREENING) [Information for applicants - SZP 2016. Payment for climate- and environment-friendly agricultural practices (Greening)]. Available at: https://www.szif.cz/cs/CmDocument?rid=%2Fapa_anon%2Fcs%2Fzpravy%2Fplatby_na_zaklade_jz%2Fsaps%2Fgreening%2F1457510247949.pdf.

Vasin, J., Belić, M., Nešić, L., Ninkov, J. and Zeremski-Škorić, T. (2010): Influence of physical properties of saline soils in Vojvodina at biomass production. *Savremena poljoprivredna tehnika*, vol. 36(3), 220-227.

VÚMOP (2015): Trvalé travní porosty (TTP) [Permanent grassland]. Available at: [https://restep.vumop.cz/encyklopedie/index.php/Trval%C3%A9_travn%C3%AD_porosty_\(TTP\)](https://restep.vumop.cz/encyklopedie/index.php/Trval%C3%A9_travn%C3%AD_porosty_(TTP)).

Williams, T.A., Evans, D.R., Rhodes, I. and Abberton, M.T. (2003): Long-term performance of white clover varieties grown with perennial ryegrass under rotational grazing by sheep with different nitrogen applications. *The Journal of Agricultural Science*, vol. 140(2), 151-159.

Carbon sequestration model factsheet

BESTMAP carbon sequestration model

2022-05-25

The structure of this factsheet is largely based on the ODMAP (Overview, Data, Model, Assessment and Prediction) protocol developed by Zurell et al. 2020 [doi/full/10.1111/ecog.04960](https://doi.org/10.1111/ecog.04960)

Overview

Authorship

Contact: Fanny Langerwisch (fanny.langerwisch@upol.cz)

Model name

Model of the effect of agro-environmental measures on soil organic carbon.

Model objective

Main objective of the model is to estimate how the adoption of agro-environmental measures (AEM) affects soil carbon sequestration on field level / within landscapes (see Figure 1 for a conceptual workflow of the model).

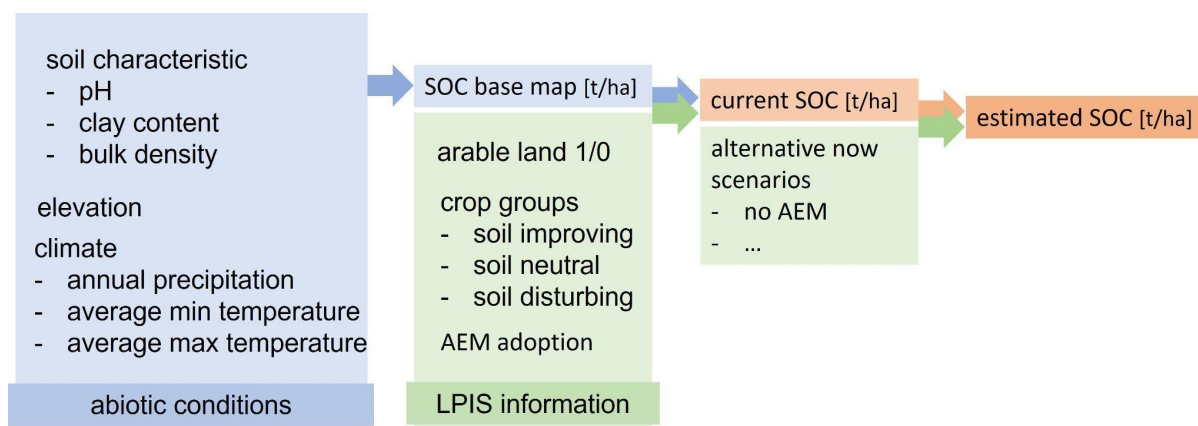


Figure 1: Conceptual figure of the workflow of the carbon model.

Model output

The model output consists of maps of soil organic carbon per field/parcel, under the current land-use patterns and AEM implementation and under alternative-now scenarios.

Data specifications

Response data type: soil organic carbon (SOC [t/ha]).

Predictor types: geospatial data (raster and polygons) on soil characteristics, climates, crops and adopted AEMs (agri-environmental schemes and ecological focus areas).

Hypotheses

We hypothesise that SOC is sensitive to the crop type and to the adoption of AEM. We also hypothesise that underlying SOC (SOC_{base}), which is only driven by abiotic factors (e.g. climate, clay content), is affected by the above mentioned land-use interventions and AEM interventions (SOC_{lu} and SOC_{curr} , respectively). To test our hypothesis we compared the simulated SOC under the current AEM implementation (SOC_{curr}) with a second scenario in which no AEM is implemented.

Assumptions

Model assumptions: (1) The soil organic carbon depends on abiotic conditions and is altered by land cover and land use. (2) Current amount of soil carbon is in equilibrium, i.e. the soil already contains organic carbon, there is no general building-up of soil organic carbon assumed. (3) There is no dependence of SOC on soil management (ploughing/mulching etc). (4) SOC is affected differently by different crop groups (soil-improving, soil-disturbing and neutral crops). (5) The rotation of each parcel over several years can be depicted by the crops rotated on all parcels per farm. This can be used to identify a 'pseudorotation', which indicates the coverage with soil-improving and soil-disturbing crops. (6) The effect of the AEM 'maintaining permanent grassland', 'buffer strips' and 'land-use conversion to permanent grassland' are similar to the effect of growing 'permanent grassland' on the parcel.

Algorithms and workflow

We calculated the soil organic carbon base for each parcel/pixel only depending on abiotic conditions, such as climate and soil characteristics (clay, pH, bulk density, elevation, annual precipitation, average min. and max. temperature, see Eq.1).

$$SOC_{base} = -e^{(\text{intercept} + \text{elev} \times c.\text{elev} + \text{clay} \times c.\text{clay} + \text{pH} \times c.\text{pH} + \text{BD} \times c.\text{BD} + \text{prec} \times c.\text{prec} + \text{Tmin} \times c.\text{Tmin} + \text{Tmax} \times c.\text{Tmax})} \quad (\text{Eq.1})$$

The coefficients for this calculation (Table 1) were extracted from LUCAS observation points making use of a quasi-poisson generalised linear model. (about 8,400, Further information and data accessibility of the LUCAS data can be found at <http://esdac.jrc.ec.europa.eu/projects/lucas>). For our study we included only the 8,554 points classified as arable, which were also by Quemada et al. 2020., also used in the DayCent model (Box 1), Quemada et al. 2020) making use of a quasi-poisson generalised linear model.

The model led to an $R^2=0.902$. The deviance residuals were distributed the following: Min=-9.7610; 1Q= -0.6710; Median=0.0440; 3Q=0.7073, Max=10.5140.

Table 1: Coefficients used in Eq.1 to calculate the SOC basemap.

Input variable	Coefficient	Value and significance
-	intercept	8.938178***
elevation (<i>elev</i>)	c.elev	-0.000077***
clay content (<i>clay</i>)	c.clay	-0.009685***
soil pH (<i>pH</i>)	c.pH	-0.022066***
bulk density (<i>BD</i>)	c.BD	-3.162275***

mean annual precipitation (<i>prec</i>)	c.prec	-0.000097***
mean maximal temperature (<i>Tmax</i>)	c.Tmax	-0.014182***
mean minimal temperature (<i>Tmin</i>)	c.Tmin	0.013269***

In a second step, we used the baseline SOC (SOC_{base}) and adapted it according to the land use to calculate the SOC_{lu} . On arable parcels, we assumed that SOC is altered by different crops. We grouped soil-disturbing crops, such as potatoes and sugar beet, which reduce the SOC, soil-improving crops, such as legumes, which increase the SOC, and neutral crops, which do not affect the SOC. This grouping was done for each case study separately. The parameters for the effects were extracted from literature. The parameters can be adapted to case study conditions. Additionally, we adapted the SOC (SOC_{lu} on permanent grassland) for parcels under permanent grassland management, assuming an increase in SOC based on Poeplau & Don (2015). Also this parameter can be adapted locally. We assumed SOC to remain unaltered in the remaining parcels, i.e. non-arable and non-permanent grassland parcels.

The last step was the modification of SOC depending on the currently applied AEM (SOC_{curr}) and alternative-now scenarios (SOC_{alt}). Here, we apply parameters for each of the following AEM groups: (1) cover crops, (2) organic farming, (3) maintaining permanent grassland, (4) buffer strips and land-use conversion (5) to permanent grassland and (6) to forest. The difference between SOC_{curr} and SOC_{alt} is the different distribution of AEM, where SOC_{curr} represents the current AEM adoption and SOC_{alt} any alternative AEM adoption. The parameters for this calculation are extracted from the literature and can be further adapted to local conditions. The parameters to calculate SOC_{lu} ($p.lu.xxx$) and SOC_{curr} and SOC_{alt} ($p.aem.xxx$) are listed in Table 2.

Calculation of SOC_{lu} and SOC_{curr} (as well as SOC_{alt}) with the following equations.

$$SOC_{lu} = SOC_{base} \times (1 + p.lu.xxx) \quad (\text{Eq. 2})$$

$$SOC_{curr} = SOC_{lu} \times (1 + p.aem.xxx) \quad (\text{Eq.3})$$

Eq.3 is applied to calculated SOC_{curr} as well as SOC_{alt} .

Table 2: Parameters used for the adaptation of the baseline SOC according to different land use and AEM application.

Parameter name	Value	Source
p.lu.soilimproving	0.35	Wu et al. 2016, Gregorich et al. 2001, Guan et al. 2016
p.lu.soildisturbing	-0.1	Goidts & van Wesemael 2007
p.lu.permgrass	0.45	Poeplau & Don 2015, Gregorich et al. 2001
p.aem.covercrops	0.1	Crystal-Ornelas et al. 2021, Poeplau & Don 2015, Abdalla et al. 2019
p.aem.organic	-0.05	Lorenz & Lal 2016, Mondelears et al. 2006, Gattinger et al. 2012

p.aem.maintgrass	0.45	Poeplau & Don 2015, Gregorich et al. 2001
p.aem.buffer	0.45	Poeplau & Don 2015, Gregorich et al. 2001
p.aem.luconvgrass	0.3	Poeplau & Don 2015, Ledo et al. 2020, Martens et al. 2003, Gregorich et al. 2001
p.aem.luconvforest	0.45	Poeplau & Don 2015, Gregorich et al. 2001, Martens et al. 2003

The resulting maps of SOC under different AEM implementation scenarios, including a “no AEM” scenario and several different AEM implementations (varying spatial arrangements of one or multiple AEM types) were used to estimate the effect of each agro-environmental measure.

Uncertainty analysis

We conducted an uncertainty analysis of the SOC basemap calculation (SOC_{base}), in which we changed the values of all input variables (see Table 1) by $\pm 5\%$ and $\pm 10\%$. The effect of changes in the bulk density (BD) was highest, which is in line with our expectations and with empirical evidence since the coefficient for BD (c_{BD}) was the biggest. The effect of variation in clay content and maximal temperature were small, while elevation, precipitation and minimal temperature had a negligible effect.

Additionally, we did a sensitivity analysis of the SOC_{adapt} and SOC_{curr} by changing the parameters listed in Table 2.

Model validation

Validation of SOC base map (SOC_{base}) and current SOC (SOC_{curr}) was done with observations from SOILGRIDS 250m organic carbon stock. Case study specific validation is possible with regional data.

Software

R version 4.1.2 ‘Bird Hippie’ (2021-11-01) R Core Team (2021).

Code availability: the R code used for the preparation of the variables and for fitting the model is available here: <https://git.ufz.de/bestmap/bestmap-carbon-sequestration>

Linking the model outputs to indicators

The model results can be linked to the following policy indicators:

C41 - Soil organic matter in arable land

The indicator consists of 2 sub-indicators: i. the total estimate of organic carbon content in arable land; ii. the mean organic carbon content. The indicator is expressed as an estimate of the total SOC stocks in topsoil (0-20) of EU Member States. The mean SOC concentration per Member State is calculated for orientation purposes (European Commission 2021). The outputs of the carbon sequestration model can be linked to the first sub-indicator of the indicator C41.

Model specifications in each case study

1) South Moravia, CZ

Location

South Moravia, Czech Republic, covering parts of Jihomoravský kraj and Zlínský kraj.

Scale of Analysis

Spatial extent: latitude 16.893 to 17.915, longitude 48.792, 49.172

Spatial resolution: field size (average 0.06km², min 0.000001km², max 3.05km²)

Temporal resolution: 2019

Boundary: administrative (field level)

Data

As spatially explicit information for South Moravia, we received the IACS/LPIS data for the years 2015 to 2019 from the Ministry of Agriculture of the Czech Republic. These data include crop type, agri-environmental schemes (AES) - all as cover per parcel, as well as user ID and parcel ID. The user ID is used to identify farms (one user represents one farm). We also received information about the ecological focus area (EFA) schemes for 2019. For the model we used the latest 2019 data.

The parameters estimating the effects of the different land use, including AEM, on SOC and their sources are reported in Table 2. These can further be adapted using regional or CS-specific data.

Geospatial information on climate, topography, soil characteristics was extracted from European-wide datasets (Table 3).

Table 3: Overview of the geospatial data used in the CZ model.

Variable	Unit of measure	Source	Original resolution of dataset
Bulk density	g/cm ³	European Soil Database Derived data , European Soil Data Centre (ESDAC)	1km
Clay content in the upper 30 cm	g/kg	Clay content, SoilGrids	250m
pH in the upper 30 cm	[-]*10	pH water, SoilGrids	250m
Elevation	m	EU-DEM v1.1 , Copernicus Land Monitoring Service	25m
Annual precipitation	mm/y	Multiannual precipitation (yearly sum), Climatologies 1981-2010 TerraClimate	~4km (1/24th degree)
Minimum temperature	°C	Multiannual minimum temperature (average), Climatologies 1981-2010	~4km (1/24th degree)

		TerraClimate	
Maximum temperature	°C	Multiannual maximum temperature (average), Climatologies 1981-2010 TerraClimate	~4km (1/24th degree)
crop types	ha	IACS/LPIS for year 2019, Ministry of Agriculture of the Czech Republic	shapefile
AEM application (separately for each AEM group, i.e. buffer areas, cover crops, land-use conversion to grassland/to forest, maintaining permanent grassland, organic farming)	ha of cover per field parcel	IACS/LPIS for year 2019, Ministry of Agriculture of the Czech Republic	shapefile

Model

To initialise the soil organic carbon (SOC) we conducted two steps. First, we used coefficients retrieved from an analysis of LUKAS observation points (about 8400, also used in the DAYCENT model, Quemada et al. 2020). The analysis showed the dependence of SOC on elevation, pH, clay content, bulk density and climate. To initialise the case study SOC basemap, we used case-study specific data for the above mentioned variables, extracted from European wide available data (Table 3).

We applied two types of alternative-now scenarios, namely noAEM and oneAEM. For the alternative-now scenario noAEM we exchanged the AEM on the parcel with the dominant crop. This means that instead of assuming any AEM on the parcel we only allowed the dominant crop on the parcel.

Variable pre-selection

Variable pre-selection: Explanatory variables were chosen to reflect environmental conditions likely to impact the soil organic carbon. These are climatic conditions (precipitation and temperature) and soil characteristics (such as pH, bulk density or clay content). The same set of variables are used in all case study areas.

Model settings

The baseline was the SOC only considering the abiotic conditions. We added the effect of the current grown crops (no AEM), and the current AEMs, additionally we calculated the SOC under the adoption of the AEM 'cover crops' on all arable parcels.

Model outputs

Estimated SOC [t/ha] for each parcel under current land use and AEM adoption, without any AEM and with a potential AEM distribution.

Uncertainty / Sensitivity

There are several aspects of the model that can incorporate uncertainty. To assess the uncertainty of the model input we conducted a sensitivity analysis of the input parameters to the SOC basemap. We change the values for each of the input variables by +/- 5% and +/-10%.

The following table shows the results for the change of 10%. The figures show the SOC values calculated with the changed input over the SOC calculated with the original values. One can clearly see that elevation, minimum temperature and precipitation lead to the smallest changes, while bulk density leads to the largest. Changes in clay content, pH and maximal temperature lead to intermediate values.

The strong reaction to changes in bulk density is correlated with the importance of this variable in the SOC calculation. Table 4 shows the coefficients with which each variable contributes to the model and the relative changes in the SOC.

Table 4: Relative change of SOC under the different changes of variables.

	coef	-10%	-5%	+/-0%	+5%	+10%
elev	-0.0001	-0.2201	-0.1100	0	0.1098	0.2195
clay	-0.0097	-2.8645	-1.4220	0	1.4018	2.7837
pH	-0.0221	-1.4879	-0.7412	0	0.7357	1.4660
BD	-3.1623	-53.8194	-24.0078	0	19.3393	34.9221
prec	-0.0001	-0.6431	-0.3210	0	0.3200	0.6390
Tmin	0.0133	-0.5841	-0.2916	0	0.2908	0.5807
Tmax	-0.0142	-3.6798	-1.8233	0	1.7906	3.5491

The change in SOC is linear to the size of the coefficient (both ln-transformed).

2) Catalonia, ES

Location

Catalonia, Spain, which serves as one of the five BESTMAP case study regions.

Scale of Analysis

Spatial extent: 0.1557295, 3.338699, 40.51405, 42.8691 (xmin, xmax, ymin, ymax; CRS= WGS84) (Approximately 32 000 ha).

Spatial resolution: field parcel

Temporal extent: 2019

Boundary: administrative

Data

As spatially explicit information for Catalonia, we received the IACS/LPIS/Single Declaration data for the years 2015 to 2019 from the Ministry of Climate Action, Food and Rural Agenda - Department of Agriculture- of the Generalitat de Catalunya. The Single Application (DUN in Catalonia) is the annual declaration that the titleholder who disposes of a productive agricultural area has to compulsorily report to carry out certain procedures, among which stand out the application for community grants (CAP). Since 2005, following the recommendations from the INSPIRE Directive, it is possible to freely consult and view LPIS data from Catalonia. The request of LPIS data caused that in the year 2012 the Department

of Agriculture set out the FREE and OPEN access to the database from Generalitat's public data portals. Its publication promotes the use of new technologies, it drives the creation of new tools and uses for the agricultural sector and, at the same time, it makes possible its analysis through "Big Data" procedures. In parallel, it accomplishes the national and community regulation obligations and recommendations in the field of transparency and reuse of public management data for the citizens. In May 2019, the Department of Agriculture was the only European administration that was currently providing free and open access to all this data.

These data include crop type, agri-environmental schemes (AES) and ecological focus areas (EFA) schemes (all as cover per parcel), as well as user ID and parcel ID. For the model we used the latest 2019 data. Geospatial information on climate, topography, soil characteristics was extracted from European-wide datasets (Table 5). The parameters estimating the effects of the different environmental variables on SOC and their sources are reported in Table 2. These can further be adapted using regional or CS-specific data should this become available for future updates of the model.

Table 5: Overview of the geospatial data used in the ES model.

Variable	Unit of measure	Source	Original resolution of dataset
Bulk density	g/cm ³	European Soil Database Derived data , European Soil Data Centre (ESDAC)	1km
Clay content in the upper 30 cm	g/kg	Clay content, SoilGrids	250m
pH in the upper 30 cm	[-]*10	pH water, SoilGrids	250m
Elevation	m	EU-DEM v1.1 , Copernicus Land Monitoring Service	25m
Annual precipitation	mm/y	Multiannual precipitation (yearly sum), Climatologies 1981-2010 TerraClimate	~4-km (1/24th degree)
Minimum temperature	°C	Multiannual minimum temperature (average), Climatologies 1981-2010 TerraClimate	~4-km (1/24th degree)
Maximum temperature	°C	Multiannual maximum temperature (average), Climatologies 1981-2010 TerraClimate	~4-km (1/24th degree)
crop types	soil improving, soil neutral, soil disturbing	IACS/LPIS for year 2019, Ministry of Agriculture of the Czech Republic	shapefile
AEM application (separately for each AEM group, i.e. buffer)	% of cover per field parcel	IACS/LPIS for year 2019, Ministry of Agriculture of the Czech Republic	shapefile

areas, cover crops, land-use conversion to grassland/to forest, maintaining permanent grassland, organic farming)			
---	--	--	--

Model

The carbon sequestration model for the ES CS was run with the same specifications as in the CZ CS; check the above CZ section for details on the variable pre-selection, model outputs, uncertainty/sensitivity analysis.

3) Humber, UK

Location

Humber River Basin, United Kingdom, which serves as one of the five BESTMAP case study regions.

Scale of Analysis

Spatial extent: -1.723979, 0.1374987, 53.05964, 54.46706 (xmin, xmax, ymin, ymax; CRS= WGS84)

Spatial resolution: field parcel

Temporal resolution: 2019

Boundary: administrative (field level)

Data

As spatially explicit information for the Humber,, we received the IACS/LPIS data for the years 2015 to 2019 from the Rural Payments Agency. These data include crop type, agri-environmental schemes and ecological focus areas schemes, as well as user ID and parcel ID. For the model we used the latest 2019 data. Geospatial information on climate, topography, soil characteristics was extracted from European-wide datasets (Table 6). The parameters estimating the effects of the different environmental variables on SOC and their sources are reported in Table 2. These can further be adapted using regional or CS-specific data should this become available for future updates of the model.

Table 6: Overview of the geospatial data used in the UK model.

Variable	Unit of measure	Source	Original resolution of dataset
Bulk density	g/cm ³	European Soil Database Derived data , European Soil Data Centre (ESDAC)	1km
Clay content in the upper 30 cm	g/kg	Clay content, SoilGrids	250m
pH in the upper 30 cm	[-]*10	pH water, SoilGrids	250m

Elevation	m	EU-DEM v1.1 , Copernicus Land Monitoring Service	25m
Annual precipitation	mm/y	Multiannual precipitation (yearly sum), Climatologies 1981-2010 TerraClimate	~4km (1/24th degree)
Minimum temperature	°C	Multiannual minimum temperature (average), Climatologies 1981-2010 TerraClimate	~4km (1/24th degree)
Maximum temperature	°C	Multiannual maximum temperature (average), Climatologies 1981-2010 TerraClimate	~4km (1/24th degree)
crop types	soil improving, soil neutral, soil disturbing	IACS/LPIS for year 2019, Rural Payments Agency	shapefile
AEM application (separately for each AEM group, i.e. buffer areas, cover crops, land-use conversion to grassland/to forest, maintaining permanent grassland, organic farming)	% of cover per field parcel	IACS/LPIS for year 2019, Rural Payments Agency	shapefile

Model

The carbon sequestration model for the UK CS was run with the same specifications as in the CZ CS; check the above CZ section for details on the variable pre-selection, model outputs, uncertainty/sensitivity analysis.

4) Mulde, DE

Location

Mulde River Basin, Saxony, Germany, which serves as one of the five BESTMAP case study regions.

Scale of Analysis

Spatial extent: 12.34771, 13.69364, 50.3809, 51.64169 (xmin, xmax, ymin, ymax, CRS=WGS84)

Spatial resolution: field parcel

Temporal resolution: 2019

Boundary: administrative (field level)

Data

As spatially explicit information for the Mulde, we received the IACS/LPIS data for the years 2016 to 2019 from the Saxon State Ministry for Energy, Climate Protection, Environment and Agriculture (Sächsisches Staatsministerium für Energie, Klimaschutz, Umwelt und Landwirtschaft, SMEKUL). These data include crop type, agri-environmental schemes and ecological focus areas, as well as a pseudonymised farmers' ID. For the model we used the latest 2019 data. Geospatial information on climate, topography, soil characteristics was extracted from European-wide datasets (Table 7). The parameters estimating the effects of the different environmental variables on SOC and their sources are reported in Table 2. These can further be adapted using regional or CS-specific data should this become available for future updates of the model.

Table 7: Overview of the geospatial data used in the DE model.

Variable	Unit of measure	Source	Original resolution of dataset
Bulk density	g/cm ³	European Soil Database Derived data , European Soil Data Centre (ESDAC)	1km
Clay content in the upper 30 cm	g/kg	Clay content, SoilGrids	250m
pH in the upper 30 cm	[-]*10	pH water, SoilGrids	250m
Elevation	m	EU-DEM v1.1 , Copernicus Land Monitoring Service	25m
Annual precipitation	mm/y	Multiannual precipitation (yearly sum), Climatologies 1981-2010 TerraClimate	~4km (1/24th degree)
Minimum temperature	°C	Multiannual minimum temperature (average), Climatologies 1981-2010 TerraClimate	~4km (1/24th degree)
Maximum temperature	°C	Multiannual maximum temperature (average), Climatologies 1981-2010 TerraClimate	~4km (1/24th degree)
crop types	soil improving, soil neutral, soil disturbing	IACS/LPIS for year 2019, SMEKUL	shapefile
AEM application (separately for each AEM group, i.e. buffer areas, cover crops, land-use conversion)	% of cover per field parcel	IACS/LPIS for year 2019, SMEKUL	shapefile

to grassland/to forest, maintaining permanent grassland, organic farming)			
---	--	--	--

Model

The carbon sequestration model for the UK CS was run with the same specifications as in the CZ CS; check the above CZ section for details on the variable pre-selection, model outputs, uncertainty/sensitivity analysis.

5) Bačka, RS

Location

Bačka region, Serbia, which serves as one of the five BESTMAP case study regions.

Scale of Analysis

Spatial extent: 18.8194, 20.31623, 45.13434, 46.18879 (xmin, xmax, ymin, ymax; CRS=WGS84)

Spatial resolution: field parcel

Temporal resolution: 2019

Boundary: administrative (field level)

Data

All spatial data used in the case study were reprojected in EPSG: 4326- WGS 84 and clipped for the Bačka region. Elevation data for the Bačka region were taken from the Copernicus Land Monitoring Service. EU-DEM v1.1 is available in Geotiff 32-bit format. It is a contiguous dataset divided into 1000 x 1000 km tiles, at 25m resolution with vertical accuracy: +/- 7 metres RMSE. GeoTIFF files are based on EPSG: 3035 (ETRS89-LAEA) projection and for this model one tile was used.

Annual precipitation intake was provided by TerraClimate. All data have a monthly time resolution and a spatial resolution of ~ 4 km (1/24 degrees). The data cover the period from January to December 2019 in raster format. For each pixel, an average annual precipitation raster map in mm was calculated using the raster calculator in QGIS. Data related to maximum and minimum temperature were also downloaded from TerraClimate. As with precipitation, the data is in raster form where each pixel has temperature values for all 12 months of the year. For the 2019 year, values were calculated using a raster calculator in QGIS. Downloaded raster files are based on EPSG:4030 projection.

As there is no IACS/LPIS data for Serbia, the data collected within the AgroSens platform at the Biosens Institute were used as input spatial data. Data on farmers and their parcels have been collected since 2017, and 2019 was taken as the reference year for this case study. These data include user ID, parcel ID, crop type and other, but are not available for the entire area of Bačka. In parallel, a land cover map was obtained from the land cover classification map owned by the BioSense Institute. The data are based on Sentinel-2A satellite images from 2019 with a spatial resolution of 10m and data collected in the field. A total of 5 types of land cover have been identified on the map, with each parcel being assigned the appropriate type of land.

As a source of biophysical parameters, a system for global digital soil mapping was used, which uses the most modern machine learning methods for mapping the spatial distribution of soil properties around the world - SoilGrids. The maps are in the form of a raster with a spatial resolution of 250 metres and for the needs of this model, maps of the following soil properties have been taken: pH, bulk density, and clay content. Downloaded raster files are based on EPSG: 4326 - WGS 84 projection.

Furthermore, for CS Bačka a remote sensing-based SOC map is available. This map is generated from Sentinel-2 satellite data with 10 m spatial resolution. Several images were collected in the winter periods between 2016 and 2020. Ground truth data collection of ~10000 soil samples of agricultural land across the broader region of Vojvodina were utilised by machine learning algorithm, Random Forest regression, to learn mapping from satellite data of bare soil and target variable - SOM. This map serves as a validation for the baseline map created by the biophysical modelling approach.

Model

The carbon sequestration model for the RS CS was run with the same specifications as in the CZ CS; check the above CZ section for details on the variable pre-selection, model outputs, uncertainty/sensitivity analysis. Additionally, the remote sensing-based SOC map available for Bačka was used as validation for the baseline SOC map obtained as output of the model.

References:

Abdalla M., Hastings A., Cheng K., Yue Q., Chadwick D., Espenberg M., Truu J., Rees R. M. & Smith P. 2019. A critical review of the impacts of cover crops on nitrogen leaching, net greenhouse gas balance and crop productivity. *Global Change Biology*. DOI: 10.1111/gcb.14644

Crystal-Ornelas R., Thapa R. & Tully K. 2021. Soil organic carbon is affected by organic amendments, conservation tillage, and cover cropping in organic farming systems: A meta-analysis. *Agriculture, Ecosystems & Environment*. <https://doi.org/10.1016/j.agee.2021.107356>.

European Commission 2021. CMEF 2014-2020 - Context indicators (update December 2021) https://ec.europa.eu/info/sites/default/files/food-farming-fisheries/key_policies/documents/context-indicator-fiches_en.pdf, last accessed on 18th May 2022.

Goidts E., van Wesemael B. 2007. Regional assessment of soil organic carbon changes under agriculture in Southern Belgium (1955–2005), *Geoderma*, Volume 141, Issues 3–4, <https://doi.org/10.1016/j.geoderma.2007.06.013>.

Gregorich E. G., Drury C. F., and Baldock J.A.. (2001). Changes in soil carbon under long-term maize in monoculture and legume-based rotation. *Canadian Journal of Soil Science*. **81**(1): 21-31. <https://doi.org/10.4141/S00-041>

Guan, X.-K., Turner, N. C., Song, L., Gu, Y.-J., Wang, T.-C., and Li, F.-M.: Soil carbon sequestration by three perennial legume pastures is greater in deeper soil layers than in the surface soil, *Biogeosciences*, 13, 527–534, <https://doi.org/10.5194/bg-13-527-2016>, 2016.

Ledo A, Smith P, Zerihun A, Whitaker J, Vicente-Vicente J L, Qin Z, McNamara N P, Zinn Y L, Llorente M, Liebig M, Kuhnert M, Dondini M, Don A, Diaz-Pines E, Datta A, Bakka H 2020. Changes in soil organic carbon under perennial crops. *Glob Change Biol*. 26: 4158–4168. <https://doi.org/10.1111/gcb.15120>

Lorenz K, Lal R, 2016. Chapter Three - Environmental Impact of Organic Agriculture, Editor(s): Sparks D. L. , Advances in Agronomy, Academic Press, Volume 139, Pages 99-152, <https://doi.org/10.1016/bs.agron.2016.05.003>.

Poeplau C. & Don A.. 2015. Carbon sequestration in agricultural soils via cultivation of cover crops – A meta-analysis, Agriculture, Ecosystems & Environment. <https://doi.org/10.1016/j.agee.2014.10.024>.

Quemada M, Lassaletta L, Leip A, Jones A, & Lugato E 2020. Integrated management for sustainable cropping systems: looking beyond the greenhouse balance at the field scale. *Global Change Biology*, 26(4), 2584-2598.

R Core Team 2018. R: A language and environment for statistical computing. R Foundation for Statistical Computing, Vienna, Austria. URL <https://www.R-project.org/>.

Wu, G.-L., Liu, Y., Tian, F.-P., and Shi, Z.-H. (2016) Legumes Functional Group Promotes Soil Organic Carbon and Nitrogen Storage by Increasing Plant Diversity. *Land Degrad. Develop.*, 28: 1336– 1344. doi: [10.1002/ldr.2570](https://doi.org/10.1002/ldr.2570).

Zurell, D., Franklin, J., König, C., Bouchet, P. J., Dormann, C. F., Elith, J., ... & Merow, C. 2020. A standard protocol for reporting species distribution models. *Ecography*, 43(9), 1261-1277. <https://doi.org/10.1111/ecog.04960>

Acknowledgements:

Emanuele Lugato

Water quality factsheet

BESTMAP Nutrient Delivery Ratio model

2022-05-16

The structure of this factsheet is largely based on the ODMAP (Overview, Data, Model, Assessment and Prediction) protocol developed by Zurell et al. 2020 [doi/full/10.1111/ecog.04960](https://doi.org/10.1111/ecog.04960)

Overview

Authorship

The model is authored by the Natural Capital Project: <https://naturalcapitalproject.stanford.edu/>

This instance of the model was run by: Dr. Arjan Gosal (a.gosal@leeds.ac.uk), Rosemary Wool (r.wool@leeds.ac.uk), Dr. Marek Bednar (marek.bednar@upol.cz) and Dr. Sanja Brdar (sanja.brdar@biosense.rs).

Model name

InVEST Nutrient Delivery Ratio: <https://naturalcapitalproject.stanford.edu/software/invest>

Model manual

A comprehensive manual is available online:

<https://invest-userguide.readthedocs.io/en/latest/ndr.html>

Model objective

The InVEST Nutrient Delivery Model (NDR) is designed to map nutrient sources, from watershed to stream. It allows nutrient retention by natural vegetation in relation to surface water quality to be investigated (Sharp *et al.*, 2018).

Model processes

The following summary is abridged from the comprehensive [InVEST documentation](#) on the NDR model. The approach the NDR model utilises is one of simple mass balance by the movement of nutrients through space (see Figure 1). Rather than use details of the nutrient cycle, the NDR model instead uses long-term, steady state flows through empirical relationships (Sharp *et al.*, 2018). Nutrient loads are associated with different land (or crop) types with nutrient delivery ratios computed for nutrient transport by surface flow (with the option for subsurface flow in the model). Surface flow is calculated using a delivery factor, which represents ability to transport nutrients without retention for downstream pixels and a topographic index (Sharp *et al.*, 2018).

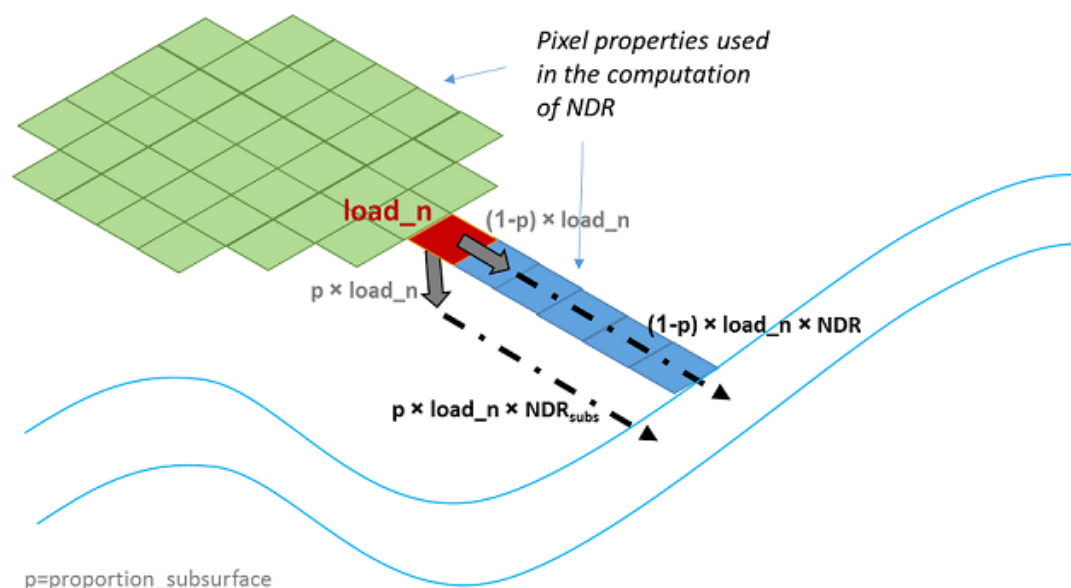


Figure 1. Conceptual representation of the nutrient delivery in the Nutrient Delivery Ratio model (source: Sharp *et al.*, 2018). The model is run assuming that the subsurface component is zero, as per Redhead *et al.* (2018).

Model output

The model provides spatial outputs. The first is a vector shapefile with the following attributes; the total nutrient loads in each watershed (i.e. the sum of the nutrient contribution from all land cover types), the total subsurface nutrient loads in each watershed, and the total nutrient export from each watershed. The second output is a raster tif file showing how much load from each pixel eventually reached the stream in kg/pixel. The model resolution of the output raster is the same resolution of the DEM provided as the input, and therefore this resolution will vary depending on the specific input data for different areas. The outputs of the model will be extracted at the farm-level in place of using the sub/watershed catchments that are outputted from the native model.

Data specifications

Geospatial information including digital elevation model (DEM), land use/land cover map (LCM), crop map, nutrient runoff proxy, watersheds delineated from a digital elevation model, and a biophysical table containing several different values on nutrients loading relating to each land use type (see Table 1).

Table 1. Description of Nutrient Delivery Model inputs.

Data type	Input	Description
Spatial	Digital elevation model (DEM)	Raster dataset with an elevation value for each pixel, given in metres
	Land use/land cover (LULC)	Raster of land use/land cover type for each pixel, where each unique integer represents a different land use/land cover class
	Nutrient runoff proxy	Raster representing the spatial variability in runoff potential, which in this case is annual precipitation
	Watersheds	Shapefile delineating the boundary of the watersheds within

		the case study area
Non-spatial	Biophysical table	A table containing information corresponding to each land use class in the LULC raster, including nitrogen/phosphorus load, maximum retention efficiency, the distance after which it is assumed that a patch of a particular LULC type retains nutrient at its maximum capacity, and the proportion of dissolved nutrients over the total amount of nutrients

Assumptions

This model has high-sensitivity to inputs, therefore errors in the biophysical table have a large effect on predictions. This includes the outputs of the model being highly sensitive to the small number of input parameters.

Algorithms and workflow

See the model specification and details of the algorithm at:
<https://invest-userguide.readthedocs.io/en/latest/ndr.html>

Model validation

This instance of the model is not validated, but has been validated in previous research for the UK: <https://www.sciencedirect.com/science/article/pii/S0048969717320909>

Uncertainty estimation

Uncertainty was ascertained using the results of Redhead et al (2018) study which validated the NDR model using regression models. We used the x solved trendline equation $x = (y-b)/m$ (where b is intercept, and m is slope). Intercept and slope values were taken for 25m resolution values, with the intercept being 0.31 for both N and P, and slope 0.67 and 0.49 for N and P respectively. We then calculated the Mean Absolute Percentage Error for each model instance.

Software

The Nutrient Delivery Ratio model as part of the InVEST Software Platform developed by the Natural Capital Project (Sharp *et al.*, 2018). The model was run using the GUI version of [InVEST](#) (version 3.9.0), though the steps can also be replicated using the InVEST Python package (version 3.9.2), which is outside the scope of this document (this additional method can be explored [here](#) and at the [Python Package Index; PyPi](#)). Many of the inputs are spatial in nature (see Table 1 and Model specifications section), these inputs were manually processed using GIS software, for example QGIS (<https://qgis.org/>).

Linking the model outputs to indicators

The outputs of this model (N and P export) are related to Gross Nutrient balance for nitrogen and phosphorus. The InVEST NDR model does not account for emissions into the atmosphere, and is limited to the retention in land/crop types to fresher water systems; 'pollution swapping' is not considered. Therefore this model contributes towards the gross calculation of nutrient balance, but does not have the function to calculate it independently.

Model

Model settings

Apart from the spatial model inputs, there are a variety of model input values that were kept constant in the model unless specified elsewhere. These were set at values according to those from Redhead et al. (2018): Threshold Flow Accumulation (1000), Borselli k Parameter (2), Subsurface Critical Length (200), and Subsurface Maximum Retention Efficient (0.8).

Assessment

Validation has been carried out by Redhead et al. (2018) for the UK. The model was found to perform well for relative magnitude of nutrient export, though absolute values of modelled nutrient export showed large percentage differences from validation data (Redhead et al., 2018).

Model specifications in case study

1) Humber, U.K.

Location

Humber River Basin, United Kingdom, which serves as one of the five BESTMAP case study regions.

Scale of Analysis

Spatial extent: xmin: 418008.24, ymin: 353867.54, xmax: 542556.68, ymax: 507394.51

Spatial resolution: 25 m

Temporal extent: Single year, with data inputs ranging between 2016 – 2019.

Temporal resolution: annual

Boundary: watersheds covering case study area.

Coordinate reference system: EPSG 27700

Two distinct models were run; (a) without the agri-environmental measures, (b) with agri-environmental measures, to investigate the change in nutrient retention for nitrogen (N) and phosphorus (P). The second model was designed to reflect a range of currently implemented AES within the Humber catchment. These were grassland management (N only), cover crops (N only), conversion to permanent grassland, woodland creation (between 2005-2016), and fallow land. Both models featured the same spatial data, but the biophysical tables contained differing values to account for the changes in nutrient loads for land with and without AEMs.

For the spatially explicit data, the DEM and LULC data was predominantly sourced from the UK Centre for Ecology & Hydrology (UKCEH) through the data provisioning platform Edina Digimap. Another LULC, which detailed information on crop type, was sourced from the Basic Payment Scheme (BPS) provided by Rural Payments Agency (RPA). Where various temporal resolutions were available for each layer the year 2019 was selected, otherwise the closest annual period to 2019 was chosen. The annual precipitation data was sourced from the UK Met Office, with the 2019 data used in this model. All layers were initially re-projected to be in EPSG 27700.

The DEM, entitled UK CEH Integrated Hydrological Digital Terrain Model, was a 50 m grid interval DEM created in 2016. The raster was resampled to 25 m to match the LCM2019

data. Sinks were identified and filled for the Digital Elevation Model to correct for any errors in the data. This was done using the 'Fill Sinks (Wang & Liu)' algorithm in QGIS Desktop 3.4.14 (Wang & Liu, 2006). The new filled sink layer was then used as the DEM input for the model. Watersheds were delineated from the filled DEM using the 'Channel network and drainage basins' algorithm using a Strahler order value of 5 in QGIS. The accuracy of watershed delineation is highly dependent on the quality of the DEM, therefore this specific DEM was chosen in part because of the extensive work that had been undertaken to ensure that the DEM would portray realistic hydrological behaviour. The delineation revealed three drainage basins within the case study area, and a new shapefile was created featuring only these. A buffer of 10 km was added around these watershed boundaries, which then functioned as the extent to which all other spatial inputs were clipped (including the filled DEM).

The model was run using a landcover input map that was created using both the UK CEH Land Cover Map (LCM) 2019 and the crop maps from Basic Payment Scheme database 2019. The UK CEH LCM featured broad habitat types based off of UK Biodiversity Action Plan (BAP) Broad Habitats classifications. The habitats were categorised using satellite imagery from 2019 and included 21 different habitats. The Basic Payment Scheme database map provided crop-level information that was provided by farmers. Some parcel types were excluded from this model run owing to their incongruity with the focus of this model (e.g. animal shelters, farm building, fallow, buffer areas). The database of the remaining 75 different crop types were joined to a parcel shapefile and parcels that did not contain any BPS crop information were removed. To create the final input map, the following layers were mosaiced in this priority order; fallow parcels, conversion to grassland, grassland management, cover crops, woodland creation, BPS crops, and the LCM layer. As multiple agri-environmental schemes can exist on the same field parcel of land, the schemes were applied in a priority order in the construction of the land use input maps into the model, with the schemes higher in the list overriding implementation of any other schemes that are applied to parcel lower in the list. This map was then clipped to the extent of the buffered watershed boundary.

The annual precipitation data was sourced from the HadUK-Grid collection of gridded climate variables from the UK Met Office. This data was based on a number of stations that were placed around 40 km apart on average, and then interpolated across the area. This data was available at a resolution of 1000 x 1000 m, and was clipped to the extent of the buffered watershed boundary.

Besides load and retention efficiency, the biophysical values were kept as their defaults (as described in the section on model settings). The load and retention efficiency values were sourced from Redhead et al. (2018), which featured an in-depth literature review. The data found by Redhead et al. (2018) had undergone sensitivity analysis and validation to evaluate the model. Redhead et al. (2018) provided nutrient load and retention efficiency for agriculture (amongst other general habitat types) as a single figure in the paper, however we were provided with further load values from Redhead (Pers Comms) for additional crop types. These load values were used for land without AEMs in both of our NDR models. Where there were disparate crop types (e.g. there was one category for beet, whilst Redhead *et al.* (2018) had two categories for beet, including sugar and fodder), averages were found between the two.

As previously mentioned, the difference between the two models (without and with AEMs) was the nutrient load values. Therefore, any land that featured AEMs had an adjusted nitrogen and/or phosphorous load and these differed across models:

1. *Cover crops*. Model (a) fields were given a value of 35.24 kg/ha for N, and 1.52 kg/ha for P (based on arable and horticulture values from Redhead et al., 2018), with model

- (b) reduced by 18.32 kg/ha for N and 0.79 kg/ha for P (based on 48% average reduction in NO₃ leaching with cover crops (Stevens and Quinton, 2009)).
2. *Maintaining grassland.* Model (a) had an N value of 92.43 kg/ha for all crop types identified as grassland (JW Redhead 2021, personal communication; Defra, 2021), and model (b) had an N of 9 kg/ha (based on low input permanent grassland (GS2 scheme) requirements of N not being increased is the rate is less than 9 kg/ha (Defra, 2022)). As the reduction of P was not that high in the UK (e.g. no increase to phosphate if the current rate is less than 23 kg/ha (Defra, 2022)), it was excluded.
 3. *Buffer areas.* Buffer areas were not included due to a range of factors; variety in published estimates of the impact on N and P, agricultural land drains, and pollution swapping. A wide range of variability exists between published studies, Kay et al. (2009) in a review of agricultural stewardship measures relating to water pollution problems found the effect of buffer zones on total nitrogen varied between 100% reduction to a 217% increase, with soluble phosphorus varying between a 30% decrease to 475% increase. In addition, land drains (also known as field or tile drains) are widely installed in the UK to prevent waterlogging (Chapman et al., 2004). These drains will reduce the efficiency of buffer areas to prevent loss of N and P. Insufficient data was available on the locations and usage of land drains in the case study. Buffer areas can also result in 'pollution swapping', a process whereby a mitigation measure reduces a pollutant, but increases a different pollutant (Stevens and Quinton, 2009). For example, riparian buffer zones can be effective at removing NO₃ from groundwater and overland flows, but there is a likelihood of high N₂O emissions from the buffer zones (Stevens and Quinton, 2009). Organic areas were not included due to a lack of information on the empirical practices of organic farmers in reducing N and P.
 4. *Organic farming.* No use of easily soluble mineral fertilisers but natural fertilisers and manure allowed. Assumed no change to N and P.
 5. *Land use conversion to permanent grassland.* Model (a) had an N of 92.43 kg/ha and P of 21.43 kg/ha for all crop types identified as grassland (JW Redhead 2021, personal communication; Defra, 2021), and model (b) had all fields marked as under the conversion to permanent grassland schemes changed to an N of 10.42 kg/ha and P of 0.63 kg/ha (based on improved grassland values from Redhead et al., 2018).
 6. *Land use conversion to forest.* Model (a) all woodland parcels had a value of 35.24 kg/ha for N, and 1.52 kg/ha for P (based on arable and horticulture values from Redhead et al., 2018), with model (b) values changed to N of 8.7 kg/ha and P of 1.8 kg/ha (based on mean values of broadleaf and coniferous woodland from Redhead et al., 2018).
 7. *Fallow land.* Model (a) all fallow parcels were given a value of 35.24 kg/ha for N, and 1.52 kg/ha for P (based on arable and horticulture values from Redhead et al., 2018), with model (b) changed to N of 3.33 kg/ha and P of 0.15 kg/ha (based on values of heather from Redhead et al., 2018).

The resulting output export maps for N and P as rasters were then used to extract the total N and P respectively using dissolved polygons of the farms by running zonal statistics in ArcMap.

2) Mulde, Germany

Location

Mulde River Basin, Saxony, Germany, which serves as one of the five BESTMAP case study regions.

Scale of Analysis

Spatial extent: xmin: 12.34771, ymin: 50.3809, xmax: 13.69364, ymax: 51.64169

Spatial resolution: 20 m

Temporal extent: Single year, with data inputs ranging from 2015 - 2020.

Temporal resolution: annual

Boundary: case study area

Coordinate reference system: CRS WGS84

Two distinct models were run; (a) without the agri-environmental measures, (b) with agri-environmental measures, to investigate the change in nutrient retention for nitrogen (N) and phosphorus (P). The second model was designed to reflect a range of currently implemented AEM within the Mulde region. Both models featured the same spatial data, but the biophysical tables contained differing values to account for the changes in nutrient loads for land with and without AEMs.

All spatial data for the German CS were initially re-projected to be in EPSG 3035. The DEM for the Mulde region was created using two sources, including DGM20 provided by the Saxony state and the Copernicus Land Monitoring Service EU-DEM v1.1. The DGM20 and EU-DEM v1.1 had a pixel size of 20 m and 25 m respectively, and were representative of the years 2020 and 2015 respectively. Two DEMs were used owing to the lack of spatial coverage in the DGM20. This was processed by clipping both of the digital elevation models to the Mulde CS region, and then filling their sinks (using the 'Fill Sinks (Wang & Lui)' algorithm in QGIS). The filled DEMs were then merged together, making sure that the DGM20 would take priority over the EU-DEM and that the EU-DEM would function only to fill in any areas that the DGM20 did not cover.

The land cover map was sourced from the APiC land cover classification map of Germany's agricultural area (Preidl et al., 2020). This data had a resolution of 20 m and was based on Sentinel-2A imagery from 2016, which identified a total of 19 land cover types. Additionally, IACS/LPIS data were provided for the years 2016-2019 by the Saxon State Ministry for Energy, Climate Protection, Environment and Agriculture (Sächsisches Staatsministerium für Energie, Klimaschutz, Umwelt und Landwirtschaft - SMEKUL), and provided spatially-explicit information on AEM application in the Mulde River Basin.

The precipitation data originated from Deutscher Wetterdienst (<https://www.dwd.de/>), the German Meteorological Service. The spatial file had a resolution of 1 km and was representative of the rainfall in 2019. The data used for the watershed boundaries was obtained from the Hydrological basins in Europe from FAO. The LCM, precipitation map and watershed boundaries were all clipped to the German CS outline.

Data for the biophysical table was taken from three sources; Düngeverordnung (2017), Döhler (2009) and Gebel et al. (unpublished). Döhler (2009) provided data on phosphorus loads for some land cover types, whilst Düngeverordnung (2017) and Gebel et al. (unpublished) had values for nitrogen loads for various crop and habitat types. A combination of these three were used to ensure that all land cover types had an N and P load that was as relevant as possible. Retention values were then extracted from Redhead et al. (2018) as this input was less likely to vary across case study regions. The remaining biophysical values were kept as their defaults, as described in the section on model settings.

The same methodology as the UK CS was utilised when assessing the differences in nutrient load across both models. The change in nitrogen and phosphorous load was, however, dependent on local agriculture policies:

1. *Cover crops*. No use of pesticides allowed after harvest of the main crop until the end of the application year, and no use of mineral N fertiliser on some catch crop AEMs.

As a result, N only from sources such as atmospheric deposition, livestock waste etc. whilst P also derived from fertiliser.

2. *Maintaining grassland.* No use of pesticides or N fertilisers in majority of cases. As a result, N only from sources such as atmospheric deposition, livestock waste etc. whilst P also derived from fertiliser.
3. *Buffer areas.* No use of fertilisers or pesticides. Therefore, both N and P only from sources such as atmospheric deposition, livestock waste etc.
4. *Organic farming.* No use of easily soluble mineral fertilisers but natural fertilisers and manure allowed. Assumed no change to N and P.
5. *Land use conversion to permanent grassland.* No information provided on adjustments to nutrient application in the policy documentation. Did not utilise in model.
6. *Land use conversion to forest.* No information provided on adjustments to nutrient application in the policy documentation. Did not utilise in model.
7. *Fallow land.* No use of fertilisers or pesticides. Therefore, both N and P only from sources such as atmospheric deposition, livestock waste etc.

3) Catalonia, Spain

Location

Catalonia, Spain, which serves as one of the five BESTMAP case study regions.

Scale of Analysis

Spatial extent: xmin: 0.1557295, ymin: 40.51405, xmax: 3.338699, ymax: 42.8691

Spatial resolution: 5 m

Temporal extent: Single year, with data inputs ranging from 2007 - 2019.

Temporal resolution: annual

Boundary: case study area

Coordinate reference system: CRS WGS84

Two distinct models were run; (a) without the agri-environmental measures, (b) with agri-environmental measures, to investigate the change in nutrient retention for nitrogen (N) and phosphorus (P). The second model was designed to reflect a range of currently implemented AEM within the Catalan region. Both models featured the same spatial data, but the biophysical tables contained differing values to account for the changes in nutrient loads for land with and without AEMs.

As with Germany, all spatial input data was re-projected to be in EPSG 3035 for the Catalan CS. The DEM was sourced from the Cartographic and Geological Institute of Catalonia (IGCG). The model is based on 2007 elevation and has a resolution of 5 m. The data was originally in multiple tiles so once these were all merged together, the 'Fill Sinks (Wang & Lui)' algorithm was run to fill any sinks present.

The LCM used was USOS Cobertes provided by the Government of Catalonia. The land cover types were classified in 2017 and had a resolution of 10 m. There were a total of 25 land cover types covered in this LCM. Information on AEM application were available from the IACS/LPIS data for the years 2015 to 2019 from the Ministry of Climate Action, Food and Rural Agenda - Department of Agriculture- of the Generalitat de Catalunya.

The annual precipitation input was provided by the Meteorological Service of Catalonia. It displayed the rainfall of 2019 in raster format at a resolution of 1000 m. Lastly, the watershed boundaries were sourced from the Government of Catalonia in vector format for 2017. The

filled DEM, LCM, precipitation and watersheds were then individually clipped to the outline of Catalonia.

Values for the biophysical table were sourced from the Ministry of Agriculture, Fisheries and Food of the Government of Catalonia. Information on the amount of phosphorus and nitrogen applied to various land cover types were provided for the year of 2016. These values were used for the N and P load, and included nutrient application in the form of mineral fertiliser, manure, other organic fertilisers, droppings of grazers, seeds, biological fixation and atmospheric deposition. An overall value was available for inputs minus outputs, however as we were only interested in the nutrient inputs for load we calculated the nutrient balance without the outputs which left us with input values. Retention values were then extracted from Redhead et al. (2018) as this input was less likely to vary across case study regions. The remaining biophysical values were kept as their defaults, as described in the section on model settings.

The same methodology as the UK CS was utilised when assessing the differences in nutrient load across both models. The change in nitrogen and phosphorous load was, however, dependent on local agriculture policies:

1. *Cover crops*. Fertiliser is allowed, however there are limits to the amount and this is highly dependent on the type of crop. Some crops see a reduction in N application (from without AEM to with AEM) whilst others see an increase. Almost all see a reduction in P application.
2. *Maintaining grassland*. No use of herbicides. Therefore, both N and P from sources such as fertiliser, atmospheric deposition, livestock waste etc. so there is very little to no effect on N and P load.
3. *Buffer areas*. No AEMs for ES CS.
4. *Organic farming*. No use of easily soluble mineral fertilisers but natural fertilisers and manure allowed. Assumed no change to N and P.
5. *Land use conversion to permanent grassland*. No AEMs for ES CS.
6. *Land use conversion to forest*. No AEMs for ES CS.
7. *Fallow land*. No data was available.

4) South Moravia, Czech Republic

This instance of the model was run by: Dr Marek Bednar (marek.bednar@upol.cz)

Location

South Moravia, Czech Republic, which serves as one of the five BESTMAP case study regions.

Scale of Analysis

Spatial extent: xmin: 16.893, ymin: 48.792, xmax: 17.919, ymax: 49.189 (xmin, xmax, ymin, ymax; CRS= WGS84)

Spatial resolution: 5 m

Temporal extent: Single year, with data inputs ranging from 2016 - 2019

Temporal resolution: annual

Boundary: case study area

Coordinate reference system: CRS WGS84

All spatial data for the Czech CS were reprojected to the WGS1984 UTM Zone 31N coordinate system. For the DEM, the DMR4G altitude model with a resolution of 5 m was

used, which was processed throughout the Czech Republic by generalising lidar data. This DEM was selected as the river network that was generated based on Flow Accumulation was more representative of the actual state in comparison to alternative DEMs as it had a finer resolution and therefore displayed subtle elevation changes more clearly. Data on water bodies from the DIBAVOD database processed at HEIS VUV T.G.M. were used for reference and comparison. The Threshold flow accumulation (input parameter of the NDR model) of 3000 showed the best correspondence.

Precipitation data were derived from the maximum daily precipitation totals with a repetition period of 20 years, which are available in the form of OGS_WMS from the ČVUT in Prague website (ČVUT, 2022). WMS data were stored in the form of a raster, then georeferenced and smoothed.

For the land cover input the KVES (consolidated layer of ecosystems) was used for the study. At the time of modelling, this was the most accurate nationwide vector spatial data basis in the Czech Republic. This layer was converted to a raster with a resolution of 5m (following the elevation model), and displayed a total of 35 land cover classes. Information on AEM application on the field parcels was extracted from the IACS/LPIS data, which were made available for the years 2015-2019 by the Ministry of Agriculture of the Czech Republic.

The area of the CZ case study is located in the Morava and Dyje river basins. When creating the hydrological area for the watershed input, the hydrologically closed unit was selected based on the 3rd and 4th order river basins. For the needs of the model, it was necessary to slightly limit the area of interest due to the hydrological units, as some of its peripheral parts already belong to other hydrological units and their incorporation would significantly expand the area studied by us. The hydrologically closed unit thus covers 96% of the CZ CS. Three sub-basins belonging to the corresponding sections were considered:

1. 4-17-01 Dyje from Svratka to the estuary
2. 4-13-02 Moravia from Olšava to Myjava
3. 4-13-01 Dřevnice and Moravia from Dřevnice to Olšava

Lastly, another important source for the calculation of nutrient outflow was the table of biophysical parameters, where for each KVES item the corresponding value of N and P load was determined, as well as N and P efficiency based on multiple sources concerning the position of the Czech Republic. Nevertheless, some parameters from KVES could be traced mainly to the works of Harmáčková & Vačkář (2015). Another source was the work of Redhead et al. (2018), Bangshuai et al. (2021) and also the InVEST spreadsheet with a list of sources and parameters. The statistical yearbooks of the Czech Republic for 2019 were used for setting up parameters for arable land. However data was more difficult to source for specific arable land types as the values change according to the sowing procedure. Individual N and P flows are not monitored in the Czech Republic at the level of individual crops, only yearly information on the total amount of nutrients for a larger administrative unit and region is available. As a result, N and P loads were derived from these regional values for 2019. N and P data at a finer spatial resolution are available from a farmer survey, in which crop-specific amounts of fertilisers were surveyed for a sample of farmers. These values may be useful within a specific area for further future improvements of the model at the local level, but they have not yet been taken into account in this instance of the CZ model.

For the second model, four of the AEM groups were taken into account:

1. *Cover crops*. No data available.
Generally Fertiliser is allowed, however there are limits to the amount and this is highly dependent on the type of crop.

2. *Maintaining grassland*. Fertilisation and limits vary according to the type of grass. For animal husbandry, there are limits per unit of livestock. Nitrogen fertilisers are not permitted in specially protected areas. N load value reduced.
3. *Buffer areas*. They usually consist of a mixture of seeds, including buckwheat, millet, cabbage and other crops, such as cereals or white lupine. The biobelt remains on the soil throughout the year (from spring sowing to ploughing the following spring). Fertilisation does not occur in these areas, therefore N and P load values reduce.
4. *Organic farming*. The structure of the landscape is mostly preserved, only organic fertilisers are used, and the total amount of N and P is reduced by 20-30%. The limits differ, e.g. in the case of organic grape production, the total amount of fertilisers applied must not exceed 96 kg N/ha, and not more than 150 kg N/ha within three years. It also depends if livestock is available. N load saw a reduction in value when this AEM is present.
5. *Land use conversion to permanent grassland*. This AEM is usually located near watercourses where fertilisation is prohibited, therefore N and P load had reduced values.
6. *Land use conversion to forest*. No AEMs for CZ CS.
7. *Fallow land*. No data available.

In general, any AEM applied in the Czech Republic is subject to strict conditions regarding the use of nitrogen fertilisers, which cannot be applied in case of unfavourable soil conditions, on arable land with a slope higher than 10 ° and TTP with a slope higher than 12 °, near watercourses.

As part of the evaluation, 15 variants of the landscape structure, with different spatial implementations of one or multiple AEMs, were subsequently processed in various combinations of individual measures, including the variant without AEMs. The results are, of course, dependent on the number of measures in the given sub-basin, but in general it follows that the application of AEMs, such as maintaining grassland and organic farming, reduces the total amount of N and P nutrients drained by about 10%. Further local models taking into account individual crops and AEMs will be developed as the project goes.

5) Bačka, Serbia

This instance of the model was run by: Dr. Sanja Brdar (sanja.brdar@biosense.rs), Predrag Lugonja (lugonjap@biosense.rs) and Miljana Marković (miljana.markovic@biosense.rs)

Location

Bačka Region, Serbia, which serves as one of the five BESTMAP case study regions.

Scale of Analysis

Spatial extent: xmin: 18.8194, ymin: 45.13434, xmax: 20.31623, ymax: 46.18879

Spatial resolution: 25 m

Temporal extent: Single year, with data inputs ranging from 2015 - 2019.

Temporal resolution: annual

Boundary: case study area

Coordinate reference system: EPSG:4326 - WGS84

Two distinct models were run; (a) without the agri-environmental measures, (b) with agri-environmental measures, to investigate the change in nutrient retention for nitrogen (N) and phosphorus (P). The second model was designed to reflect “surrogateAEM”, as AEMs do not currently exist in the Bačka region. Both models featured the same spatial data, but

the biophysical tables contained differing values to account for the changes in nutrient loads for land with and without surrogate AEMs.

All spatial layers were re-projected in EPSG: 4326 - WGS 84 and clipped to the outline of the Bačka CS region.

Elevation data was sourced from the Copernicus Land Monitoring Service. EU-DEM v1.1 is a contiguous dataset divided into 1000 x 1000 km tiles, at 25m resolution with vertical accuracy of +/- 7 metres RMSE. It is available in Geotiff 32 bits format and based on EPSG: 3035 (ETRS89-LAEA) projection. One tile was used for the Bačka region, and data was representative of 2015.

Annual precipitation data were derived from the TerraClimate dataset using Google Earth Engine (GEE). TerraClimate provides data of ~4 km (1/24 degrees) spatial resolution and monthly temporal resolution. Image Collection 'TerraClimate: Monthly Climate and Climatic Water Balance for Global Terrestrial Surfaces, University of Idaho' was imported in GEE script and filtered for the period from 1st of January to 31st of December 2019. Also, the Bačka region was used for filtering as the area of interest. The band 'pr', which refers to precipitation accumulation in mm, was selected and the function sum was applied in order to sum up values per each pixel for all 12 months of the year. The final step was the extraction of the data in raster format, based on EPSG:4030 projection.

The land cover map was obtained from the crop classification map produced by the BioSense Institute. Using Sentinel-2A satellite images from 2019 with a spatial resolution of 10m, vegetation indices and ground truth data collected on-site, crop classification was generated by applying a machine learning algorithm: Random Forest classifier. The final result was a classification map with 5 types of main crops: wheat, soybean, maize, sunflower and sugar beet.

Watershed boundaries were sourced from the Hydrological basins in Europe from FAO as an ESRI shapefile. The case study area of Bačka belongs to the major Danube hydrological basin and three sub-basins: Duna, Drava and Tisza.

Source of local biophysical parameters of nitrogen and phosphorus nutrient loads (Load_n, Load_p) for the crops in the crop classification map were extracted from the internal BioSense database of agricultural production collected from field books of farmers and companies in the Bačka region through non-disclosure agreements and averaged per crop type. Obtained values are furthermore verified with advisory recommendations for farmers on local agricultural portals (Agro Info Net, 2022; Poljomarket, 2019; AgroKlub, 2022a,b).

For the second model, "surrogate" AEMs were used since AEMs do not currently exist in Serbia:

1. *Cover crops*. No "surrogate" AEMs for RS CS.
2. *Maintaining grassland*. The "surrogate" for the maintaining grasslands AEM was derived from the Nature Conservation of Vojvodina Province data (PZZP). These areas were designed in a way to encourage farmers to keep open grassland and pasture, prevent vegetation succession towards woody encroachment and disable land use conversion. There is non-fertilization practice in Bačka for meadows and pastures; hence N and P loads are set to zero in the model.
3. *Buffer areas*. Linear elements were used as AEM "surrogates". They were derived from Sentinel 2 images (which were available for the peak of the vegetation season in 2019) and processed on Google engine. An NDVI time series was generated, and a threshold selected to detect permanent vegetation locations along roads and arable fields in the RS CS region. Identified areas were then used as "surrogates" for buffer areas and flower strips in arable fields. There is no fertilisation of these areas.

4. *Organic farming*. No use of easily soluble mineral fertilisers, but organic fertilisers and manure allowed. Assumed no change to N and P.
5. *Land use conversion to permanent grassland*. No “surrogate” AEMs for RS CS.
6. *Land use conversion to forest*. No “surrogate” AEMs for RS CS.
7. *Fallow land*. The “surrogate” file for fallow land was developed within the agricultural field zones from Sentinel 2 images by developing and applying an in-house algorithm for ploughing detection. We determined areas where in three consecutive years no ploughing activity was detected. The developed binary files were masked with grassland maintenance and grassland maps. There is no fertilisation of these areas.

References:

Agro Info Net (2022). Basic fertilisation in the fall for wheat. Agro Info Net. <https://agroinfo.net.com/poljoprivreda/ratarstvo/osnovno-dubrenje/>

AgroKlub (2022a). Sugar beet. AgroKlub. <https://www.agroklub.rs/sortna-lista/rep-krompir/secerna-repa-35/>

AgroKlub (2022b). Sunflower. AgroKlub. <https://www.agroklub.rs/sortna-lista/uljarice-predivo-bilje/suncokret-84/>

Bangshuai H., Reidy A. and Li, A. (2021). Modeling nutrient release with compiled data in a typical Midwest watershed. *Ecological Indicators*, 121(107213).

Chapman, A. S., Foster, I. D. L., Lees, J. A., Hodgkinson, R. J., & Jackson, R. H. (2004). Sediment and phosphorus delivery from field to river via land drains in England and Wales. A risk assessment using field and national databases. *Soil Use and Management*, 19(4), 347–355. <https://doi.org/10.1079/sum2003208>

ČVUT (2022) WMS viewing of daily maximum precipitation totals. ČVUT. <https://rain.fsv.cvut.cz/webapp/webove-sluzby/ogc-wms/>

Defra. (2021). *The British Survey of Fertiliser Practice: Fertiliser use on farm crops from crop year 2020*. <https://www.gov.uk/government/statistics/british-survey-of-fertiliser-practice-2020>

Defra. (2022). *GS2: Permanent grassland with very low inputs (outside SDAs)*. Countryside Stewardship Grants. <https://www.gov.uk/countryside-stewardship-grants/permanent-grassland-with-very-low-input-s-outside-sdas-gs2>

Döhler, H. (14ed.). (2009). *Faustzahlen für die Landwirtschaft*. KTBL.

Düngeverordnung vom 26. Mai 2017 (BGBl. I S. 1305), die zuletzt durch Artikel 97 des Gesetzes vom 10. August 2021 (BGBl. I S. 3436) geändert worden ist

Gebel, M., Uhlig, M., Bürger, S., & Halbfaß, S. (unpublished). Nährstoffeinträge in sächsische Gewässer - Zeitschnitt 2018. Landesamt für Umwelt, Landwirtschaft und Geologie. Freistaat Sachsen.

Harmáčková, Z. V. and Vačkář, D (2015). Modelling regulating ecosystem services trade-offs across landscape scenarios in Třeboňsko Wetlands Biosphere Reserve, Czech Republic. *Ecological Modelling*, 295, 207-215.

Kay, P., Edwards, A. C., & Foulger, M. (2009). A review of the efficacy of contemporary agricultural stewardship measures for ameliorating water pollution problems of key concern to the UK water industry. *Agricultural systems*, 99(2-3), 67-75.

Poljomarket (2019). Fertilize corn before sowing. Pljomarket. <http://poljomarket.rs/blog/76-dubrenje-kukuruza-pre-setve>

Preidl, S., Lange, M., & Doktor, D. (2020). Introducing APiC for regionalised land cover mapping on the national scale using Sentinel-2A imagery. *Remote Sensing of Environment*, 240, 111673.

Redhead, J. W., May, L., Oliver, T. H., Hamel, P., Sharp, R., & Bullock, J. M. (2018). National scale evaluation of the InVEST nutrient retention model in the United Kingdom. *Science of the Total Environment*, 610–611, 666–677. <https://doi.org/10.1016/j.scitotenv.2017.08.092>

Sharp, R., Tallis, H.T., Ricketts, T., Guerry, A.D., Wood, S.A., Chaplin-Kramer, R., Nelson, E., Ennaanay, D., Wolny, S., Olwero, N., Vigerstol, K., Pennington, D., Mendoza, G., Aukema, J., Foster, J., Forrest, J., Cameron, D., Arkema, K., Lonsdorf, E., Kennedy, C., Verutes, G., Kim, C.K., Guannel, G., Papenfus, M., Toft, J., Marsik, M., Bernhardt, J., Griffin, R., Glowinski, K., Chaumont, N., Perelman, A., Lacayo, M. Mandle, L., Hamel, P., Vogl, A.L., Rogers, L., Bierbower, W., Denu, D., and Douglass, J. (2018). InVEST +VERSION+ User's Guide. The Natural Capital Project, Stanford University, University of Minnesota, The Nature Conservancy, and World Wildlife Fund.

Stevens, C. J., & Quinton, J. N. (2009). Diffuse Pollution Swapping in Arable Agricultural Systems. *Critical Reviews in Environmental Science and Technology*, 39(6), 478–520. <https://doi.org/10.1080/10643380801910017>

Wang, L., & Liu, H. (2006). An efficient method for identifying and filling surface depressions in digital elevation models for hydrologic analysis and modelling. *International Journal of Geographical Information Science*, 20(2), 193-213.

Socio-economic effects model factsheet**BESTMAP viable farm income model**

2022-11-04

The structure of this factsheet has been influenced by the ODMAP (Overview, Data, Model, Assessment and Prediction) protocol developed by Zurell et al. 2020 [doi/full/10.1111/ecog.04960](https://doi.org/10.1111/ecog.04960)

Overview**Authorship**

George Breckenridge, Guy Ziv, Arjan Gosal, Anne Paulus, Katharina Schneider, Tomáš Václavík, Stephanie Roilo.

Contact: g.ziv@leeds.ac.uk

Model name

Model of the socio-economic effects of the adoption of agri-environmental schemes.

Model objective

The main objective of the model is to estimate how the adoption of agri-environmental schemes (AES) affects the estimated total income per farm (per worker) in different case studies across Europe.

Model output

The model output comprises the estimated change in total income between adoption/non-adoption of AES scenarios, by calculating the change in estimated Farm Net Value Added (FNVA) for a given year per farm. These results can then be aggregated.

Location

European BESTMAP areas (see Ziv et al., 2020). Example 'case study' regions: South Moravia, Czech Republic; Catalonia, Spain; Mulde, Germany; Humber, UK. No model/results for Serbia as no FADN available for this region.

Assumptions

1. All relevant impacts of AES adoption on production area / crop selection / yield are accurately assessed in the food and fodder standard output modelling. All inputs from dependencies on the food and fodder model are complete, accurate and not erroneous.
2. Between the scenarios of AES adoption/non-adoption, there is no change in the other components involved in calculating FNVA aside from the *Value of Agricultural Production* and *Pillar II (AES) payments*. So e.g. national subsidies, VAT, intermediate consumption, farm taxes (exc. income), depreciation etc. remain equal.

Outline of model algorithms and workflow

Output from the BESTMAP food and fodder model at the farm-level contains estimates for net crop income for AES non-adoption, and for real-life AES adopters, an adjusted estimated net crop income for the scenario of AES adoption. Building on top of this, the viable farm income model presented here harnesses field-level 'IACS/LPIS' data information to estimate the amount of CAP AES subsidy income to add on top for the AES adoption scenario, to create an estimate for unstandardised Farm Net Value Added (FNVA) for each farm across the adoption scenarios (for those farms which adopt AES in real life).

Also, FNVA is standardised by a measure of labour: Annual Work Units (AWU). AWU is largely unavailable in 'IACS/LPIS' and so the analytical concept was devised to harness its inclusion in FADN microdata (as 'SE010', 'Total labour input') to construct a regression model which could be applied at the farm-level using substitute variables of similar/equivalent meaning to estimate AWU per farm in 'IACS/LPIS'. This estimate is dynamic insofar as it responds to whether AES are being adopted or not for economic size.

To make this a reality, first FADN columns with all 0.0 values / NaN values were removed from the analysis. Then, the sample of FADN farm records is weighted, by replicating rows to as many whole farms they represent according to the weighting 'SYS02' field. Selected area-based continuous variables in FADN on land use, in addition to particular categorical variables of potential use in FADN on farm characteristics, are then declared. Continuous variables are first put through an algorithm to eliminate multicollinearity (of absolute $r > 0.8$) whilst preserving as many valuable variables as possible in bivariate relation to SE010. At this point, remaining variables are input into a feature-selecting Lasso() regression model against SE010, which aims to output the coefficients of insignificant terms as 0. Remaining variables with coefficients not as 0 are then re-input into a multi-linear regression model against SE010, with coefficients saved for later use.

For each farm, field-level data on land use and other information is then harnessed to find alternative raw input values from 'IACS/LPIS', with these being substituted into the FADN-derived regression model for 'Total labour input' in AWU. Once an estimate for AWU is regressed for each farm, for each adoption scenario, this is then what the unstandardised FNVA value is divided by, in order to create a standardised estimate for FNVA for each farm, for each scenario of AES (adoption or non-adoption). De-identified farm-level results can then be aggregated by region to indicate for a region the aggregate impact of AES adoption on estimated farm incomes. Percentage change between AES adoption and non-adoption on mean and median average will be a key indicator to assess whether AES subsidies offer enough return to be worthwhile from a rational financial standpoint, all else being equal. It is assumed throughout that other components of FNVA other than *Value of Agricultural Production* and *Pillar I/II payments* remain equal between AES adoption scenarios.

Linking the model outputs to indicators

The model results are linked to the following policy indicator (European Commission, 2022):

C.27 I.4 Supporting viable farm income / I.5 Contributing to territorial balance: 'Farm income by type of farming, region, by farm size, in areas facing natural and other specific constraints'

Software

Software: Python v3.7.11 (Python, 2018), using Geopandas 0.9.0 (Jordahl et al., 2021), sklearn 1.0.1 (cited as Pedregosa et al., 2011), matplotlib 3.4.3 (Hunter, 2007) and seaborn 0.11.2 (Waskom, 2021).

Code availability: Code to be made available via the UFZ GitLab repository.

Data availability: Data not publicly available or on request from authors. FADN microdata access available from European Commission DG Agri subject to specific request. 'IACS/LPIS' data access available from national and regional governments subject to specific request.

Data

Data sources and specifications

To calculate AES adoption impacts (in BESTMAP Food & Fodder Model which pre-processes output file for input here):

- Geospatial (e.g. raster and shapefile data) information on agricultural land-use, including management information like AES adoption (cover crops, buffer areas/flower strips, land use conversion, maintaining grasslands) and type of crops grown as well as spatially explicit yield data of agricultural crops of interest.
- Standard Output coefficients per crop per NUTS1 region, sourced from EUROSTAT (2021): <https://ec.europa.eu/eurostat/web/agriculture/data/ancillary-data>.

To calculate socio-economic effects of pre-calculated AES adoption estimates, in each BESTMAP case study region:

- 'IACS/LPIS' data containing field-level information on crop type, field area (.shp), AES uptake at group level of detail (i.e. 'cover crops' / 'maintaining grassland' etc.).
- Output data from BESTMAP food and fodder model containing farm-level estimated standard output values (in Euros) for overall income from crops, both for AES non-adoption scenario ('so') and, where applied, for AES adoption ('so_mod'). As stated, in turn this calculation used NUTS1-specific EUROSTAT (2021) standard output coefficients and scientific literature to achieve these estimates.
- FADN microdata on selected variables (mostly continuous and area-based) for 2017. Full input selection (to be filtered for all-0s/NaN columns, weighted by 'SYS02', then filtered for multicollinearity, then feature-selected using Lasso() regression model): ['SE005','SE025','SE030','SE035','SE041','SE042','SE046','SE050','SE054','SE055','SE065','SE071','SE073','SE074','SE075','AGE','TF8','SEX','REGION','ALTITUDE','ANC'].
- Expert judgement from agricultural academics on available AES schemes and their typical/distinct payment rates for the BESTMAP region, in Euros per ha per year, across these types/'groupings' of AES: 'cover crops', 'flower strips', 'maintaining grassland', 'converting arable land to grassland'.
- Expert judgement from agricultural academics on crop type classification in given local regions according to typical purposes of crops / crop classifications. Judgements are applied for AWU regression parameterization from 'IACS/LPIS' data.

Data specifications in South Moravia, Czech Republic

The application of the socio-economic model to the BESTMAP case study region of South Moravia in Czech Republic used annual administrative data from 2017 at the field/farm scale. 'IACS/LPIS' data for South Moravia for 2015-2019 was sourced from the Ministry of Agriculture of the Czech Republic, though only 2017 data was used for consistency. FADN microdata for Czech Republic (FADN region 745) for 2017 was accessed from the Directorate-General for Agriculture and Rural Development at the European Commission.

As crop type and AES uptake were arranged in a complex way in the Czech 'IACS/LPIS' data, further pre-processing completed by the BESTMAP food and fodder model team was used in the implementation of the farm income algorithm. This involved the use of the *input file* to the food and fodder model, detailing crop use at the field-level (otherwise usually taken from the 'IACS/LPIS' file(s)), in addition to the routine use of the *output file* containing information on the ordinary and adjusted standard output values according to AES uptake.

Location

South Moravia, Czech Republic, one of the five BESTMAP case study regions.

Scale of Analysis

Spatial extent: 16.893 17.919, 48.792, 49.189 (xmin, xmax, ymin, ymax; at CRS = WGS84)

Spatial resolution: field scale

Temporal extent: 2017

Temporal resolution: annual

Boundary: administrative

Model

Model algorithms and workflow

FNVA is a statistical definition of the indicator C.27 in the approved [Context and Indicators Impact guidelines](#) for the new Performance Monitoring and Evaluation Framework (PMEF) of the post-2020 EU Common Agricultural Policy (CAP), officially adopted in December 2021.

Farm Net Value Added (FNVA) is calculated by formula (European Commission, 2022: 54):

FNVA = Value of agricultural production + Pillar I and Pillar II payments + any national subsidies + VAT balance
- intermediate consumption - farm taxes (excluding income taxes) - depreciation.

FNVA is standardised through Annual Work Units (AWU). FNVA is calculated per AWU *“in order to take into account the differences in the scale of farms and to obtain a better measure of the productivity of the agricultural workforce”* (European Commission, 2022: 54).

Our viable farm income model estimates the difference in Farm Net Value Added ('FNVA') between the scenarios of adoption / non-adoption of AES per farm in the European context.

The *net* contribution of AES adoption to FNVA is therefore deduced through calculating:

(Value of agricultural production + Pillar I and Pillar II payments + any national subsidies + VAT balance
- intermediate consumption - farm taxes (excluding income taxes) - depreciation) with AES payments/yield changes

-
(Value of agricultural production + Pillar I and Pillar II payments + any national subsidies + VAT balance
- intermediate consumption - farm taxes (excluding income taxes) - depreciation) without AES payments/yield changes.

Our estimation of FNVA is partial insofar as we do not incorporate FNVA components other than *Value of Agricultural Production* and *Pillar II payments*. We assume that other aspects do not change between the scenarios of AES adoption and AES non-adoption.

First, we take the output of the BESTMAP food and fodder model, which for a given BESTMAP case study region outputs a table of all unique farms and their associated modelled standard output values (in Euros). These are values rather than coefficients as they are understood here to represent the total modelled net income for an individual farm. These are calculated both for AES non-adoption ('so') and, where applied, for AES adoption ('so_mod'), with the modelling for AES adoption capturing the changes in crop coverage and respective yield implications in the calculations. This is the case though *only* on those farms with which AES is applied in real-life: otherwise, the value of 'so_mod' is always equal to the value for 'so'. These modelled estimations of the *Value of Agricultural Production* component of FNVA are derived from AES uptake information available in 'IACS/LPIS', as well as EUROSTAT (2021) data on NUTS1 Standard Output coefficients.

Second, the value of Pillar II payments is initially determined through research into local Agri-Environmental Schemes (AES) using expert knowledge by local agricultural researchers, in the case of the 5 BESTMAP Case Study regions (see Table 1 below). Difficulties were experienced in reconciling the complex agri-environment scheme policy landscape with this generalised schematic, although all values were based on expert judgement and/or statistical summarisation. We then estimate the modelled Pillar II payments due (AES) by summing up the areas of modelled AES adoption (at the field level from 'IACS/LPIS' data) multiplied by their researched payment rates per ha (Table 1).

Table 1: Data on AES payment rates per BESTMAP Case Study Region. Data Source: Consultation with subject/country experts by/within BESTMAP.

BESTMAP CS Region	Flower strips (inc. buffers) (/ha per annum)	Catch/cover crops (/ha per annum)	Maintaining Grassland (/ha per annum)	Conversion of arable land to grassland (/ha permanent)
UK	(AB8): €615.59	(SW6): €130.20	(GS6, ~GS2/GS9): €207.86	(SW7): €355.19
DE	(AL5c): €835.00	(AL4): €78.00	(GL5a): €330.00	-
CZ	(10.1.6): €591.00	- (Not as AES in CZ)	(10.1.4 Ošetřování travních porostů): €180.00	(10.1.5 Zatrávňování orné půdy): €400.00 (no permanent AES)
ES	-	(~AES_367): €95.92 (variable so split by crop group in model)	(~AES_363): €280.80 (~AES_368): €30.00	-
RS	~€662.00	~€287.00	~€136.00	~€551.00

Finally, we calculate an estimation for AWU from a model trained using FADN microdata. Our model for the socio-economic indicator uses FADN microdata to determine a linear regression model which can, for each given area, determine the variables from FADN which best account for the variance in farm labour as expressed through Annual Work Units (AWU). This FADN data is filtered to include only data from within NUTS2 and/or NUTS3 areas overlapping with the BESTMAP Case Study regions (see Ziv et al., 2020), unless the overlap was clearly not meaningful and therefore would have likely distorted the results more from including the NUTS region than from excluding it. With FADN data the weighting estimated by the 'SYS02' column representing 'farms represented' was used at all stages from collinearity analysis onwards to calculate appropriate relationships between variables in

the FADN data. This was accounted for in practical terms by replicating the rows within the FADN table as many times as the 'rounded down' integer value cast from SYS02.

In the first instance, FADN columns with entirely 0.0 values / NaN values were removed from the analysis. Then, an algorithm was developed to automatically remove extreme levels of multicollinearity, so as to address the assumption that variables are truly independent. Variables were automatically removed if they had an absolute Pearson correlation coefficient (r) greater than 0.8 with another independent variable and generated a lower relative R^2 value when modelled as a single input variable against SE010 (Total Labour in AWU) in a bivariate linear regression model. This process occurred for all (unique) sets of collinear variables identified in the [corr\(\) correlation matrix](#) until a list of unique 'variables to remove' were determined for that iteration. This entire process iterated until no unique sets of collinear variables remained. The value of this approach beyond automatically removing all variables with collinearities was that despite a higher computational demand, particularly valuable explanatory variables could still remain in the model as (truly) independent entities so long as they only presented collinearities with less individually-explanatory input variables across the weighted FADN table.

For each case study area a [feature-selecting Lasso regression model](#) is then fitted which runs by aiming to reduce as many variable coefficients as possible to 0, leaving only significant features in the model. Continuous variables are [normalized using StandardScaler\(\)](#) and categorical variables are [encoded using the OneHotEncoder\(\) function](#) to ensure suitable incorporation into this first Lasso regression model. At this point, the selected variables from each case study were then input as Fixed Effects into a [Linear Mixed Effects Regression \(LMER\) Model](#), with selected categorical variables included as the declared Random Effects, in part to see if we can further improve the predictability of AWU (as measured through AIC). Although this was a worthwhile methodological exploration, it was ultimately determined that this farm income model would instead rely on the outputs of re-running a [statsmodel linear regression](#) using the feature-selected variables from the Lasso regression model output.

Having derived this statistical relationship to AWU from FADN variables, we can then return exclusively to data from 'IACS/LPIS' in order to build a socio-economic indicator through modelling change in Farm Net Value Added (FNVA) according to adoption/non-adoption of AES, as standardised through Annual Work Units (AWU). By taking, wherever pragmatically possible, variables of equivalent meaning from the 'IACS/LPIS' data to those selected in the FADN model for AWU, we are then able to use the estimated model for predicting AWU derived from FADN microdata and thenceforth deduce a more accurate estimate for AWU per farm in the 'IACS/LPIS' data across European places in order to complete our methodology for estimating (standardised) FNVA in both adoption scenarios. This estimate of AWU for standardisation was 'dynamic' insofar as it responded, in some instances, to changes in the adoption scenario when calculating proxy values from 'IACS/LPIS' to put into the AWU regression. As such, on a given individual farm, the estimated AWU value used to standardise estimations of FNVA was different according to if AES were being adopted.

Once an AWU-standardised value for the *Value of Agricultural Production* is therefore calculated for both adoption scenarios, the estimated percentage change in FNVA between AES non-adoption and AES adoption is calculated per farm. Tabular outputs from the model are at this point de-identified (assuming a sufficient sample of individual farms was input, e.g. $n \geq 10$) though they are also then typically aggregated as summary statistics to indicate the overall effect of AES adoption on farmer incomes across a given geographical region. All boxplot figures were generated using the *matplotlib* (Hunter, 2007) graphics environment in Python, with both *matplotlib* and *seaborn* (Waskom, 2021) libraries used for the histogram and scatterplot figures.

Assessment

Uncertainty analysis

Uncertainty is relatively high for this farm income model, as it is a result of the outputs of the BESTMAP food and fodder model, as well as for being the outcome of the application of a linear regression from one dataset within the available ('best-fit') fields from another.

In the first instance the regression model for SE010 'Total labour input' (AWU) for CZE shows excellent ($R^2 > 0.85$) but nevertheless not perfect performance, despite best efforts to use a feature-selecting Lasso model to determine which variables should be included after excluding multicollinear columns. This is inevitable but clearly represents uncertainty and the model may be able to generate different levels of explainability in other European contexts.

The model specified below, from the Czech FADN region ($n = 3,350$ rows after weighting), produced an Adjusted R^2 value = 0.862, the same as its unadjusted R^2 value = 0.862:

$$SE010 = 0.7986 + 0.0097(SE005) + 0.1178(SE054) + 0.0212(SE071)$$

Here, the equal R^2 and Adjusted R^2 values (to 3 d.p.) and the large sample size indicate a relatively low risk of overfitting for a regional agricultural study.

In the application of this regression model to 'IACS/LPIS' data, there is inherent uncertainty introduced into the accuracy of the result, owing to the difficulty in accurately and consistently estimating an FADN category using 'IACS/LPIS' fields. In some cases values were unavailable, weren't readily available, or had uncertain degrees of crossover between categories and classifications.

As for measures to counter uncertainty, the uncertainty in the statistical model for AWU was countered through repeated, iterative efforts to improve the regression scores, including the Adjusted R^2 value. This included passing in a large number of both continuous and categorical variables, using feature-selection techniques, and experimenting with running more complicated models. In the case of classifications, avoiding unacceptable levels of uncertainty was helped through referencing the May 2019 European Commission (2019) Definitions for FADN wherever possible. Consulting regularly with local experts internal to BESTMAP also reduced uncertainties arising from classification issues between data sets, case study regions, and languages.

Model validation

Country-level EU data for validation assessments for farm income per AWU was identified to be available as C.25/C.26 in the old CAP CMEF framework, the closest available metric. These are currently available at:

1. <https://agridata.ec.europa.eu/extensions/IndicatorsSectorial/AgriFactorIncome.html> [Accessed 24/05/22]. C.25 in CMEF.
2. <https://agridata.ec.europa.eu/extensions/IndicatorsSectorial/AgriculturalEntrepreneurialIncome.html> [Accessed 24/05/22]. C.26 in CMEF.

Although a model validation exercise wasn't systematically conducted, using these statistics facilitates a qualitative evaluation of the model outputs, indicating that our model outputs in the test case study are within the correct expected magnitude (~5 pre-decimal figures i.e. €10 000s) for income per AWU in late-2010s EU agricultural settings.

In some respects, it is actually unsurprising that our average *Value of Agricultural Production* estimate value would present disparities to the value contained here as on top of being a separate, new CAP indicator, not covered by the old CMEF indicator framework directly, our modelling also did not incorporate many of the stated components deducting from the total income figure in FNVA or similar metrics, including intermediate consumption, farm taxes and asset depreciation (European Commission, 2022: 54).

Data from FADN in Total labour output (SE010) can be used similarly to indicate reasonable bounds for estimating AWU at the farm level, with our model outputs appearing to roughly align, indicating efforts to estimate AWU using 'IACS/LPIS' data were acceptably accurate.

Prediction

SOUTH MORAVIA, CZECH REPUBLIC

Investigating Biases from Spatial Exclusions: South Moravia, Czech Republic

Data from South Moravia posed challenges and presented potential biases. Firstly this was owing to the relatively high number of records output from the food and fodder model which were unable to determine standard output values for Czech farms. Unfortunately this meant that in 446 of the 1104 unique farms in South Moravia results for farm income could not be produced as the inputs were not available. In many other cases farms were not recorded as adopting AES in ground-truth data and therefore could not be represented in our results, which depend upon real distinction between the AES non-adoption and adoption scenarios within the input data format. As such, only 257 (23.28% to 2 d.p.) farms could be included.

As stated, such exclusions in the South Moravia case study occurred *in part* due to methodological choices and data issues in the food and fodder model, which was applied in the Czech Republic to ensure consistency between BESTMAP case studies. Firstly, the use of the WOFOST simulation predictions (Hristov et al., 2020) to generate yield predictions for six crops (maize, sugar beet, wheat, sunflower, winter rapeseed, spring barley), in addition to the Czech-specific ReSteP yield model for permanent and temporary grassland (VÚMOP, 2015), meant that whilst many crop types were catered for, many were also left without the yield information necessary for income modelling. Secondly, in the case of the Czech Republic, an abnormal number of crop entries in the EUROSTAT data on standard output coefficients contained 0/NaN values which also prevented *Values of Agricultural Production* from being calculated with EUROSTAT (2021) coefficients.

To informally understand the biases these exclusions may introduce, the nature and spatial patterns of fields for farmers with no income estimation were examined in Python and GIS software. Firstly, a CSV file was created with the farm IDs of farms which were unable to be included in the final results. This generated a file which could be joined - as a delimited text layer - to the field-level South Moravia 'IACS/LPIS' shapefile in QGIS, with 'not null rows' highlighted for visual examination. It became immediately apparent that the majority of total field area did not belong to this set of excluded farm IDs, despite this set of IDs representing 76.72% of all farms in the South Moravia case study region. This initial impression was supported by statistical evidence that both the mean and median average field size was lower for excluded fields (4.38 ha, 0.61 ha respectively) than for all fields in the region (6.01 ha, 0.91 ha respectively), and that 66.77% (2 d.p.) of total field area in South Moravia was used in the final results. So, in conclusion, the fields attached to farmer IDs ('ID_UZ') whose income cannot be estimated represent in fact the minority of fields, as well as disproportionately representing smaller area fields. All this said, it is nevertheless true that a slim majority of fields in South Moravia were excluded from the results due to being associated with an excluded farmer: 53.84% (to 2 d.p.). Both the largest and the smallest

fields were excluded from the analysis so the range of field sizes affected was as broad as theoretically possible. Returning to the findings of the visual inspection, it was clear that although many fields were scattered across the region, many also clustered together (as may be expected given fields are excluded on the basis of a common owner, and usually owned/managed locally in any case). Regions with higher than average presence of excluded fields were overlaid across an OpenStreetMap (2022) base layer which illustrated that clusters were not consistently found in urban centres. Although there was a degree of spatial grouping amongst *excluded* fields, the same could not be said for the remaining *included* fields, as they formed a larger part of the landscape, which was itself discontinuously represented across space by the vector shapefile fields in existence.

As such, it is concluded that it is more likely than otherwise that the biases introduced by these (involuntary) exclusions were disproportionately on groups of small holdings, and that they didn't prevent the majority of agricultural land (and for that matter, probably agricultural income) from being represented in the farm income analysis. The results of this farm income model application are therefore expected to be broadly representative of South Moravia. The code for this investigation into spatial biases is included in the main code file as an appendix.

Results: South Moravia, Czech Republic

Results for the demonstrative implementation of the BESTMAP socio-economic model are represented in Table 2, Figure 1 and Figure 2. They illustrate the FNVA value as standardised per Annual Work Unit (AWU) for South Moravia, Czech Republic, using 2017 data, for those farms ($n = 257$) for which income for both scenarios could be modelled.

The results indicate that the aggregate impact of AES adoption in this region is a major increase in net farm income, with a mean percent change of +67.72% (to 2 d.p.). This relates to mean average *Value of Agricultural Production* figures of €12,325.00 for non-adoption of AES, in comparison to €13,295.69 in the scenario of AES adoption. On average, therefore, it can be deduced that the income from AES subsidies estimated by this analysis is more than compensating sufficiently for the changes in land use and crop yield that are needed to fulfil, or a consequence of, agri-environment scheme requirements. Interestingly, the median average for non-adoption stands at the far lower level of €2,042.95, compared to €3,566.74 in the scenario of AES adoption.

The median average is many times closer to the minimum *Value of Agricultural Production* figures (€17.22, €33.14) than it is to the maximum figures which stood at €89,290.60 and €89,355.18 for non-adoption/adoption of AES respectively (see Table 2). A large range of values for the *Value of Agricultural Production* were predicted here, even within the single region of South Moravia, and despite the possible biases from excluding smaller holdings. Similarly, a large range of estimated percent changes in Farm Net Value Added (FNVA) are also predicted, ranging from a minimum value of -64.93% to a maximum value of +194.27%.

Given the *major* percentage increase, *both* in mean and median average terms, it was investigated whether unrealistic farm receipts were driving this summary statistic, as investigated by Figure 3. At various thresholds for inclusion on the basis of income levels in the scenario of AES non-adoption it was recorded the mean average value of estimated percent changes in FNVA, to examine this relationship between a selected sub-sample and aggregate results. Figure 3 reports results of the mean average FNVA change upon AES adoption statistic at the increasing thresholds of every €200 between €0 and €15,000. The results evidence a strong non-linear relationship between the size of the farm before AES adoption and the proportion of FNVA (income) increase reported overall (despite AES subsidy payments being calculated per ha). The mean percent change drops to below +30% once the lower half of the farms are excluded, as per the sequential Q1/Q2/Q3 grey lines

shown. These results indicate that the effect of AES adoption on income is highly associated with levels of pre-AES adoption income, possibly due to similar levels of area being dedicated to the AES schemes irrespective of the size of the farm, which would naturally produce higher levels of proportionate income increase in farms with a smaller overall size.

Table 2: Aggregated summary statistics (all to 2 d.p.) for farm-level FNVA outputs, generated using `pandas.DataFrame.describe()` (records with €0 for either AES scenarios removed), South Moravia, 2017.

Summary statistics for 'Value of Agricultural Production' estimations in socio-economic model
South Moravia, Czech Republic, 2017 [Data: FADN, 'IACS/LPIS']
 [€0 income farms removed]

			Value of Agricultural Production (€)		Percent change
			No AES adoption	AES adoption	
summary	records	count	257	257	257
	average	mean	12325.00	13295.69	67.72
	variance	std	22604.38	22394.46	59.26
percentiles	min	0%	17.22	33.14	-64.93
	-	25%	864.13	1798.17	4.36
	median	50%	2042.95	3566.74	78.09
	-	75%	7608.46	9407.57	112.34
	max	100%	89290.60	89355.18	194.27

Data Acknowledgements: FADN data in methodology for ESP (2017) from Directorate-General for Agriculture and Rural Development, European Commission. 'IACS/LPIS' data (2017) is from Ministry of Agriculture of the Czech Republic.

Figure 1: Boxplots of distributions for estimated FNVA, South Moravia, 2017.

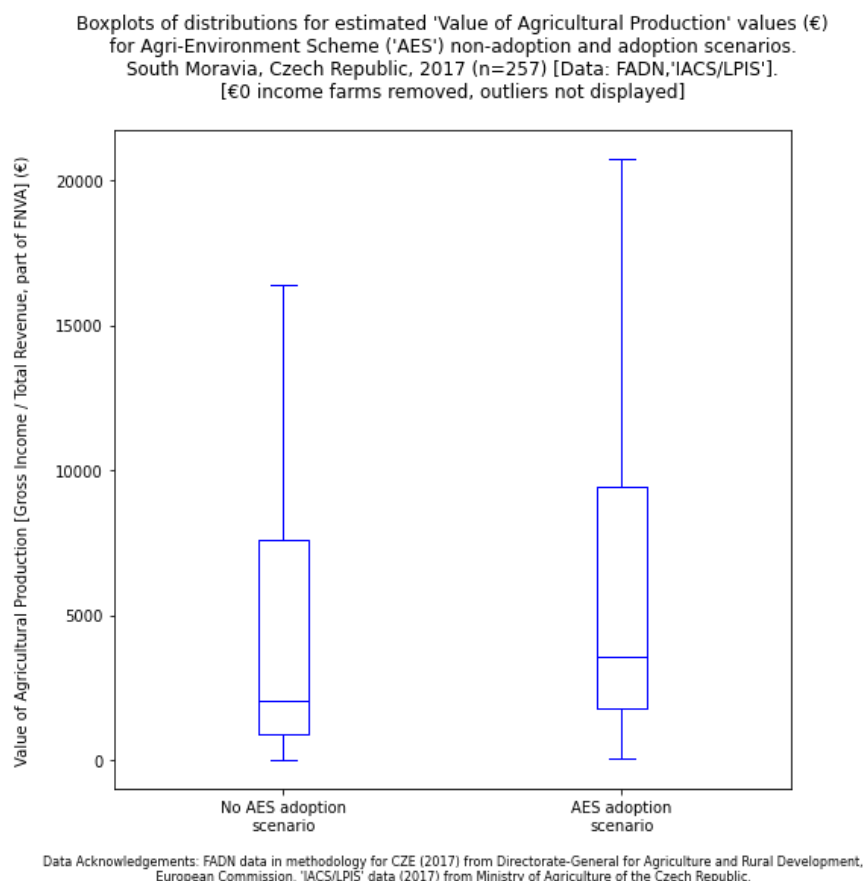
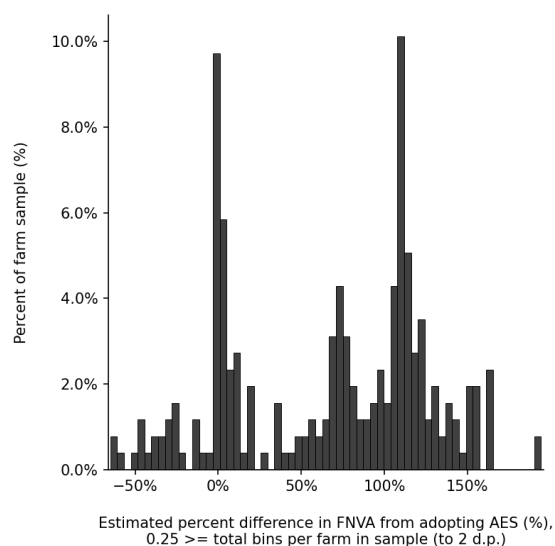


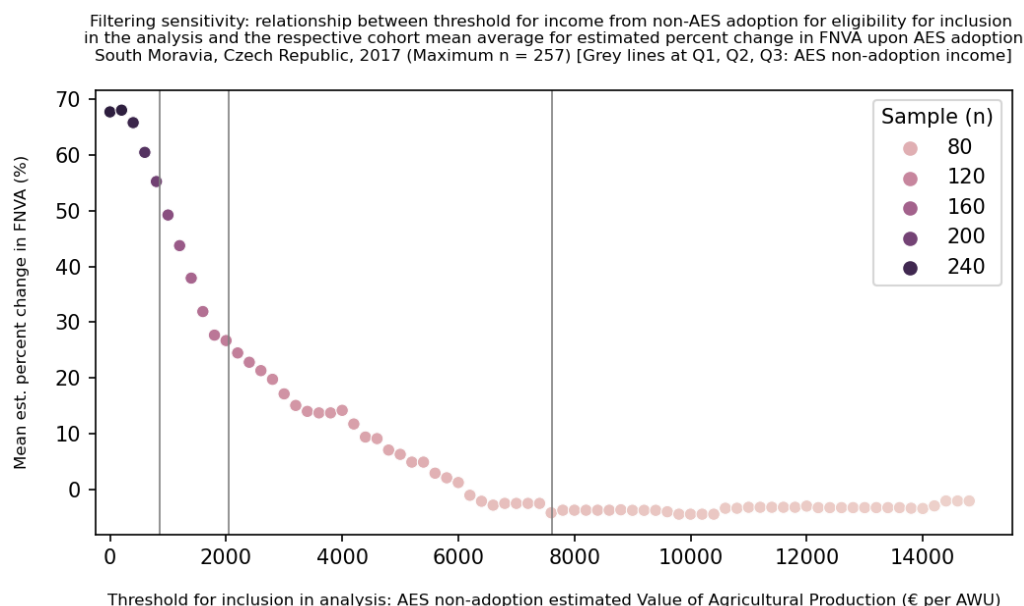
Figure 2: Histogram of distribution for farm-level *percentage difference* for FNVA between AES non-adoption and AES adoption, South Moravia, 2017.

Proportion of farm sample (n = 257) exhibiting (approximate) estimate percent difference in Farm Net Value Added ('FNVA', C.27 PMEF) from adopting AES. South Moravia, Czech Republic, 2017 [Data: FADN, 'IACS/LPIS']. [€0 income farms removed]



Data Acknowledgements: FADN data in methodology for CZE (2017) from Directorate-General for Agriculture and Rural Development, European Commission. 'IACS/LPIS' data (2017) from Ministry of Agriculture of the Czech Republic.

Figure 3: Scatterplot of relationship between sample inclusion threshold according to AES non-adoption income, and the cohort's respective mean average farm-level *percentage difference* for FNVA between AES non-adoption and AES adoption, South Moravia, 2017. [Data Acknowledgements: FADN for CZE (2017) from Directorate-General for Agriculture and Rural Development, European Commission. 'IACS/LPIS' data (2017) from Ministry of Agriculture of the Czech Republic.]



Specifications for other BESTMAP case study regions are currently under development and will in future be made available in the UFZ GitLab page (<https://git.ufz.de/>).

References

European Commission (2019). *Definitions of Variables used in FADN standard results. COMMITTEE FOR THE FARM ACCOUNTANCY DATA NETWORK (FADN)*. Directorate-General for Agriculture and Rural Development, European Commission.

European Commission (2022). *Context and Impact indicators*. CAP Performance Monitoring and Evaluation Framework. Directorate-General for Agriculture and Rural Development, European Commission. Available at: https://ec.europa.eu/info/sites/default/files/food-farming-fisheries/key_policies/documents/pmef-context-impact-indicators_en.pdf. [Accessed 24/05/22]

EUROSTAT (2021). Standard output coefficients. Available at: <https://ec.europa.eu/eurostat/web/agriculture/data/ancillary-data>.

Hristov, J., Toreti, A., Perez Dominguez, I., Dentener, F., Fellmann, T., Elleby, C., et al. (2020). *Analysis of climate change impacts on EU agriculture by 2050*. EUR 30078 EN, Publications Office of the European Union, Luxembourg, ISBN 978-92-76-10617-3, doi:10.2760/121115, JRC119632.

Hunter, J. D. (2007). "Matplotlib: A 2D Graphics Environment". *Computing in Science & Engineering*, vol. 9, no. 3, pp. 90-95, doi: 10.1109/MCSE.2007.55.

Jordahl, K., Van den Bossche, J., Fleischmann, M., McBride, J., Wasserman, J., Gerard, J., et al. (2021). *geopandas/geopandas: v0.9.0*. <https://doi.org/10.5281/zenodo.4569086>.

OpenStreetMap (2022). OpenStreetMap: About. Available at: <https://www.openstreetmap.org/about>. [Accessed 27/05/22]

Pedregosa, F., Varoquaux, G., Gramfort, A., Michel, V., Thirion, B., Grisel, O. et al. (2011). Scikit-learn: Machine learning in Python. *The Journal of Machine Learning Research* 12: 2825-2830.

Python (2018). *Python Documentation contents*, v.3.7.13 <https://docs.python.org/3.7/contents.html>.

VÚMOP (2015). *Trvalé travní porosty (TTP)* [Permanent grassland]. Available at: [https://restep.vumop.cz/encyklopedie/index.php/Trval%C3%A9_travn%C3%AD_porosty_\(TTP\)](https://restep.vumop.cz/encyklopedie/index.php/Trval%C3%A9_travn%C3%AD_porosty_(TTP)).

Waskom, M. L. (2021). Seaborn: statistical data visualization. *Journal of Open Source Software*, 6(60), 3021. <https://doi.org/10.21105/joss.03021>

Ziv, G., Beckmann, M., Bullock, J., Cord, A., Delzeit, R., Domingo, C., et al. (2020). BESTMAP: behavioural, Ecological and Socio-economic Tools for Modelling Agricultural Policy. *Research Ideas and Outcomes*, 6, e52052. <https://doi.org/10.3897/rio.6.e52052>